THE ASTROPHYSICAL JOURNAL

AN INTERNATIONAL REVIEW OF SPECTROSCOPY AND ASTRONOMICAL PHYSICS

VOLUME 99 MAY 1944 NUMBER 3

HEBER DOUST CURTIS*

1872–1942

The passing of Heber Doust Curtis, on January 9, 1942, deprived his associates of a true friend, and the world of a scientist and scholar who was a leader in fostering the great observing tradition of American astronomy. He is survived by his wife, Mary D. Rapier Curtis; a daughter, Margaret Evelyn (Mrs. Alexander Walters); and three sons—Rowen Doust, Alan Blair, and Baldwin Rapier.

Professor Curtis was born in Muskegon, Michigan, on June 27, 1872, the son of Sarah Doust and Orson B. Curtis, and received his early schooling in the Detroit public schools. Perhaps influenced by the fact that his father was a Union veteran of the Civil War, he wished to enter Annapolis, but he could not meet the height requirement. In 1889 he entered the University of Michigan, graduating with the A.B. degree three years later, having specialized in the classical languages—Latin, Greek, Hebrew, and Sanskrit. After a year of graduate study, he received his A.M. degree from the University of Michigan in 1893. His first seven years after leaving the university were spent as a teacher. During the academic year 1893–1894 he taught English and algebra in the Detroit High School, after which he became professor of Greek and Latin at Napa College, California. In 1896 he was appointed professor of mathematics and astronomy at the College of the Pacific. It was at this time that his interest in astronomy became aroused. Interestingly enough, during his four years at the University of Michigan, Curtis did not once enter the observatory that he was later destined to direct. But the stimulus of teaching mathematics and astronomy and keeping, as he put it, "one jump ahead of the class," attracted him to the possibilities of astronomical research. His growing enthusiasm for astronomy was encouraged by Director Edward S. Holden of Lick Observatory, where he spent several summers as a volunteer assistant.

In the summer of 1900 Curtis accompanied the Lick Observatory–Crocker Eclipse Expedition to Thomaston, Georgia, as a volunteer observer, the first of eleven such expeditions that were later to take him all over the world. Having determined to make astronomy his life work, he applied for and received the Vanderbilt Fellowship at the University of Virginia, where he studied at the Leander McCormick Observatory under Professor Ormond Stone and received his Ph.D. degree in 1902. For eighteen years, starting in 1902, Curtis was associated with the Lick Observatory. From 1902 to 1906 he served as assistant and assistant astronomer; from 1906 to 1909 as acting astronomer in charge of the D. O. Mills Expedition to the Southern Hemisphere at Santiago, Chile; and

* Reprinted from the *American Philosophical Society Yearbook, 1942*, pp. 339–344.

from 1909 to 1920 as astronomer. During the war years 1917–1918 he organized and conducted a navigation school for the United States Shipping Board in San Diego, California, taught navigation at the Naval Officers' School in Berkeley, and was a research physicist in the Optical Section of the National Bureau of Standards in Washington, D.C., where for a time he was acting head of the Optical Section. In 1920 he was called to the directorship of the Allegheny Observatory of the University of Pittsburgh, serving in that capacity for ten years. In 1930 Curtis accepted the post of director of the observatories of the University of Michigan, serving in that position until his death, five months prior to his scheduled retirement.

He was a member of many learned and popular societies, including, in addition to the American Philosophical Society (elected in 1920), the Astronomical Society of the Pacific (president, 1912); Fellow, the American Association for the Advancement of Science (vice-president, Section D, Astronomy, 1924); American Astronomical Society (vice-president, 1926); National Academy of Sciences; Royal Astronomical Society (associate); Astronomische Gesellschaft; International Astronomical Union (Commission 13, Solar Eclipses); Phi Beta Kappa; Sigma Xi; and Phi Kappa Phi. He was Henry Russell Lecturer at the University of Michigan in 1938. The University of Pittsburgh conferred upon him the honorary degree of Doctor of Science, in 1930.

Dr. Curtis' professional bibliography of 135 titles is a monument to his versality and habit of clearheaded and concise thinking. Gifted with an unusual mechanical ingenuity, he was able to modify existing equipment or to design and build new instruments that would enable him to make the types of exacting observations he felt were a prerequisite for an understanding of the nature and workings of the universe. His researches were as varied as they were fundamental, including contributions to the fields of the meteors, cometary orbits, stellar positions, asteroid observations, stellar spectroscopy, orbits of spectroscopic binaries, photographic studies of comets, solar eclipses, galactic and spiral nebulae, cosmogony, and instruments.

Probably the most fruitful of Professor Curtis' researches were carried out during his association with the Lick Observatory. Curtis joined the staff one year following the assumption of the directorship by W. W. Campbell. Under Campbell's leadership, Curtis participated in an ambitious project for measuring the radial velocities of all the stars in the northern skies brighter than magnitude 5.5. This program and others established standards of precision that have made Lick Obseratory renowned for its high-quality observations. As a by-product of the radial velocity program, Curtis discovered many new spectroscopic binaries and computed their orbits. A southern counterpart of the radial velocity program was pursued by Curtis at Santiago, Chile, while he was in charge of the D. O. Mills Expedition.

While in Chile, Curtis found time to make spectrographic and photographic observations of Comet Morehouse, in 1908. His return to Lick in 1909 coincided with the reappearance of Halley's great comet. From September, 1909, to July, 1910, Curtis made 360 photographs of this famous visitor—a collection that should be of immense value to the astronomers in 1985, when Comet Halley is expected to return once more.

In 1910 Professor Curtis began his new classic photographic studies of the planetary, diffuse, and spiral nebulae, described in Volume XIII of the "Lick Observatory Publications." This work helped lay the groundwork for the now generally accepted view that our Milky Way system is one of hundreds of millions making up the observable universe. Curtis was particularly interested in the "coal sacks" and starless regions in or near the Milky Way. His careful observations led him to conclude, in 1918, that "it is difficult to avoid the impression that something is blotting out everything beyond . . . ." and lent strong support to the present belief that the Milky Way is strewn with great clouds of obscuring dust and gas.

The years immediately preceding and following 1920 were exciting ones for astrono-

mers, who were then engaged in debating a question of great significance, both astronomically and philosophically. The question was whether the many thousands of spiral nebulae observed visually and on the photographic plate belonged, like the diffuse and planetary nebulae, within the confines of our Galaxy or whether each constituted a separate Milky Way of stars, clusters, and nebulae, located millions of light-years from the sun. Curtis had made an extensive study of dark "lanes" in spirals. To him the almost complete absence of spiral nebulae near the plane of the Milky Way indicated a similar belt of obscuration, which suggested a close resemblance between the structures of the Galaxy and of the spiral nebulae. These studies, together with the discovery of novae in spirals by him and by Ritchey, led him to champion the "island universe" theory of spirals. The evidence for the opposing view seemed equally convincing, however; and for a time, as he put it, he was practically an "Irish majority" in his vigorous adherence to the island-universe theory. The issue was finally settled beyond all doubt in 1924, when Hubble's discovery of Cepheid variable stars in the Andromeda nebula with the powerful 100-inch reflector demonstrated that the nebula was not a "nebula" at all but a stellar aggregation one million light-years away.

Dr. Curtis had a love for fine instruments, which found ample opportunity for expression in the three institutions he served for over forty years. At Lick Observatory the mechanical modifications of the Crossley reflector, which he made to facilitate his observational program, gave him as much personal satisfaction as the observations themselves. During the decade 1920–1930, when Curtis was director of the Allegheny Observatory, his penchant for machine work and the design of apparatus found expression in the many instruments that he designed and constructed, primarily for use by the Allegheny Observatory, including those transported on four eclipse expeditions. He also built, in the Allegheny shops, a long-screw measuring engine for the Sproul Observatory of Swarthmore College. The problems that he encountered and solved in constructing an accurate screw led him to make preliminary plans for a grating ruling engine. He always regarded a successful ruling engine as "the most perfect man-made mechanism" and was eager to try to build one. To the University of Michigan, Curtis came in 1930 prepared to design a large reflecting telescope for the university observatory at Ann Arbor. Unfortunately, by the time he had personally completed the design and drawings of the telescope, the 1932 depression was at its "lowest," and funds were no longer available for its construction. The 97-inch Pyrex disk (the gift of the late Tracy W. McGregor) which he ordered is now stored at the observatory; and, when the time comes to build the telescope, his designs should be of great value to his successor.

Dr. Curtis' preparation for, and attendance at, eleven eclipse expeditions provided ideal opportunities for exercising both his mechanical talents and limitless energy. In addition to the 1900 eclipse already mentioned, he journeyed to Solok, Sumatra, in 1901; Cartwright, Labrador, in 1905; Brovary, Russia, in 1914; Goldendale, Washington, in 1918; Yerbaniz, Mexico, in 1923; New Haven, Connecticut, in 1925; Benkoelen, Sumatra, in 1926; Takengon, Sumatra, in 1929; Gerlach, Nevada, in 1930; and Fryeburg, Maine, in 1932. One of his great disappointments was that illness prevented his attendance at his twelfth planned eclipse expedition, to Canton Island, in 1937. His spectrum photographs of the solar corona and chromosphere, obtained in 1925, in New Haven, were the first ever secured of the infrared region of the spectrum.

Although Professor Curtis' researches reached to the observable limits of the universe, his first love was the star nearest home, the sun. Thus it was natural that he should take a deep interest in the McMath-Hulbert Observatory, the development of which as a private institution was well under way when he came to Michigan in 1930. Dr. Curtis was a never ending source of encouragement and inspiration to the writer and his associates at Lake Angelus. His contributions to the McMath-Hulbert Observatory cannot be assessed too highly.

During the last eleven years Professor Curtis and the writer were together constantly, both socially and professionally. First, last, and always, Heber D. Curtis was a man. Sympathetic understanding was always available for those in need; clearheaded, concise thinking about all problems was one of his many fine characteristics; but when the situation demanded, he could be all "iron." To the highly privileged writer, he was always a "guide, philosopher, and friend."

Astronomers will recall the note by Campbell regarding Professor Curtis, at the time of the 1900 eclipse: "We do not see how we could have dispensed with his services, nor how anyone could have met the exacting demands better than he did."

ROBERT R. MCMATH

McMATH-HULBERT OBSERVATORY
UNIVERSITY OF MICHIGAN

LINE INTENSITIES AND THE SOLAR CURVE OF GROWTH

K. O. WRIGHT*

Dominion Astrophysical Observatory, Victoria, B.C.

Received March 15, 1944

ABSTRACT

The solar curve of growth is redetermined by combining the best available equivalent-width data (those of Allen and the Utrecht photometric atlas) with King's laboratory gf-values for lines of *Ti* I and *Fe* I. A comparison of laboratory intensities with theoretical intensities, calculated for LS coupling, shows that the latter may be seriously in error for complex atoms. Excitation temperatures for the reversing layer of the sun are found to be 4550° ± 125° K for *Ti* I lines and 4900° ± 125° K for *Fe* I lines; this difference appears to be real. Solar gf-values may be calculated for any atomic line with a known solar equivalent width if an excitation temperature of 4700° K is assumed.

The theory of the curve of growth for absorption lines in stellar spectra was first given by Minnaert and Slob[1] in 1931, when they showed how the intensity of a stellar absorption line, measured by its equivalent width, depended on the "number of active atoms" involved in the electron transition. The theory was extended in 1936 by Menzel[2] and again in 1938 when Unsöld[3] gave a complete review of the subject. Detailed, practical applications of the theory to the sun and stellar spectra have been attempted, among others, by Menzel, Baker, and Goldberg,[4] Greenstein,[5] Miss Steel,[6] and the author[7]; but in all cases the scatter of observed intensities about the mean curve of growth has been much greater than might have been desired. Three main contributing factors producing this scatter are: (*a*) The theory is very much oversimplified, largely because more probable assumptions concerning the passage of radiation through a stellar atmosphere involve mathematical equations which have not yet been solved. (*b*) Line intensities calculated from theoretical models of the atom (LS coupling) are not accurate for complicated atoms, such as iron and titanium; and extensive lists of laboratory intensities are available for the spectra of very few atoms. (*c*) The accurate measurement of stellar line intensities for this purpose requires a detailed study of high-dispersion spectra; a great many lines covering as wide an intensity range as possible are desired for each element, and, under such conditions, systematic errors in measurement may be introduced. It is the purpose of this paper to use the best available data for *b* and *c* for the sun and to show that certain difficulties still remain with regard to *a*.

The theory of the curve of growth indicates that for weak lines the intensity, measured by log (W/λ), is directly proportional to the "number of active atoms," N, according to the Doppler principle; and for strong lines it is proportional to the square root of N if produced by a combination of radiation and collision damping effects. The transition portion of the curve, which represents the sum of these effects as the line becomes saturated, has not yet been completely studied mathematically; the best representation of the curve has been given by Baker,[8] although his formula, given in equation (1), applies

* On loan to the Department of Physics, University of British Columbia, during the 1943–44 session.

[1] *Proc. kgl. Acad., Amsterdam*, **34**, 542, 1931.

[2] *Ap. J.*, **84**, 462, 1936.

[3] *Physik der Sternatmosphären*, pp. 264–285, Berlin: Springer, 1938.

[4] *Ap. J.*, **87**, 81, 1938.

[5] *Ap. J.*, **95**, 161, 1942.

[6] Unpublished.

[7] *Pub. A.A.S.*, **10**, 34, 1940.

[8] *Ap. J.*, **84**, 474, 1936.

only to the sun and very similar stars:

$$\log \frac{W}{\lambda} = \log X_0 \frac{v}{c}\sqrt{\pi} - \tfrac{1}{2}\log(1+X_0) - \frac{\tfrac{1}{2}\log 4\sqrt{\pi}\,\frac{v}{c}\,\frac{\nu}{\Gamma}}{1+1.5e^{-2\log X_0}}, \qquad (1)$$

where W is the equivalent width, λ the wave length in Angstrom units, X_0 the optical depth at the center of the line, and c/v and Γ/ν are constants which must be derived from the observed curve of growth. As X_0 is not known at the beginning of an investigation, $\log (W/\lambda)$ must be plotted against known values which are proportional to $\log X_0$. Theory indicates that, for a Boltzmann distribution of energy within the atom, X_0 is proportional to $Ss/\Sigma s\ e^{-E_i/kT}$ or to $\mathrm{gf}\cdot\lambda\cdot e^{-E_i/kT}$, where $Ss/\Sigma s$ is the theoretical line strength on the basis of pure LS coupling, gf is the observed laboratory intensity, and E_i is the excitation potential of the lower level of the atomic transition. In this paper $\log (W/\lambda)$ has been plotted against $\log X_f$ as defined by

$$\log X_f = \log \mathrm{gf} + \log\lambda - \frac{5040}{T}E_i, \qquad (2)$$

where T is the excitation temperature of the given atoms and may be determined from the curve itself. In previous work the stellar intensity has been plotted against the theoretical intensity for all lines in the same transition array, and the various segments have been shifted along the X_0-axis to form the best mean curve of growth; or the stellar intensities have been compared with the values of X_0' determined by Menzel[4] for the sun.

For complex atoms it is known that LS coupling does not represent the interaction of electrons well, but line intensities are not readily calculable for other models. Laboratory intensities should be more reliable if the necessary corrections for self-reversal, temperature, and frequency are made. Laboratory emission intensities have been published;[9] but only Seward[10] and Allen and Hesthal[11] have completely corrected the observed values. An attempt was made to use Seward's intensities for *Mn* I, and satisfactory results were obtained for lines in the region λλ 4000–4800; but when lines in the region λλ 3500–3900 were included, the scatter about the mean curve of growth was so greatly increased that the *Mn* I intensities have been omitted. The laboratory intensities upon which this investigation is based are the gf-values measured in absorption in the electric furnace for *Ti* I and *Fe* I by A. S. and R. B. King.[12]

In Figure 1, $\log (Ss/\Sigma s)$ has been plotted against $\log (\mathrm{gf}\cdot\lambda)$ for the transition arrays of *Ti* I and *Fe* I for which King and King have published laboratory intensities. The straight line in each diagram indicates a one-to-one correspondence between theoretical and laboratory intensities. As King and King consider that the probable error of their measurements is about 10 per cent, the failure of LS coupling in these atoms seems to be the most likely cause for the observed scatter in the diagrams. In general, it appears that the intensity rules hold fairly well within individual multiplets, but the theoretical multiplet strengths (S) are frequently in error. These diagrams indicate that large errors may be introduced if theoretical intensities are used for complicated atoms. Laboratory intensities should, therefore, be employed whenever possible.

In order to obtain the best available solar intensities, the values published by Allen[13] and measures made by the author from the *Utrecht Photometric Atlas of the Solar Spectrum*[14] have been used. Equivalent widths of about seven hundred lines in the atlas

[9] See list in Unsöld, *op. cit.*, p. 207.

[10] *Phys. Rev.* **37**, 344, 1931.

[11] *Phys. Rev.*, **47**, 926, 1935.

[12] *Ap. J.*, **87**, 24, 1938.

[13] *Mem. Comm. Solar Obs., Canberra*, No. 5, 1934; No. 6, 1938.

[14] By Minnaert, Mulders, and Houtgast, Amsterdam, 1940.

in the region λλ 3500–6700 were obtained by counting squares after corrections for blending with other lines and for the position of the continuous spectrum had been made. The agreement between Allen's data and the Utrecht values is very satisfactory. The probable error of any given equivalent width is about 7 per cent for very weak lines ($W < 0.050$ A) and slightly less than 6 per cent for all stronger lines. As no appreciable systematic differences have been detected, average values have been used wherever a line was available in each publication. Woolley[15] and Mulders[16] have also published tables of solar line intensities, but these have not been used because they cover only limited regions of the spectrum. Phillips[17] published solar intensities for the region λλ 3500–3900; but, since the scatter when compared with the Utrecht measures was great and since the Utrecht measures agreed well with those by Allen in other regions, Phillips' observations have been omitted.

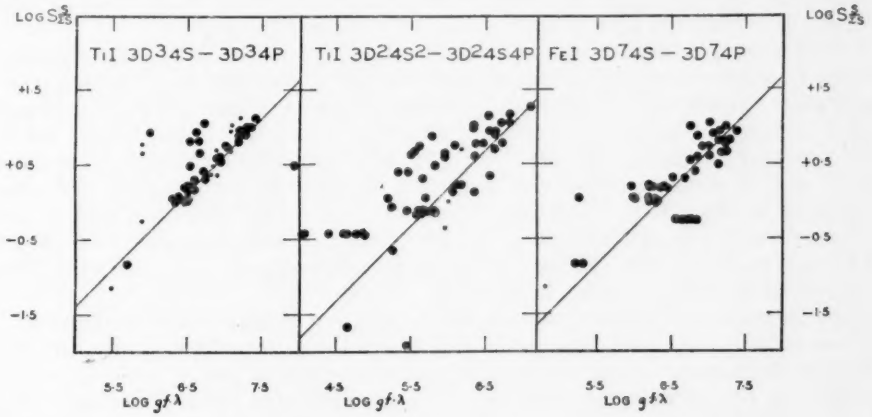

FIG. 1.—Comparison of theoretical intensities ($S\frac{S}{\Sigma S}$ and laboratory intensities ($gf \cdot \lambda$) for lines of *Ti* I and *Fe* I.

The solar curve of growth has been derived by plotting log (W/λ) against log X_f (eq. 2) for all available lines of *Ti* I and *Fe* I. All lines in the solar spectrum from which the blending of other lines could be eliminated were used, with weights ranging from 4 (a line almost free from blends) to 1 (a line of uncertain equivalent width). Both solar and laboratory intensities were available for 160 lines of neutral titanium and 97 lines of neutral iron. As a first approximation, the temperature, T (in eq. 2), was assumed to be 4400° K—a value obtained by Menzel[4] and also by King.[18] The titanium and iron observations were treated separately at first, and the best empirical curve was drawn through each set of points, adopting only the criteria that the slope of the lower Doppler region be 1.0 and that of the radiation-damping portion be 0.5. As the slopes of the transition portions of the two curves were very nearly equal and as the gf-values were only relative, the two curves were moved along the X_f-axis until the single curve with the least scatter was obtained. The observational points were grouped, and a smooth curve was drawn through the weighted mean values. Improved excitation temperatures were then calculated from the formula

$$Y = \log X_f - \log \mathrm{gf} - \log \lambda = L - \frac{5040}{T} E_i , \qquad (3)$$

[15] *Ann. Solar Phys. Obs., Cambridge*, **3**, Part II, 1933.

[16] *Zs. f. Ap.*, **10**, 297, 1935. [17] *Ap. J.*, **96**, 61, 1942. [18] *Ap. J.*, **87**, 40, 1938.

in which Y is defined from the first half of the equation, log X_f is taken from the curve for each value of log (W/λ), and L is a constant which should equal zero in this case if the correct excitation temperature has been assumed but which is proportional to the abundance of the atom in the solar reversing layer when the theoretical value of X_0 (as given in Baker's formula [eq. 1]) is used. Temperatures of 4550° for *Ti* I and 4850° for *Fe* I were derived from least-squares solutions of this equation.

In order to cover the transition portion of the curve more completely, W. Petrie's calibration[19] of King's eye-estimates[20] of emission-arc intensities, in terms of the laboratory gf-values, was used for lines of *Fe* I. Although laboratory intensities have been obtained only for lines with lower excitation potentials of less than 1.6 volts, the relation appears to be linear; and, in order to use the weak iron lines, Petrie's curves were extrapolated up to a lower excitation potential of 4.0 volts. These calibrated gf-values may be in error for individual lines, but the two hundred additional lines, each of weight 1, extended the transition portion of the curve for the iron lines 0.5 units along the log X_f-axis with very little increase in scatter about the mean curve.

Several attempts were made to reconcile the different temperatures obtained for *Ti* I and *Fe* I; but when a mean temperature of 4700° K was used to form the curve, the temperature calculated for *Ti* I lines became 4300° K, and that for *Fe* I lines was increased to 4950° K. The adopted curve of growth for the sun shown in Figure 2 is based on an assumed temperature of 4500° for *Ti* I, which leads to a calculated temperature of 4575° ± 125° and an assumed temperature of 4850° for *Fe* I, which leads to a calculated value of 4750° ± 150° for all iron lines and 4975° ± 100° for lines with measured gf-values. When Y is plotted against E_i, the mean points fit a straight line very well, and there is no appreciable change in slope with excitation potential, such as W. Petrie[21] has observed for chromospheric intensities.

The adopted curve of growth for the sun is the mean of the two curves obtained from the observations of neutral titanium and of neutral iron lines, as indicated above. The overlap of these curves is only on the flat transition portion, and, in order to obtain an objective fit, this section was considered to be straight, and the best straight line was drawn through the points on each curve. As the slopes were nearly identical it was readily found that a factor of 3.00 must be added to log X_f for the titanium lines in order to make the best fit with the relative gf-values for the iron lines. An additional factor (−3.73) has been added to all observations in order to make the scale agree with the absolute gf-values for neutral iron as determined by King.[22] Thus the present scale along the X_f-axis is based on the absolute gf-values for iron. The weighted mean values of the observed points for both titanium and iron are given in Table 1 and points taken from the smooth curve are given in Table 2. Log X_f may be obtained directly from this curve for any line whose solar intensity, log (W/λ), is known and absolute gf-values on the iron scale are readily derived by means of the equation

$$\log \mathrm{gf}_{\odot} = \log X_f - \log \lambda + \frac{5040}{T} E_i . \qquad (4)$$

The most uncertain quantity in this equation is T, which apparently should be 4550° for *Ti* I lines and 4900° for *Fe* I lines. As, however, the factor $(5040/T)E_i$ varies slowly with T for lines of low excitation potential, this discrepancy is small, and a mean value of $T = 4700°$ K for lines of atoms other than *Ti* I and *Fe* I might well be used.

In order to compare this empirical curve of growth for the sun with the theoretical curve, it was related to the family of curves computed by Menzel[23] to obtain the damp-

[19] *Pub. A.A.S.*, **10**, 257, 1942.

[20] *Ap. J.*, **37**, 239, 1913; **56**, 318, 1922.

[21] *J.R.A.S. Canada*, Vol. **38** (in press).

[22] *Ap. J.*, **95**, 78, 1942.

[23] *Pop. Astr.*, **47**, 74, 1939.

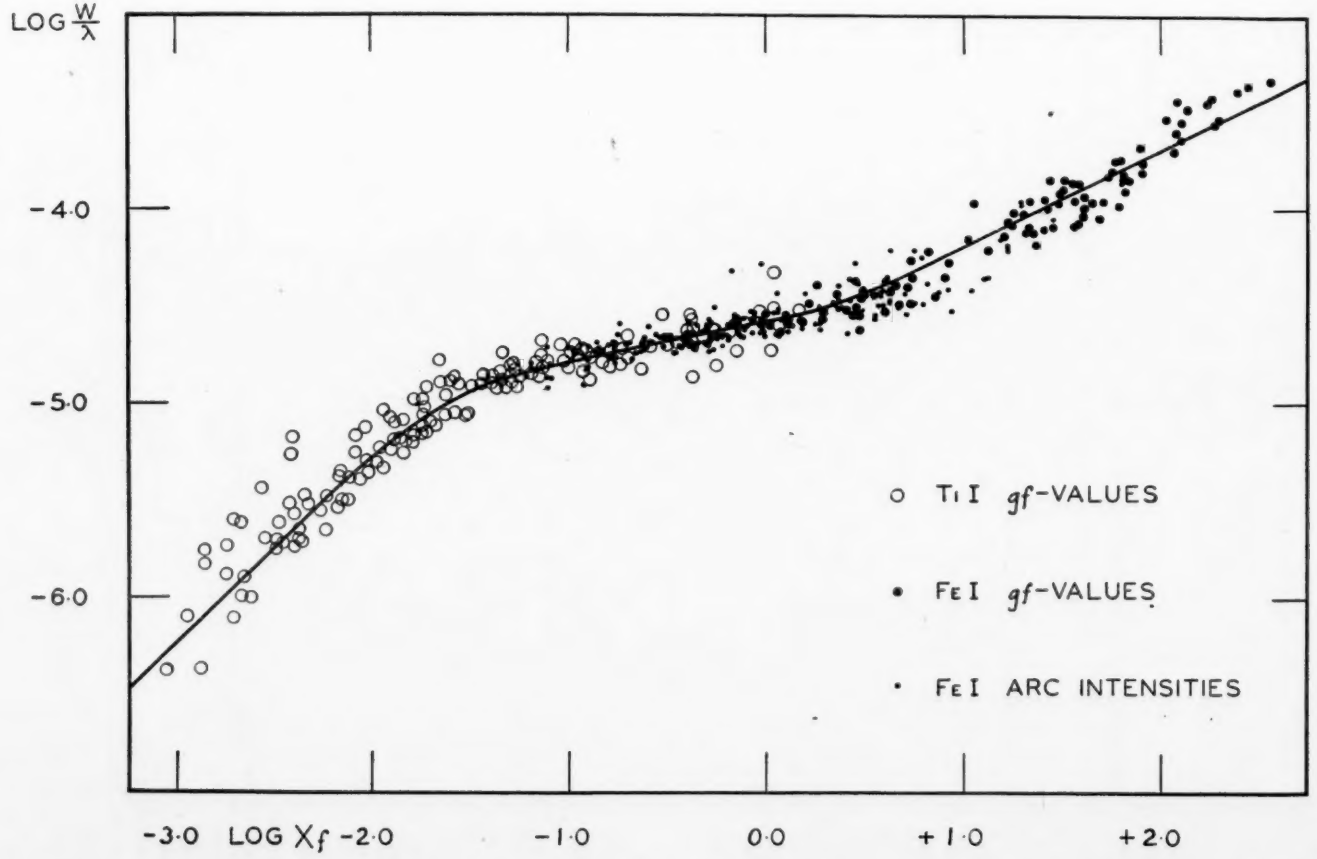

FIG. 2.—Curve of growth for the sun obtained from equivalent-width measurements (Allen and the *Utrecht Photometric Atlas*) and King's laboratory gf-values for lines of *Fe* I and *Ti* I. In drawing the mean curve the weights of individual points have been considered.

ing factor, Γ/ν, and the turbulent velocity, v. The best fit between empirical and theoretical curves is obtained by adding +1.81 to log X_f, and these values, together with the difference (Empirical − Theoretical) for a given value of log (W/λ) are given in columns 3, 4, and 5 and columns 8, 9, and 10 of Table 2. The empirical curve is definitely above the theoretical curve of best fit where the Doppler region changes to the transition por-

TABLE 1

MEAN VALUES OF OBSERVED POINTS ON SOLAR CURVE OF GROWTH

Ti I			*Ti* I			*Fe* I			*Fe* I		
log (W/λ)	log X_f	Wt.	log (W/λ)	log X_f	Wt.	log (W/λ)	log X_f	Wt.	log (W/λ)	log X_f	Wt.
−6.18	−2.92	6	−4.87	−1.33	53	−4.83	−1.13	8	−4.39	+0.80	32
5.99	2.68	17	4.81	−1.14	36	4.76	−0.90	12	4.07	1.28	48
5.63	2.50	15	4.77	−0.95	24	4.71	−0.70	31	3.94	1.61	33
5.58	2.35	17	4.78	−0.73	20	4.68	−0.43	36	3.79	1.84	25
5.44	2.15	28	4.67	−0.42	24	4.62	−0.19	48	3.56	2.10	24
5.25	1.95	43	4.65	−0.24	19	4.58	+0.03	35	3.49	2.27	10
5.12	1.76	44	−4.54	+0.06	15	4.50	+0.33	40	−3.36	+2.47	9
−4.96	−1.56	22				−4.45	+0.56	45			

TABLE 2

COMPARISON OF OBSERVED AND CALCULATED CURVES OF GROWTH FOR THE SUN*

log (W/λ)	log X_f	log X_0			log (W/λ)	log X_f	log X_0		
		Observed	Calculated	O−C			Observed	Calculated	O−C
−7.00	−3.77	−1.96	−1.96	0.00	−4.70	−0.58	+1.23	+1.17	+0.06
6.50	3.27	−1.46	−1.45	− .01	4.60	−0.08	1.73	1.59	.14
6.00	2.76	−0.95	−0.93	.02	4.50	+0.31	2.12	1.96	.16
5.50	2.24	−0.43	−0.37	.06	4.40	+0.58	2.39	2.26	.13
5.25	1.96	−0.15	−0.04	.11	4.25	+0.90	2.71	2.64	.07
5.00	1.60	+0.21	+0.37	.16	4.00	+1.41	3.22	3.19	+ .03
4.90	1.40	+0.41	+0.58	.17	−3.50	+2.41	+4.22	+4.22	0.00
−4.80	−1.05	+0.76	+0.83	−0.07					

* Note added April 5, 1944: In a recent letter Dr. Menzel has pointed out that line strengths based on $(Ss/\Sigma s)$ values are more important in theoretical discussions than gf-values. Therefore, the scale for the X_f-axis given in columns 3 and 8 of Table 2 may prove more useful than the data given in columns 2 and 7. As these values differ only by the additive constant (+1.81), the same notation may be used.

tion, and it is below the theoretical curve where the transition portion changes to the damping region. This curve corresponds to a turbulent velocity, v, of 0.9 km/sec and a damping factor, $\Gamma/\nu = 2.61 \times 10^{-6}$; Menzel and Rubenstein's solar curve[24] gives corresponding values of 0.6 km/sec and 1.7×10^{-6}.

A comparison of the present curve of growth for the sun with those obtained previously shows that the scatter of individual points about the mean curve has been considerably decreased by the use of accurate solar intensities combined with reliable laboratory

[24] *Ap. J.*, **92**, 114, 1940.

intensities. Observations of weak lines ($0.004 < W < 0.030$ A) indicate that the theory for the Doppler portion of the curve agrees well with observation. The well-defined shoulder of the empirical curve between the Doppler and the transition portions indicates that at that point log (W/λ) is greater than provided by Baker's formula. The status of the damping portion of the curve is uncertain. King[25] observed that the strong iron lines fitted a curve with $T = 4800°$ better than one with $T = 4400°$, but he attributed the discrepancy to variations in the damping factor. As King and Minkowski[26] have pointed out, a study of the natural widths of these lines indicates that this factor is much smaller than that observed for lines in stellar spectra and that it should vary considerably from line to line. However, they conclude that differences in line width plus pressure effects do not account for the observed scatter about the curve of growth. The best straight line through the observed points on the damping portion of the empirical curve has a slope of 0.57 rather than the theoretical value of 0.50, but in the absence of satisfactory justification for the higher value, the theoretical slope has been adopted in this paper.

This communication presents the further results of a paper read before the American Astronomical Society in May, 1943. The author wishes to thank his colleagues at the Dominion Astrophysical Observatory for many helpful discussions, Dr. W. Petrie for the use of his calibration of King's arc intensities, and Lt. Commdr. D. H. Menzel, U.S.N.R., for his continued interest in the work.

[25] *Ap. J.*, 95, 78, 1942.

[26] *Ap. J.*, 95, 86, 1942.

NOTE ON THE SPECTRUM OF α^2 CANUM VENATICORUM*

W. A. HILTNER
McDonald and Yerkes Observatories
Received October 26, 1943

ABSTRACT

Certain lines of *Fe* II are observed to be double in the spectrum of α^2 Canum Venaticorum at a phase near *Eu* II maximum. All lines showing duplicity are of type B. The doubling in α^2 Canum Venaticorum is very similar to that in ϵ Ursae Majoris.

In September, 1943, Struve and Hiltner[1] announced that, in addition to variation in intensity of absorption lines found by Guthnick,[2] certain lines of *Cr* II, *Fe* II, *V* II, and of some other elements in ϵ Ursae Majoris became double at phases 1.5 and 3.7 days after the epoch of minimum intensity of the *Ca* II K line. As was emphasized in this article, it is difficult to explain the doubling in terms of binary motion, since only some of the lines show doubling and, more significantly, the total width of the lines remains constant throughout the period of 5.09 days.

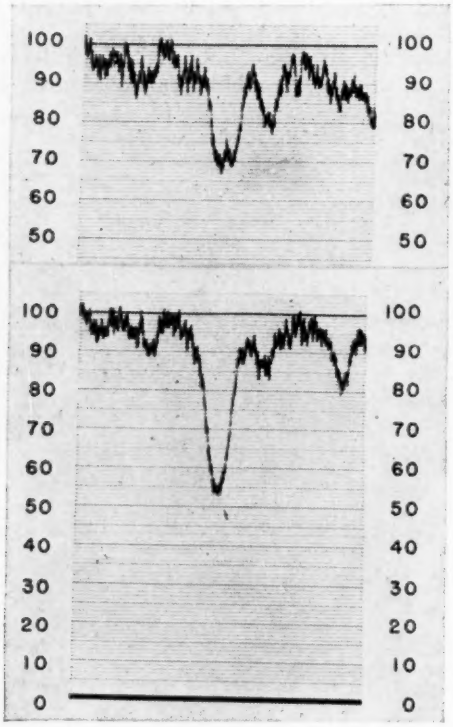

FIG. 1.—Tracings of *Fe* II 4233 in α^2 Canum Venaticorum. *a*, Phase 0.085 day; *b*, Phase 1.559 days.

At the time of this announcement no periodic doubling of lines in other peculiar A stars had been observed. However, on analyzing a series of Coudé spectrograms obtained at McDonald Observatory for a spectrophotometric study of α^2 Canum Venaticorum, the strong *Fe* II line λ 4233.2 was found to be double on a plate taken on May 13.307, 1943, U.T. This corresponds to phase 0.085 day after *Eu* II maximum as computed with the formula obtained by Miss G. Farnsworth.[3] The duplicity of this line can be seen on Plate XII and is vividly shown by the intensity tracings in Figure 1. Struve and Swings[4] consistently measured the line single. The separation of the two components is about 0.26 A.

The doubling is almost certainly not a consequence of blending. In addition to λ 4233.2, other lines of *Fe* II consist of two components at phase 0.085 day. For example, $\lambda\lambda$ 4177.7, 4273.3, and 4303.2 show the effect conspicuously. The last two belong to the same multiplet as *Fe* II 4233.2. The wave lengths of the center of gravity remain ap-

* *Contributions from the McDonald Observatory, University of Texas*, No. 85.

[1] *Ap. J.*, **98**, 225, 1943.

[2] *Sits.-Ber. Preuss. Akad. Wiss. Berlin*, p. 27, 1931.

[3] *Ap. J.*, **75**, 364, 1932.

[4] *Ap. J.*, **98**, 437, 1943.

PLATE XII

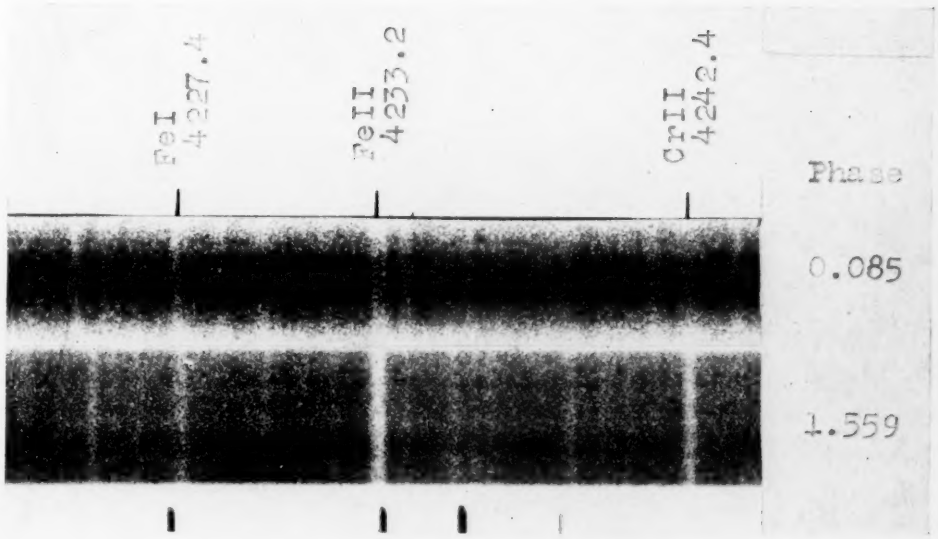

THE SPECTRUM OF α^2 CANUM VENATICORUM

proximately constant in the transition from the double to the single stage. If doubling resulted from blending with lines of type A (intensities vary in phase with *Eu* II lines) of appreciable strength as indicated by the relative intensities of the two components, then the lines that show doubling would probably no longer fall in type B (intensities vary oppositely to type A), since the lines of type A, such as *Eu* II, usually possess a much greater intensity variation than the *Fe* II lines of type B. All lines observed as double at phase 0.085 day are of type B. The residual central intensities are greater when the lines are double, and, as in ϵ Ursae Majoris, the total widths of the lines remain constant.

Although the Coudé spectrographs of ϵ Ursae Majoris have not been analyzed spectrophotometrically, from visual inspection it appears that the equivalent widths of the lines that become periodically double are smaller when the lines are double and the central intensities greater.[5] The same relationship is observed for α^2 Canum Venaticorum. The variations in profiles of α^2 Canum Venaticorum and ϵ Ursae Majoris must certainly have a common origin. The evidence suggests that emission in the center of the lines may produce the observed duplicity in certain lines of these two peculiar A stars.

In ϵ Ursae Majoris, *Cr* II shows doubling relatively more often than other elements, while in α^2 Canum Venaticorum, *Fe* II has a greater tendency to become double. In fact, no line of *Cr* II has thus far been observed double and only one line each of *Ti* II and *Fe* I. *Mg* II 4481 and *Si* II 4128 and 4131 remain single throughout the period of 5.47 days.

[5] See *Ap. J.*, **98**, Pl. XX, *Fe* II 4033 and *Cr* II 4052.

THE SPECTRUM VARIABLE ε URSAE MAJORIS*

J. W. SWENSSON
Yerkes and McDonald Observatories
Received February 8, 1944

ABSTRACT

A list of absorption lines between λ 3307 and λ 4638 is given for the spectrum variable ε Ursae Majoris. This is supplemented by a brief description of the periodic variations in the line intensities.

A recent paper by O. Struve and W. A. Hiltner[1] called attention to changes in the line contours of the spectrum variable ε Ursae Majoris. P. Guthnick,[2] in a study of the variations of the total intensities of absorption lines in this star, has given a table of lines for the range λλ 3933–4589; this has appeared inadequate in the light of present-day laboratory material. A new table of lines in the region λλ 3307–4638 is given, together with a brief description of the periodic variations in the line intensities. The identifications in the present table are essentially in agreement with those given by P. Swings and M. Désirant[3] for the region λλ 3671–3931.

The observational material consisted of 36 spectrograms taken in June and July, 1943, by O. Struve, C. A. Bauer, and G. Münch with the Cassegrain quartz spectrograph and the 500-mm camera of the McDonald Observatory and 5 spectrograms taken in May and June, 1943, by C. A. Bauer and O. Struve with the Bruce spectrograph of the Yerkes Observatory. The dispersions for the two groups of plates are 55 and 26 A/mm at $H\gamma$, respectively; the exposures are all on Eastman Process plates. Owing to the choice of the exposure times, the region of the Balmer limit is either underexposed or overexposed, and the study is therefore somewhat deficient in this region.

From a study of a great number of spectra Guthnick[4] has established that the K line of *Ca* II is periodically variable with intensity minima on

$$(1931 \text{ April } 5.01 = \text{JD } 2246437.01) + 5.0887E\,.$$

Many of the other lines are slightly weakened when the K line is strong.

Eye estimates were made of the intensity of *Ca* II K indicating minima on the following dates: JD 2430904.6, 2430920.6, 2430925.7, and 2430930.6. A period of roughly 5.2 days is obtained, which is in accord with Guthnick's more accurate determination. Using his value of $P = 5.0887$ days, the above four epochs give for the K line an intensity minimum on JD 2430925.5. Guthnick's elements give JD 2430925.24, differing by only 0.3 day. This difference is of the same magnitude and sense as was obtained by Struve and Hiltner[5] in their study based on coudé spectrograms taken a few weeks earlier than the plates used in the present work, but this is probably due to the relatively small number of plates taken and the unfavorable distribution of the exposure times.

A list of the measured absorption lines is given in Table 1. Two spectrograms were measured in the ultraviolet region; they were taken on June 29 and July 8, at phases 4.79 and 3.62 days, respectively, the former plate being of much better quality and showing more lines. For the strong, well-defined lines the measures from the two plates agreed

* *Contributions from the McDonald Observatory, University of Texas*, No. 88.

[1] *Ap. J.*, **98**, 225, 1943.

[2] *Sitz. Preuss. Akad. Wiss. Berlin*, No. 27, 1931.

[3] *Ap. J.*, **83**, 31, 1936.

[4] *Op. cit.*, No. 30, 1934.

[5] *Op. cit.*

TABLE 1

LIST OF MEASURED ABSORPTION LINES IN ε URSAE MAJORIS

λ	Int.	Int. (α Cyg)	Identification		
			Element	λ	Int.*
3306.96	3	3	Cr II	3306.95	50
			Cr II	3307.04	50
3308.75	2	2	Cr II	3308.15	18
			Ti II	3308.82	8
3310.41	2	2	Cr II	3310.65	35
3311.96	4	4	Cr II	3311.93	40
			Cr II	3312.18	40
3314.43	4	2	(Fe II	3314.00	1)
			c Cr II	3314.06	18
			c Cr II	3314.57	35
3315.43	3	2	c Cr II	3315.29	12
			c Ti II	3315.33	10
			Fe II	3315.52	pr
3316.94	2	.....	.....	.....	.....
3318.12	2	3	c Ti II	3318 03	10
			(Fe II	3318.61	pr)
3320.29	1	1	.....	.....	.....
3321.56	3	.....	Fe II	3321.49	1
		3	V II	3321.54	150
			c Ti II	3321.71	25
3322.93	5+	6	Cr II	3322.69	12
			c Ti II	3322.93	75
			c Fe II	3323.07	8
			Ti II	3323.40	pr
		.....	Cr II	3323.53	8
3324.15	6+	5	Cr II	3324.06	25
			Cr II	3324.10	20
			c Cr II	3324.35	50
3326.74	5+	3	Ti II	3326.78	20
3328.22	2+	2	Cr II	3328.35	20
3329.37	4+	5	Ti II	{3329.44	70
				{3329.52	
3330.81	2	.....	.....	.....	.....
3332.15	4	4	Ti II	3332.11	30
3335.28	6+	6	Ti II	{3335.17	40
				{3335.22	
			Cr II	3335.28	40
			Cr II	3335.46	30
3336.25	6+	.....	(Cr II	3336.16	2)
		5	c Cr II	3336.33	40
3337.43	1	1	V II	3337.85	200
			Ti II	3337.85	2
3338.62	1	1	Fe II	3338.52	3
3340.00	6	7nv	c Cr II	3339.80	50
			(Si II	3339.84	3)
			Cr II	3339.90	20
			c Ti II	{3340.33	35
				{3340.39	
3342.26	6n	5	c Ti II	3341.84	100
			Cr II	3341.98	5
		.....	c Cr II	3342.51	50
		5			
3343.42	2	3	Ti II	3343.78	10
3346.77	3+	4	Ti II	{3346.73	15
				{3346.77	
3347.90	3+	5	Cr II	3347.84	40
3349.26	10	10	Ti II	3348.91	10?
			c Ti II	3349.00	75
			Cr II	3349.34	6
			c Ti II	{3349.39	125
				{3349.47	
3350.31	1	1	Ni II	3350.41	5
3352.93	4nn	1	Ti II	3352.07	5
		3n	c Cr II	3353.12	20
3355.17	2	.....	Fe I	3355.23	6
3356.13	2	1n	Fe II	3356.27	2
3357.38	3+	2	Cr II	3357.40	40
3358.62	6+	5	Fe II	3358.25	3
			c Cr II	3358.50	75
3360.28	6+	4	Fe II	3360.10	3
			c Cr II	3360.30	100
3361.66	6+	9	c Ti II	3361.19	125
			Cr II	3361.77	30
3363.82	2+	2n	Cr II	3363.71	12
3364.92†	1+	0–1	Fe II	3365.41	1
3368.11	7v+	1	c Fe II	3366.96	3
		7	Cr II	3367.42	12
			c Cr II	3368.05	150
3369.10	4+	2	Cr II	3368.73	10
			c Cr II	3369.05	18
			Ti II	3369.22	2
			c Fe II	3369.35	3
3370.91	2+	1	Fe I	3370.80	10
3372.50	6+	0–1	Cr II	3372.13	15
			Ti II	3372.23	10?
		7	c Ti II	{3372.77	100
				{3372.86	
3374.56	4+	3	Ni II	3373.98	4
			Ti II	3374.35	8
3376.49	4+	2	Cr II	3376.27	10
		1–0	Cr II	3376.72	5
3377.49	0–1	1–0	Cr II	3377.36	5
3378.37	3+	4	Cr II	3378.34	25
3379.91	8n+	6n	Cr II	3379.37	30
			c Cr II	3379.83	60
			c Ti II	{3380.26	30
				{3380.31	
		.....	(Sr II	3380.75	50)
		1–0	(Fe II	3381.00	4)
3382.69	6+	4	Cr II	3382.68	60
3383.79	6+	6	Ti II	3383.77	125

* When the intensity is given as two numbers within parenthesis, the identification is from the *M.I.T. Tables*. The first number in the parenthesis is the arc intensity; the second, the spark intensity.

† Unidentified in α Cygni.

TABLE 1—*Continued*

λ	Int.	Int. (α Cyg)	Identification			λ	Int.	Int. (α Cyg)	Identification		
			Element	λ	Int.*				Element	λ	Int.*
3385.38...	0–1	.....	.....	.....	.....	3440.79...	5+	1	c *Fe* I	3440.63	150
3386.62...	0–1	.....	*Fe* II	3386.45	1				*Fe* I	3441.02	75
			Fe II	3386.72	2	3441.99...	5+	8	c *Mn* II	3441.98	100
3387.84...	7+	5	*Cr* II	3387.73	5				*Fe* II	3442.24	3
			c *Ti* II	3387.85	50	3444.16...	4	.....	*Fe* I	3443.89	50
			Fe II	3388.13	2			4	*Ti* II	3444.33	30
3389.17...	1n	.....	*Ti* II	3388.76	8			.....	*Cr* II	3444.34	4
3391.33...	4+	4	*Fe* II	3391.30	1	3445.17...	2	.....	*Cr* II	3445.04	5
			c *Cr* II	3391.43	35			.....	*Fe* I	3445.13	20
3392.99...	4+	.....	*Fe* I	3392.63	15	3446.58...	2	2	(*K* I	3446.72	8)
		3	c *Cr* II	3393.00	35	3449.31...	3++	.....	*Co* I	3449.18	60
3394.38...	6+	6nv	*Cr* II	3393.86	30			.....	*Co* I	3449.45	60
			Cr II	3394.32	35	3450.70...	0–1	.....	*Fe* I	3450.34	10
			Ti II	3394.55	40			0–1	*Cr* II	3450.84	3
3395.76...	3+	2	*Fe* II	3395.34	4	3452.77...	2bd	-1	*Ti* II	3452.48	4
			Cr II	3395.62	20			.....	*Co* I	{3453.49 3453.57}	200
3398.29...	1	2	*Fe* II	3398.36	4	3455.22...	2	2	*Ni* II	3454.17	5
3399.46...	4	.....	*Fe* I	3399.36	15			1	c *Cr* II	3454.98	35
		1n	c *Cr* II	3399.54	18	3457.80...	2n	3	*Ti* II	3456.40	20
3402.46...	2	3	*Ti* II	3402.42	8				*Fe* II	3456.93	5
			c *Cr* II	3402.43	25			2	*V* II	3457.15	300
3403.37...	6+	6	*Cr* II	3403.32	100				*Cr* II	3457.62	30
3404.85...	4n+	.....	*Co* I	{3405.09 3405.17}	150	3460.18...	5v+	.....	*Cr* II	3459.29	25
								.....	*Mn* II	3460.04	8
3407.18...	4+	4	*Ti* II	3407.21	3			6	c *Mn* II	3460.31	75
			Ni II	3407.32	8	3461.52...	3+	4	*Ti* II	3461.50	20
		.....	*Fe* I	3407.47	20	3462.85...	2+	.....	*Cr* II	3462.73	6
3408.77...	7r	6	*Cr* II	3408.77	150			.....	*Mn* II	3462.88	5
								.....	*Mn* II	3463.33	6
3414.37...	2nn	.....	*Fe* I	3413.14	15	3464.26...	2+	1n	*Fe* II	3463.97	1
		0–1	*Fe* II	3414.14	2				*Cr* II	3464.02	4
		.....	(*Ni* I	3414.78	150)			.....	*Mn* II	3464.04	7
		4	(*Fe* II	3416.02	5)			.....	(*Sr* II	3464.48	50)
									Fe II	3464.50	3
3418.02...	1	.....	*Fe* I	3417.87	12	3465.79...	2+	3	*Ti* II	3465.65	3
		0–1	*Fe* II	3418.03	pr			.....	*Co* I	3465.77	100
3421.26...	5+	7	*Cr* II	3421.20	75			.....	*Fe* I	3465.88	60
3422.71...	6+	7	*Cr* II	3422.74	125	3467.29...	2+	.....	*Cr* II	3467.09	pr
3424.20...	1	.....	*Fe* II	3424.17	pr	3468.77...	3+	4	*Fe* II	3468.68	8
		.....	*Fe* I	3424.30	10	3472.01...	3bd+	4	(*Ni* II	3471.35	2)
3426.75...	3n+	2	(*Fe* II	3425.58	3)				c *Cr* II	3472.07	25
		.....	*Cr* II	3426.13	8						
		.....	*Fe* I	3427.13	20	3474.12...	7++	6	*Fe* II	3473.83	2
3428.50...	3+	1n	*Fe* II	3428.63	pr			.....	*Co* I	{3473.97 3474.06}	100
			Cr II	3428.94	7				c *Mn* II	3474.04	50
									c *Mn* II	3474.12	40
3430.45...	2+	0–1	*Fe* II	3430.15	pr	3475.40...	6++	2	c *Cr* II	3475.13	20
			Cr II	3430.42	3				*Fe* II	3475.25	pr
3431.97...	3+	.....	*Co* I	3431.59	50			.....	c *Fe* I	3475.46	70
		.....	*Co* I	3433.03	60				*Fe* II	3475.74	pr
3433.44...	8++	8	*Cr* II	3433.30	75	3476.98...	4++	.....	*Fe* I	3476.71	40
								4	*Ti* II	3477.19	15
3435.98...	2+	3	*Fe* II	3436.11	5	3478.45...	2	1–0	*Cr* II	3478.17	3
3438.34...	2bd+	.....	(*Zr* II	3438.24	100)	3479.73...	2	1	*Fe* II	3479.91	2
		3	*Mn* II	3438.98	20						

TABLE 1—*Continued*

λ	Int.	Int. (α Cyg)	Identification		
			Element	λ	Int.*
3482.74	6+	6	*Fe* II	3482.43	2
			Cr II	3482.58	12
			e *Mn* II	3482.91	40
3484.23	2	1	e *Cr* II	3484.15	20
			Fe II	3484.35	1
3485.62	1n	1–0	*V* II	3485.92	250
3488.78	8++	5	*Fe* II	3487.99	3
			e *Mn* II	3488.68	40
3490.83	4++	3	e *Fe* I	3490.60	100
			Ti II	3491.06	10
3493.14	4n	.....	(*Ni* I	3492.98	150)
		8	*V* II	3493.16	150
			Fe II	3493.47	10
		.....	(*Cr* II	3494.52	4)
		1	(*Fe* II	3494.67	5)
3495.49	8++	8	*Cr* II	3495.37	25
		.....	*Cr* II	3495.56	20
			Fe II	3495.62	4
			Mn II	3495.83	40
3497.45	7++	6nv	e *Mn* II	3496.81	20
			V II	3497.03	200
			e *Mn* II	3497.54	25
			Fe II	3497.72	pr
		.....	e *Fe* I	3497.84	40
3500.47	3	2	*Fe* II	3499.88	4
		.....	(*Ti* II	3500.34	2)
3502.57	1	.....	*Co* I	{3502.26 3502.33}	100
3503.53	1	1–0	*Cr* II	3503.36	3
			Fe II	3503.47	2
3504.79	3+	5	*V* II	3504.43	400
			e *Ti* II	{3504.88 3504.92}	80
3506.62	1	.....	*Co* I	3506.33	80
3508.06	1	2n	*Fe* II	3507.39	3
			Fe II	3508.21	1
3510.86	2++	4	*Ti* II	3510.85	60
3511.78	2++	3	*Cr* II	3511.84	35
3513.63	0–1	5	*Cr* II	3513.03	10
			Fe I	3513.83	30
			Ni II	3513.94	8
3515.22	0–1	.....	*Ni* I	3515.07	150
		.....	*Fe* II	3515.82	2
3517.28	0–1	2	*V* II	3517.30	800
3518.49	2+	.....	*Co* I	3518.35	50
		.....	*Cr* II	3518.62	3
3520.06	2+	3	*V* II	3520.02	120
			Ti II	3520.26	20
3521.44	1	.....	*Fe* I	3521.27	25
3524.40	2+	1n	*Ni* I	3524.54	200
			V II	3524.71	200
3526.30	4++	1	*Fe* I	3526.04	20
		.....	*Fe* I	3526.17	15
		.....	*Co* I	3526.85	100
3527.66	2	.....	*Fe* II	3527.17	1
		.....	(*Fe* I	3527.80	4)
3529.78	2	.....	*Co* I	3529.82	80
		.....	*Fe* I	3529.82	6
3532.62	3n+	2	(*V* II	3530.77	500)
		.....	*Mn* I	3532.00	50
		.....	*Mn* I	3532.12	50
		.....	*Fe* II	3532.65	2
		1	*Fe* I	3533.20	10
3535.75	2	3	e *Ti* II	3535.41	40
			Fe II	3535.63	2
3538.22	2++	1	(*Fe* II	3537.50	1)
			(*V* II	3538.24	50)
3540.98	2++	1n	*Fe* I	3541.10	15
3545.15	3++	3	*V* II	3545.19	1000
3547.71	3++	.....	*Mn* I	3547.80	50
		.....	*Mn* I	3548.03	40
		.....	*Mn* I	3548.19	30
3554.92	3++	1	e *Fe* I	3554.94	40
			Fe II	3555.08	pr
3556.84	3++	3	*V* II	3556.80	1500
3558.43	3++	2	*Fe* I	3558.53	30
3561.33	0–1+	2n	*Ti* II	3561.58	3
3565.82	7bd++	.....	*Cr* II	3565.31	5
		2	*Fe* I	3565.38	60
		3	*Ti* II	3565.97	6
			Fe II	3566.05	2
			Fe II	3566.15	3
			V II	3566.18	200
3570.07	7++	.....	*Mn* I	3569.51	60
		.....	*Mn* I	3569.82	40
		.....	*Mn* I	3570.05	20
		2	e *Fe* I	3570.14	100
		.....	*Fe* I	3570.28	20
3571.84	2	.....	*Cr* II	3571.37	3
		.....	*Fe* II	3572.02	6
3573.91	2	2	*Ti* II	3573.74	20
3574.92	2	.....	(*V* II	3574.34	60)
3576.50	2	7	*Ni* II	3576.76	3
3578.48	4++	1–0n	*Cr* I	3578.69	200
3581.33	4++	5	*Fe* I	3581.21	250
3585.37	9++	10	e *Cr* II	3585.31	60
		.....	*Fe* I	3585.34	30
			e *Cr* II	3585.54	40
		.....	*Fe* I	3585.72	20
3587.14	1	.....	*Fe* I	3586.99	30
		2	*Ti* II	3587.15	12
3589.18	1	3	*V* II	3589.75	1000
3591.92	1	2	*V* II	3592.01	800
3593.48	4++	1	*V* II	3593.32	600
			e *Cr* I	3593.50	160
3596.31	2	3	*Ti* II	3596.06	50
3599.01	0–1	0–1	(*Y* II	3600.74	300)
3601.81	1	.....	*Zr* I	3601.20	400
3603.73	6	.....	*Fe* I	3603.21	10
		6	e *Cr* II	3603.61	20

TABLE 1—*Continued*

λ	Int.	Int. (α Cyg)	Identification			λ	Int.	Int. (α Cyg)	Identification		
			Element	λ	Int.*				Element	λ	Int.*
			c *Cr* II	3603.80	40	3669.82...	2+	4	*V* II	3669.41	300
			c *Cr* II	3603.86	20				(*H* 25	3669.47	.....)
								.....	*Fe* I	3669.52	10
3605.30...	4+	1n	c *Cr* I	3605.34	140						
			Fe I	3605.48	15	3677.79...	6	4	*Cr* II	3677.69	40
									c *Cr* II	3677.86	50
3608.57...	4++	3n	*Cr* II	3608.66	3				*Cr* II	3677.93	30
			c *Fe* I	3608.87	100						
						3679.66...	2	6	*H* 21	3679.36	.....
3610.45...	2+	.....	*Fe* I	3610.17	20			.....	*Ti* II	3679.69	pr
								.....	*Fe* I	3679.92	40
3613.25...	4r+	4	*Cr* II	3613.21	20						
		.....	*Cr* II	3613.26	15	3682.68...	2	8	c *H* 20	3682.81	.....
		2	(*Fe* II	3614.87	5)			.....	*Fe* I	3683.09	10
3618.77...	4+	3n	c *Fe* I	3618.78	125	3685.24...	4s+	5	*Ti* II	3685.20	250
			V II	3618.92	200						
		.....	*Ni* I	3619.40	150	3687.16...	7	.....	*Cr* II	3686.67	20
								9	c *H* 19	3686.83	.....
3621.56...	4	5	*V* II	3621.20	150			.....	*Fe* I	3687.47	40
			c *Fe* II	3621.27	6						
		.....	*Fe* I	3621.47	15	3691.53...	7	10	*H* 18	3691.56	.....
3623.93...	1	1	*Zr* I	3623.92	300	3693.97...	1	0–1	*Fe* I	3694.03	20
									(*Yb* II	3694.20	200)
3624.83...	4+	4	*Ti* II	3624.84	70						
		.....	*Fe* II	3624.89	5	3697.20...	11	12	c *H* 17	3697.15	.....
								.....	(*Cr* II	3698.00	35)
3627.63...	1	1	*Fe* II	3627.17	1						
						3703.97...	11	15	*H* 16	3703.86	.....
3631.59...	7+	8	*Fe* I	3631.48	125						
			Cr II	3631.49	50	3705.73...	2	.....	c *Fe* I	3705.58	100
			Cr II	3631.72	40			6	(*Ca* II	3706.04	10)
									(*Ti* II	3706.22	20)
3632.85...	1	.....	*Fe* II	3632.29	3						
						3707.55...	1	.....	*Fe* I	3707.83	20
3634.61...	2	2n	*Cr* II	3634.04	10						
			Fe II	3634.89	5	3709.42...	3	2n	c *Fe* I	3709.26	75
									(*Y* II	3710.29	500)
3636.57...	2	.....	*Fe* II	3636.61	pr						
						3712.17...	12	15	c *H* 15	3711.97	.....
3638.16...	1	1	*Fe* I	3638.31	12			5	(*Cr* II	3712.97	35)
3639.66...	2	.....	(*Fe* I	3640.40	15)	3715.33...	3	5	*Cr* II	3715.19	20
									Cr II	3715.45	20
3641.59...	2+	4	*Fe* II	3641.22	pr				*V* II	3715.48	1200
			c *Ti* II	3641.34	100						
						3720.12...	2	3	c *Fe* I	3719.95	250
3643.12...	2+	2	*Cr* II	3643.22	10				*Fe* II	3720.17	pr
3644.75...	2+	2	*Cr* II	3644.70	10	3722.17...	12	15	c *H* 14	3721.94	.....
								.....	(*Fe* I	3722.59	50)
3647.65...	4++	2	*Cr* II	3647.40	8						
			c *Fe* I	3647.85	100	3727.40...	4	4	*V* II	3727.35	1000
									Cr II	3727.37	40
3649.85...	3++	.....	*Fe* I	3649.51	12				*Fe* I	3727.64	50
		1	c *Cr* II	3650.37	40						
						3734.76...	15	15	c *H* 13	3734.37	.....
3651.58...	3++	.....	*Fe* I	3651.48	20				(*Fe* I	3734.88	300)
		1	*Cr* II	3651.68	12						
						3743.63...	4	2	*Fe* I	3743.37	20
3653.87...	2+	.....	(*Ti* I	3653.50	100)	3745.55...	2	4	*Fe* II	3745.36	pr
									c *Fe* I	3745.58	100
3655.90...	2+	.....	.....	.....	.....				*V* II	3745.81	800
								.....	*Fe* I	3745.91	40
3657.85...	3+	0–1	*Cr* II	3658.19	20						
						3749.99...	16	.....	(*Fe* II	3748.49	8)
3659.66...	2+	2	*Ti* II	3659.76	60			.....	(*Fe* I	3749.50	200)
								15	c *H* 12	3750.15	.....
3661.19...	1	2	*V* II	3661.38	200						
						3757.54...	2r	5	*Ti* II	3757.69	30
3662.54...	1	2	c *Ti* II	3662.24	40				c (*Fe* I	3758.25	150)
		.....	(*Zr* I	3663.70	300)						
						3759.18...	2	6	*Ti* II	3759.30	200
3664.82...	1	2	(*H* 28	3664.68	.....)				*Fe* II	3759.46	6
			Cr II	3664.95	30						
						3761.65...	5	6	c *Ti* II	3761.32	200
3666.55...	2	2	(*H* 27	3666.10	.....)				*Cr* II	3761.69	7
									Ti II	3761.88	15
3667.96...	0–1	2	(*H* 26	3667.68	.....)				*Cr* II	3761.90	8

TABLE 1—*Continued*

λ	Int.	Int. (α Cyg)	Identification		
			Element	λ	Int.*
3763.80...	5+	4	c *Fe* I	3763.81	100
			Fe II	3764.11	pr
3765.63...	2	2	*Cr* II	3765.62	8
3770.56...	17	7	*H* 11	3770.63	.....
3781.49...	1	1	*Fe* II	3781.51	1
3783.34...	2	5	*Fe* II	3783.35	4
3786.10...	3+	1	(*Ti* II	3786.33	pr)
3787.99...	3+	1	(*V* II	3787.24	150)
			c *Fe* I	3787.89	50
			(*Y* II	3788.70	200)
3798.03...	18	20	*H* 10	3797.90	.....
3806.85...	2	2nn	*Fe* I	3806.70	10
3813.51...	4bd	1	c *Fe* I	3812.96	40
			Ti II	3813.40	2
			Cr II	3814.00	12
	.....	4	c *Fe* II	3814.12	4
			(*Ti* II	3814.60	4)
3815.81...	2	3	*V* II	3815.38	200
			c *Fe* I	3815.85	100
3821.07...	4	4	c *Fe* I	3820.44	250
		.....	(*Fe* I	3821.19	10)
3824.37...	4	.....	*Fe* I	3824.45	50
		4	(*Fe* II	3824.91	4)
3835.47...	19	20	*H* 9	3835.39	.....
3840.83...	2	3	c *Fe* I	3840.45	80
			c *Fe* I	3841.06	80
			Fe II	3841.36	pr
3845.17...	1	.....	*Co* I	3845.47	60
3846.69...	2	.....	*Fe* I	3846.81	8
3849.73...	4+	.....	*Ni* II	3849.58	2
		3	c *Fe* I	3849.98	40
3852.50...	2	.....	*Fe* I	3852.58	6
3854.28...	2	3	(*Si* II	3853.67	3)
3856.06...	3	5	*Si* II	3856.03	8
			Fe I	3856.38	50
3859.84...	3+	3	c *Fe* I	3859.92	300
			Fe II	3860.11	pr
3862.34...	1	6	*Si* II	3862.60	6
3863.84...	2+	0–1	*Fe* II	3863.41	1
			(*V* II	3863.81	60)
			Fe II	3863.95	1
3865.87...	4	2	*Fe* I	3865.54	30
			c *Cr* II	3865.59	75
3867.25...	1n	.....	*Cr* II	3866.54	7
		.....	*Fe* I	3867.23	7
3872.50...	3+	4	*Fe* I	3872.51	60
3874.81...	2	.....	.....	.....	.....
3878.45...	7+	4n	c *Fe* I	3878.03	60
			c *Fe* I	3878.58	100
			V II	3878.72	300
3889.01...	20	20	*H* 8	3889.05	.....
3898.06...	3+	.....	*Fe* I	3897.90	8
		.....	*Fe* I	3898.01	10
		.....	(*V* II	3899.14	200)
3900.43...	3++	5	*Ti* II	3900.54	70
3903.29...	3++	.....	*Fe* I	3902.95	20
		2	*V* II	3903.27	250
3905.89...	5++	.....	(*Si* I	3905.53	10)
		4	*Cr* II	3905.64	25
			Fe II	3906.04	5
3908.90...	1+	.....	*Cr* I	3908.76	25
3911.47...	2+	.....	c *Mn*	3911.12	(20–)
		.....	*Cr* II	3911.32	3
		.....	c *Mn*	3911.42	(15–15)
		.....	(*Sc* I	3911.83	100)
3913.66...	3	5	c *Ti* II	3913.47	60
		3	(*V* II	3914.33	250)
			(*Fe* II	3914.48	2)
3916.40...	2	2	*V* II	3916.42	200
3918.56...	4++	1	*Mn*	3918.32	(40–50)
		.....	*Cr* I	3919.16	35
3920.65...	4+	1	*Fe* I	3920.27	20
		.....	*Cr* I	3921.05	20
3922.89...	1+	1	*Fe* I	3922.93	25
3925.74...	3++	.....	(*Fe* I	3925.65	4)
		1	(*Mn*	3926.47	(40–50))
3927.96...	3++	1	*Fe* I	3927.94	30
3930.02...	2++	3	*Fe* I	3930.31	25
3932.16...	1	2	*Ti* II	3932.02	2
3933.52...	6	15	*Ca* II	3933.68	400
3935.79...	2+(+)	.....	*Fe* I	3935.81	8
		3	c *Fe* II	3935.94	6
3937.39...	1	.....	*Mn*	3936.76	(25–50)
3938.63...	4	5nr	*Fe* II	3938.29	2
			Fe II	3938.97	4
3941.71‡...	4+	1–0n	(*Cr* I	3941.50	20)
3944.44...	4	.....	(*Al* I	3944.02	10)
3947.08...	4+	1	*O* I	3947.33	10
			O I	3947.51	7
			O I	3947.61	4
3952.83...	4+	2	(*V* II	3951.97	500)
			Mn	3952.84	(60–75)
3956.31...	4n+(+)	2	*Fe* I	3956.69	12
3969.98...	20	.....	(*Ca* II	3968.49	350)
		20	c *He*	3970.08	.....
3976.82...	3+(+)	0	*Cr* I	3976.70	25
		.....	*Mn*	3977.08	(50–100)
3978.02...	1	0	*Fe* I	3977.75	12
3979.68...	2+(+)	4	*Cr* II	3979.51	20

‡ Unidentified in α Cygni.

TABLE 1—*Continued*

λ	Int.	Int. (α Cyg)	Identification		
			Element	λ	Int.*
3981.83...	3+	0	*Fe* II	3981.61	pr
			Fe I	3981.78	7
		.....	c *Mn*	3982.17	(12–25)
		.....	c *Mn*	3982.58	(20–30)
3984.15...	2+(+)	0	*Cr* I	3983.92	20
			Fe I	3983.97	10
		.....	*Mn*	3984.18	(20–20)
3985.86...	2+	.....	*Mn*	3985.24	(75–100)
		.....	*Mn*	3986.83	(40–75)
3990.48...	3n	.....	(*Cr* I	3991.13	20)
3994.40¶...	3	.....	.....	.....	.....
3997.10...	4	1	*V* II	3997.13	200
		.....	*Mn*	3997.21	(12–25)
		.....	*Fe* I	3997.40	15
4002.44...	4+(+)	3	*Fe* II	4002.07	2
		2	*Fe* II	4002.55	3
		1	(*Cr* II	4003.33	25)
4005.06...	5	1	*Fe* I	4005.26	25
		4	*V* II	4005.71	800
4007.17...	0–1	0	*Cr* II	4007.04	pr
			Fe I	4007.28	6
		1	(*Fe* II	4007.72	pr)
4012.51...	4++(+)	6	*Ti* II	4012.39	4
			Fe II	4012.47	1
			c *Cr* II	4012.50	30
4017.75...	4	.....	*Mn*	4018.10	(80–60)
4020.36...	0–1	.....	(*Sc* I	4020.40	75)
4022.03...	4r+	0	*Fe* I	4021.87	12
		3	(*V* II	4023.39	600)
4024.99...	4+	5	c *Fe* II	4024.55	5
		2	(*Ti* II	4025.14	2)
4027.48...	1	5	(*Ti* II	4028.35	7)
4030.55...	4++(+)	0	*Cr* II	4030.28	pr
			c *Mn* I	{4030.73 / 4030.80}	200
4032.84...	3+(+)	3	*Fe* II	4032.95	3
			c *Mn* I	4033.08	150
4035.25...	0–1	1n	*Mn* I	4034.49	100
		3	*V* II	4035.63	400
4037.60...	0–1	2n	*Cr* II	4038.03	25
4043.95...	2+	2	*Fe* II	4044.01	pr
		.....	(*K* I	4044.15	8)
4045.74...	4(+)	5	*Fe* I	4045.83	60
4048.97...	4++(+)	3	*Fe* II	4048.83	3
			Cr II	4049.14	18
4051.91...	2+(+)	3	*Cr* II	4051.97	12
4054.01...	2+	3	*Ti* II	4053.83	8
		3	*Cr* II	4054.11	8
4058.37...	1	1	(*Fe* I	4058.23	4n)
		.....	*Cb* I	4058.99	2000
4063.41...	5++(+)	3	*Fe* I	4063.61	45
4066.96...	5++(+)	5	c *Ni* II	4067.05	30
			Cr II	4067.05	pr
4071.55...	5bd	2	*Cr* II	4070.90	10
		3	c *Fe* I	4071.75	40
		1	(*Cr* II	4072.56	4)
4077.26...	5	2n	*Cr* II	4076.87	3
			c *Fe* II	4077.16	?3
		.....	*Cr* II	4077.50	4
		4	c *Sr* II	4077.73	400
4079.68...	2	.....	*Cb* I	4079.73	1000
		0	(*Fe* I	4079.85	4)
4101.83...	20	20	*Hδ*	4101.75	.....
4110.77...	3++(+)	3	*Cr* II	4111.01	18
4113.11...	3+	0	(*Cr* II	4113.24	5)
4118.61...	3+	0	*Fe* I	4118.56	15
4122.50...	3++(+)	5	*Fe* II	4122.64	4
4128.14...	5++(+)	8	*Si* II	4128.05	8
		3	*Fe* II	4128.74	3
4132.35...	3v+(+)	8	c *Si* II	4130.88	10
		0	c *Fe* I	4132.07	25
		1	*Cr* II	4132.41	7
4137.78...	3++	0	.....	.....	.....
4143.19...	4++(+)	1	*Fe* I	4143.42	15
		2	c *Fe* I	4143.88	30
4146.55...	4n+	2	*Cr* II	4145.77	25
		0	(*Cr* II	4146.45	1)
		.....	(*Cr* II	4146.50	pr)
4154.19...	3v+(+)	.....	*Cr* I	4153.81	20
		.....	*Fe* I	4153.91	10
		0	*Cr* II	4154.29	pr
			Fe I	4154.51	12
4159.10...	0–1	.....	(*Fe* I	4158.80	4)
4161.30...	0–1	2n	*Cr* II	4161.05	2
			Cr II	4161.27	pr
			(*Ti* II	4161.52	1)
			Cr II	4161.56	pr
4164.08...	2	.....	*Cr* I	4163.66	20
		5	c *Ti* II	4163.66	40
4172.16...	9bd+(+)	4	c *Ti* II	4171.91	30
		.....	*Cr* II	4171.92	3
		1	*Cr* II	4172.60	2
		8	c *Fe* II	4173.45	8
4175.79...	1+	1n	*Fe* I	4175.65	10
4179.14...	5++(+)	8	c *Fe* II	4178.86	8
		0	*Cr* II	4179.43	12
4181.99...	2++(+)	.....	*Fe* I	4181.76	15
		1	(*V* II	4183.44	250)
4184.43...	2++	.....	(*Fe* I	4184.90	10)
4187.41...	4++	1	*Fe* I	4187.05	20
		2	*Fe* I	{4187.79 / 4187.86}	20
4191.51...	2	.....	c *Fe* I	4191.44	15
		0	(*Ni* II	4192.02	1)
4195.69...	4++(+)	1	(*Fe* I	4195.34	5)
		.....	*Cr* II	4195.41	10
4198.35...	4+	0	*Fe* I	4198.34	20

¶ Measured on plate taken on July 13, 1943, at phase 3.53 days.

TABLE 1—*Continued*

λ	Int.	Int. (α Cyg)	Identification			λ	Int.	Int. (α Cyg)	Identification		
			Element	λ	Int.*				Element	λ	Int.*
4201.90	2+(+)	1	*Fe* I	4202.04	30	4300.07	3	1	(*Fe* I	4299.25	18)
			V II	4202.35	150			8	c *Ti* II	4300.06	60
4205.27	1n+	1n	*V* II	4205.08	250	4303.28	3nn	4	*Ti* II	4301.93	15
			Fe II	4205.48	pr			9	c *Fe* II	4303.17	8
4209.89	3++	.....	*Fe* I	{4210.34	15	4308.01	3n	4	*Ti* II	4307.91	40
				4210.40}					*Fe* I	4307.91	35
4212.88	1+	.....	.....	.....	.....	4313.96	4nn+(+)	5	*Ti* II	4312.88	35
4215.67	3++	3	c *Sr* II	4215.55	300				*Fe* II	4313.03	1
		.....	(*Cr* II	4215.77	2)			4	*Fe* II	4314.29	4
		.....	(*Fe* I	4216.19	8)			4	*Ti* II	4314.98	40
									Fe I	4315.10	10
4217.77	2+	.....	*Cr* I	4217.56	15	4320.13	4n+	1	(*Fe* II	4319.72	1)
4219.42	1	0	*Fe* I	4219.36	12			3	(*Ti* II	4320.96	1)
4222.43	1	0	*Fe* I	4222.22	12	4325.45	5+	.....	*Cr* I	4325.08	15
								3	c *Fe* I	4325.76	35
4224.74	4++	3	*Cr* II	4224.85	20	4340.52	20	20	*Hγ*	4340.48	.....
4227.52	4+	2	*Fe* I	4227.44	30						
		.....	*Zr* I	4227.76	200	4344.50	1	2n	*Cr* I	4344.51	40
4233.33	6++(+)	12	c *Fe* II	4233.17	11	4346.75	2	.....	*Cr* I	4346.83	10
		.....	*Cr* II	4233.25	10						
		.....	*Fe* I	4233.61	18	4348.63	2	.....	(*Mn* II	4348.49	1)
								.....	*Fe* II	4348.57	pr
4235.82	3++	1	*Fe* I	4235.95	25	4351.91	7r++(+)	10	c *Fe* II	4351.76	9
4239.53	3++(+)	.....	*Zr* I	4239.31	150			.....	*Cr* I	4351.77	60
									(*Mg* I	4351.92	30)
4242.44	3+(+)	7	*Cr* II	4242.38	30	4357.59	3+	2	*Fe* II	4357.57	4
4244.79	1	.....	*Fe* II	4244.58	pr						
		1	*Ni* II	4244.81	1	4359.59	2+	0n	*Cr* I	4359.63	20
4247.41	3+	.....	*Fe* I	4247.43	12	4361.36	2+	2	*Fe* II	4361.25	2
4251.26	3r++(+)	0	*Fe* I	4250.13	25	4363.22	3+	1	(*Cr* II	4362.93	3)
		1	*Fe* I	4250.80	25						
		3	*Cr* II	4252.62	10	4365.22	1	0	(*Mn* II	4365.29	1)
4254.41	3++(+)	2	*Cr* I	4254.35	500	4367.94	3+	2	*Ti* II	4367.68	15
								1	*Fe* II	4368.26	1
									O I	4368.30	10
4260.74	3bd+	4	*Fe* II	4258.16	3						
		2	*Fe* I	4260.49	35	4369.65	2+	3	*Fe* II	4369.40	2
		5	*Cr* II	4261.92	20				*Fe* I	4369.77	7
4269.71	3v++(+)	2	*Cr* II	4269.28	10	4371.39	2	.....	*Cr* I	4371.29	20
4271.96	3++(+)	1	*Fe* I	4271.17	20	4374.47	3n+	2	(*Ti* II	4374.83	1)
		2	*Fe* I	4271.78	35				*Y* II	4374.95	300
4273.95	2+(+)	5	*Fe* II	4273.32	3	4377.03	1	.....	.....	.....	.....
		1n	*Cr* I	4274.81	400						
						4379.80	1n	.....	(*V* I	4379.24	150)
4275.74	3+	4	*Cr* II	4275.57	30	4383.92	5	5	c *Fe* I	4383.56	45
4282.37	1+(+)	1	*Fe* I	4282.41	12			6	(*Mg* II	4384.64	8)
			Mn II	4282.50	3						
4284.26	3+(+)	.....	*Mn*	4284.08	(80–20)	4385.27	5	.....	*Cr* I	4384.99	20
		3	*Cr* II	4284.21	20			8	c *Fe* II	4385.38	7
						4388.48	0–1n	0	*Fe* I	4388.42	10
4289.82	3+(+)	5	*Cr* I	4289.73	350			.....	*Fe* II	4388.59	pr
			Ti II	4290.23	50						
						4391.54	2n	3	(*Mg* II	4390.59	10)
4291.96	1+	0	(*Fe* I	4291.46	4)						
		0	(*Mn* II	4292.28	2)	4395.45	4	7	c *Ti* II	4395.04	60
								1	(*Ti* II	4395.85	2)
4294.74	0–1	7	*Fe* I, *Ti* II?	{4294.05	15						
				4294.15}		4399.57	3	4	*Ti* II	4399.78	35
4296.15	3	.....	*Cr* I	4295.76	15						
		7	c *Fe* II	4296.58	6	4401.66	0–1	.....	.....	.....	.....

TABLE 1—*Continued*

λ	Int.	Int. (α Cyg)	Identification		
			Element	λ	Int.*
4403.10	3+	2	*Fe* II	4402.88	2
4404.87	3+	3	*Fe* I	4404.76	30
4407.66	0-1	.....	(*Ti* II	4407.68	1)
			Fe I	4407.72	5
4410.99	0-1	2	*Ti* II	4411.08	15
4414.74	2nn	2	*Fe* I	4415.14	20
4416.88	3r	6	*Fe* II	4416.82	7
		4	*Ti* II	4417.73	40
4422.72	4	.....	(*Fe* I	4422.58	6)
4427.71	3	0	*Fe* I	4427.31	10
		1n	*Mg* II	4428.00	7
4430.29	3	.....	(*Fe* I	4430.62	6)
4432.05	1	0	(*Fe* II	4431.63	1)
4433.82	1	2	*Mg* II	4433.99	8
4435.67	1	.....	.....	.....	.....
4444.04	4	7	*Ti* II	4443.81	50
4447.89	0-1	0	*Fe* I	4447.73	9
4450.17	1	4	*Ti* II	4450.49	10
4451.67	1	3	*Fe* II	4451.55	4
4455.06	1	3	*Fe* II	4455.26	3
4456.98	0-1	.....	.....	.....	.....
4459.19	1	.....	*Fe* I	4459.14	10
4461.75	4(+)	3	*Fe* I	4461.66	8
			c *Mn*	4462.02	(40-60)
4464.48	1	2	(*Ti* II	4464.46	1)
4465.94	1	0	*Fe* I	4466.55	12
4468.76	3r	5	c *Ti* II	4468.50	50
		0	(*Fe* I	4469.39	5n)
4472.93	0-1	3	*Fe* II	4472.92	2
4476.04	2	.....	*Fe* I	4476.02	10
4478.18	0-1	.....	(*Mn* II	4478.74	1)
4481.15	12	16	*Mg* II	{4481.14 4481.34}	100
4484.24	0-1	.....	*Fe* I	4484.23	4
4485.67	0-1	.....	(*Fe* I	4485.69	2n)
4487.68	0-1	3	*Ti* II	4488.33	15
4488.99	4	5	*Fe* II	4489.19	4
4491.54	1	6	*Fe* II	4491.40	5
4494.49	1	.....	*Fe* I	4494.58	12
4501.22	2	5	*Ti* II	4501.28	40
4504.01	1	.....	.....	.....	.....
4507.93	4bd	7	*Fe* II	4508.28	8
4512.12	1	0	*Cr* II	4511.82	pr
		.....	*Cr* I	4511.90	10
4515.43	4	7	*Fe* II	4515.34	7
4518.19	0-1	1n	.....	.....	.....
4520.23	3	6	*Fe* II	4520.23	7
4522.63	4(+)	7	*Fe* II	4522.63	9
4525.14	1	0n	*Fe* I	4525.15	5n
4526.66	1	0	*Fe* II	4526.58	pr
4529.26	1n	0	*V* II	4528.51	300
			Fe I	4528.63	18
4531.13	1n	.....	*Fe* I	4531.16	8
4533.96	3(+)	7	c *Ti* II	4533.97	30
			Fe II	4534.17	2
4536.28	1n	.....	*Cr* I	4535.71	15
4540.79	2bd	4	*Cr* I	4540.71	10
			c *Fe* II	4541.52	4
4545.19	1n	0	*Cr* I	4545.96	20
4549.58	10(+)	15	*Fe* II	4549.21	4
			c *Fe* II	4549.47	10
			c *Ti* II	4549.62	60n
4555.64	4v+(+)	4	*Cr* II	4555.02	20
		6	c *Fe* II	4555.89	8
4558.68	5+(+)	6	*Cr* II	4558.66	100
4563.64	1	5	*Ti* II	4563.77	30
4565.46	1	1	*V* II	4564.59	200
		2	*Cr* II	4565.78	10
4572.03	1	5	*Ti* II	4571.98	50n
4576.51	1	4	*Fe* II	4576.33	4
4579.88	1	1	*Fe* II	4579.52	1
		2n	*Cr* I	4580.06	20
			Fe II	4580.06	1
4583.69	4v	4	*Fe* II	4582.84	3
		9	c *Fe* II	4583.83	11
4588.21	4+(+)	5	*Cr* II	4588.22	75
4590.01	0-1	3	*Cr* II	4589.89	3
4592.18	0-1	4	*Cr* II	4592.09	20
4595.80	0-1	3	*Fe* II	4595.68	pr
4616.57	3	.....	*Cr* I	4616.13	25
		4	*Cr* II	4616.64	18
4618.89	3	6	*Cr* II	4618.83	35
4625.82	2n	1	*Fe* II	4625.91	1
		.....	*Cr* I	4626.18	20
4629.21	3	9	c *Fe* II	4629.34	7
		.....	*Ti* II	4629.34	15
4634.86	3bd	5	*Cr* II	4634.11	25
		4	*Fe* II	4635.33	5
4637.83	0-1	.....	*Fe* I	4637.51	3
		1	*Fe* I	4638.02	3

NOTES TO TABLE 1

The tables below give approximate conversions from stellar to laboratory intensities for some of the elements present in ϵ Ursae Majoris. Near the head of the Balmer series, where many lines are almost lost in the wings of the hydrogen lines, these conversions are sometimes considerably in error.

Cr II

Star	Lab.
0–1	4
2	20
3	30
4–5	100
6–7	125

Fe I

Star	Lab.
0–1	10
2	30
3	50
4	100
5–7	125

Mn I

Star	Lab.
0–1	100
2–3	150
4	200

Mn II

Star	Lab.
0–1	7
2	20
3–6	75

Ti II

Star	Lab.
0–1	5
2	20
3	30
4–6	100

Fe II

Star	Lab.
0–1	2
2–3	4
4–5	6
6	12

Mg II

Star	Lab.
1	10
12	100

Sr II

Star	Lab.
3	300
5	400

Cr I

Star	Lab.
0–1	15
2	30
3–4	300

V II

Star	Lab.
0–1	100
2	300
3	1000

Si II

Star	Lab.
0–1	5
2–3	8
4–5	10

Co I

Star	Lab.
0–1	50
2	80
3–4	125

well within the errors of measurement. Thus, for the stronger lines in the region to the violet of λ 3632, the wave lengths given in the first column of the table are the averages of the measures from the two plates. For each plate the radial velocity was computed from about 40 lines, giving a mean of ± 10 km/sec. The regions λλ 3727–4341 and λλ 4341–4638 were measured on plates taken on July 25 and May 5, at phases 0.26 and 0.39 day, respectively.

The *M.I.T. Wavelength Tables* were extensively used in identifying lines, although the identifications given in the table are, for the most part, from C. E. Moore's table.[6] For *Fe* II and *V* II the works of J. C. Dobbie[7] and of Meggers and Moore[8] were used. Unpublished material was used for *Cr* II, *Mn* II, *Ni* II, and predicted lines. Whenever possible, the most important contributor or contributors of the star lines have been designated by the letter "c," placed directly before the element, in the fourth column of Table 1. Some identifications which are very minor contributions, which are somewhat doubtful, or which differ appreciably in wave length are given in parentheses. The hydrogen lines are very broad; and many lines are therefore masked, thus accounting for the absence in Table 1 of lines near the stronger members of the Balmer series. When a line is given as a blend, including a strong hydrogen line, the contribution of the other elements is usually rather small. The intensities in the second column are eye estimates, the intensities of the faintest lines in the table being 0–1. The letters "s," "bd," "n," "nn," "r," and "v" mean, respectively, "sharp," "broad," "nebulous," "very nebulous," "shaded toward the red," and "shaded toward the violet." The identifications were compared with those in the tables by O. Struve[9] and by O. Struve and P. Swings[10] for α Cygni (Sp. c A2), and the intensities in α Cygni are given in the third column of Table 1. For the two stars the blending elements are, of course, not always the same. In α Cygni the ultraviolet region ($\lambda < 3957$) was investigated on plates taken at the McDonald Observatory with the Cassegrain quartz spectrograph and the 500-mm camera. The visual region ($\lambda > 3957$) was studied on high-dispersion spectrograms taken with the coudé spectrograph, and therefore the intensities in these two regions are not strictly comparable.

We proceed with a discussion of the identifications. The comparisons are with α Cygni and refer to ϵ Ursae Majoris. The spectral type is A0p.

[6] *A Multiplet Table of Astrophysical Interest.*

[7] *Ann. Solar Phys. Obs.*, Vol. 5, Part I, 1938.

[8] *Natl. Bur. of Standards Res. Paper 1317.*

[9] *Ap. J.*, **90**, 699, 1939.

[10] *Ap. J.*, **94**, 344, 1941.

H: Present. Very strong and broad lines.
O I: Present. May be stronger.
Mg I: The strongest lines are masked. Only λ 4351.92 may be present.
Mg II: Present. About the same intensity.
Al I: Only λ 3944.02 is listed. λ 3961.54 is masked.
Al II: Absent or very weak.
Si I: Uncertain. λ 3905.53 may be present in a blend.
Si II: Present. Weaker.
K I: Two lines may be present. The ionization potential is only 4.33 volts.
Ca II: Present. Weaker.
Sc I: Uncertain. Only two coincidences.
Sc II: Absent or very weak.
Ti I: λ 3653.50, one of the strongest laboratory lines, is listed.
Ti II: Present. About the same intensity.
V I: λ 4379.24, the strongest laboratory line in the region studied, is listed.
V II: Present. Weaker.
Cr I: Present. Stronger.
Cr II: Present. About the same intensity.
Mn I: Present.
Mn II: Present. About the same intensity.
Fe I: Present. About the same intensity.
Fe II: Present. About the same intensity.
Co I: Present.
Co II: Absent or very weak.
Ni I: Presence not quite certain, but probable.
Ni II: Present. Weaker.
Sr II: Present. About the same intensity.
Y II: Probably present. About the same intensity.
Zr I: Present. Slightly stronger.
Zr II: Absent or weak. Only one coincidence.
Cb I: The two strongest lines are listed. Presence not quite certain.
Yb II: λ 3694.20 listed in a blend. Uncertain.

In addition to a few identifications in parentheses which are questionable or which do not seem completely to account for the observed lines, 15 lines in Table 1 have been left completely unidentified, 2 of which are also unidentified in the table of Struve and Swings[11] for α Cygni. The strongest unidentified lines are λ 3994.40 and λ 4137.78.

A comparison of the spectrograms has confirmed Guthnick's finding that many of the lines are weakened when *Ca* II K is at maximum intensity, although the writer has not been convinced of Guthnick's observation that the weak lines are broader and less sharp at the time of the maximum of *Ca* II K. In identifying the variable lines, comparisons were made in the regions λλ 3307–3388, 3388–3722, 3722–4341, and 4341–4638 between spectrograms taken, respectively, on July 12 (phase = 2.54 days) and July 14 (phase = 4.54 days); June 23 (phase = 3.90 days) and June 29 (phase = 4.79 days); July 25 (phase = 0.26 day) and July 13 (phase = 3.53 days); and May 25 (phase = 0.39 day) and June 23 (phase = 3.97 days). Since the variations in the line intensities are slight and a large proportion of the lines show some variation in intensity, it was decided not to use the method of line ratios in estimating the variable lines. Instead, direct comparisons were made, taking the intensity of the continuum into account, between the two spectrograms listed in each of the above four groups. The plates used for the region λλ 3722–4341 were of good quality, the intensities of the continuous backgrounds at corresponding points being very nearly the same throughout the range; little difficulty was encountered in picking out the variable lines. However, in the ultraviolet region the study may not be so reliable, owing to the slightly poorer quality of the plates.

[11] *Ibid.*

The material available for the region to the red of λ 4341 was poor for a study of line-intensity variations, and therefore the reality of the intensity variations in the few lines listed in this region as variable is uncertain.

Lines which were found to be stronger when *Ca* II K is weak have been designated by a plus sign in the second column of Table 1; those lines showing a slightly stronger variation than average, by two plus signs. Guthnick[12] has listed several lines which seem to vary in the same sense as *Ca* II K. The writer has been unable to confirm this except for an unidentified line at λ 3994.40 (not listed by Guthnick). For the region λλ 3933–4589 Guthnick has given a list of lines showing the strongest variations. These lines, almost all of which were independently discovered by the writer, are designated by a plus sign in parentheses in the second column of Table 1, indicating that the variation is, in sense, opposite to that of the K-line variation. The present identifications given for many of the lines are,

TABLE 2

DISTRIBUTION OF LINES IN ε URSAE MAJORIS

Element	Lines Relatively Constant in Intensity			Variable Lines Marked +			Variable Lines Marked ++			Total Number of Lines
	Weak (Int. 0–1)	Intermediate in Intensity (Int. 2–3)	Strong (Int. ≥ 5)	Weak (Int. 0–1)	Intermediate in Intensity (Int. 2–3)	Strong (Int. ≥ 5)	Weak (Int. 0–1)	Intermediate in Intensity (Int. 2–4)	Strong (Int. ≥ 5)	
Cr II	3(0.06)	4(0.08)	3(0.06)	0(0)	24(0.46)	9(0.17)	0(0)	7(0.14)	2(0.04)	52
Fe II	9(0.32)	8(0.29)	0(0)	1(0.04)	6(0.21)	1(0.04)	0(0)	1(0.04)	2(0.07)	28
Fe I	10(0.15)	15(0.23)	0(0)	2(0.03)	16(0.24)	4(0.06)	0(0)	18(0.27)	1(0.02)	66
Ti II	4(0.11)	9(0.25)	2(0.06)	1(0.03)	12(0.33)	6(0.17)	0(0)	2(0.06)	0(0)	36
V II	5(0.50)	2(0.20)	0(0)	1(0.10)	0(0)	0(0)	0(0)	2(0.20)	0(0)	10
Mn II	0(0)	0(0)	0(0)	1(0.11)	1(0.11)	3(0.33)	0(0)	0(0)	4(0.44)	9
Mn I	0(0)	0(0)	0(0)	0(0)	2(0.40)	0(0)	0(0)	2(0.40)	1(0.20)	5
Cr I	0(0)	1(0.10)	0(0)	1(0.10)	5(0.50)	0(0)	0(0)	3(0.30)	0(0)	10
*Mn**	1(0.09)	2(0.18)	0(0)	0(0)	6(0.55)	0(0)	0(0)	2(0.18)	0(0)	11

* *Mn* lines for which the stage of ionization is uncertain.

however, quite different from those of Guthnick. Fewer lines are designated as variable in Guthnick's list than are designated as such for the same region in Table 1, owing partly to the fact that many more lines are given for Guthnick's region in Table 1. Moreover, Guthnick has listed only those lines showing the strongest variation. For many of the lines, especially the fainter ones, it was impossible to definitely ascertain whether or not the intensity of the line varies, and therefore the absence of a plus sign does not necessarily mean that the line was considered to be definitely constant in intensity; it appears that a large number of the lines are variable, and, indeed, they all may very well be, to some extent, variable.

No attempt was made to ascertain whether or not the very broad and strong Balmer lines are variable; nor to verify or study the rapid changes in the contour of $H\gamma$ or the rapid changes in the intensity of *Ca* II K which have been reported by Guthnick.[13]

For the unblended or slightly blended lines in the region λλ 3322–4340, Table 2, which is self-explanatory in the headings, was prepared. The numbers of lines falling in the categories given at the top of the table are tabulated for a number of the elements pres-

[12] *Op. cit.* [13] *Ibid.*

ent. The numbers appearing in parentheses after each of these numbers are the fractional parts of the total number of lines listed for each element. In the case of the weak lines, it was usually impossible definitely to ascertain variability, thus accounting for the large proportion of weak lines in the second column of Table 2. In addition to the elements given in Table 2, *Ni* II, *Si* II, *O* I, and *Sr* II are represented by unblended or slightly blended lines marked plus or double plus; it appears that the variations are not confined to any particular elements. In Table 2 there is a suggestion that the lines of *Cr* II, *Cr* I, *Mn* II, and *Mn* I show a greater tendency toward variability than those of the other elements.

The investigation was suggested by Dr. O. Struve, and the writer is thankful for his advice given during the course of the work. He also wishes to record his indebtedness to Miss Jeannette Ringstad for her assistance with the reductions.

RADIAL VELOCITIES OF PROPER-MOTION STARS*

GUIDO MÜNCH
McDonald and Yerkes Observatories
Received January 20, 1944

ABSTRACT

Radial velocities have been determined for 39 stars of large proper motion. New spectral types are given, except for the M dwarfs and the white dwarfs. For these, Kuiper's spectral types have been adopted. Three dwarfs have the H and K lines of *Ca* II in emission, and one of these (BD+55°1823, M1) also shows the hydrogen lines in emission.

The present list of radial velocities is a continuation of two earlier lists by D. M. Popper under the same title.[1] The spectrograms used were obtained with the 82-inch telescope of the McDonald Observatory and the Cassegrain spectrograph equipped with glass prisms and an $f/2$ Schmidt camera, giving a dispersion of 76 A/mm at $H\gamma$. In a few cases, a set of two quartz prisms and a 500-mm camera, giving a dispersion of 55 A/mm, were used.

The arrangement of the results, given in Table 1, is the same as that used in the earlier papers by Popper. The visual magnitudes were given by Kuiper, except for the HR stars and the magnitudes shown in italics, which are photovisual determinations by Seyfert.[2] The probable errors, given in the sixth column, were computed in the usual way, except when two spectrograms were obtained; in the latter case, the probable error was taken as one-third of the difference between the measured velocities. The "quality" of a velocity depends on the number of lines measured on each spectrogram, the number of spectrograms, and their probable errors. The highest quality is indicated by "A"; the lowest, by "F." In the fourth column is given the number of spectrograms secured for measurement; an asterisk following the number indicates that these plates have a dispersion of 55 A/mm at $H\gamma$; otherwise, the spectra have 76 A/mm in $H\gamma$.

The H and K lines were found to be in emission in the following dwarfs:

Star	Type
BD+55°1823	M1
BD+51°2402	K5
BD−17°6769	K8

The hydrogen lines also appear in emission in the spectrum of BD+55°1823.

I wish to record my thanks to Dr. Gerard P. Kuiper for suggesting this list of objects and for the use of unpublished data. Dr. O. Struve and Mr. C. A. Bauer have kindly secured for me a few of the spectrograms.

* *Contributions from the McDonald Observatory, University of Texas*, No. 89.

[1] *Ap. J.*, **95**, 307, 1942; **98**, 209, 1943.

[2] *Ap. J.*, **91**, 117, 1940.

TABLE 1

RADIAL VELOCITY AND SPECTRA OF PROPER-MOTION STARS

Star	α (1900)	δ (1900)	m_V	Type	No.	Vel.	P.E.	Quality	Notes
−31°325	0h48m1	−30°54′	7.2	dK4	2	+ 2	± 3	B	
−23°693	1 48.0	−22 56	8.7	dK9	2	+ 28	2	D	
HR 857	2 47.7	−13 11	6.1	dK1	3	+ 17	4	C	
Furuhjelm 10	3 02.8	+45 22	10.1	dM2	2	+ 5	3	C	
40 Eri B	4 10.7	− 7 49	9.6	wA	2	− 20	9	F	
+21°652	4 23.1	+21 41	9.2	dK9	1	− 35	6	D	
HR 1614	4 55.9	− 5 52	6.5	dK4	3	+ 35	4	C	1
γ Lep B	5 40.3	−22 29	6.3	dK3	2	− 11	1	C	2
+26°2606	14 44.6	+26 08	9.8	dF0	2	+ 34	2	A	
−20°4399	15 59.7	−20 11	7.4	dK2	2	+ 34	2	A	
+55°1823	16 14.9	+55 32	10.1	dM1	2	− 34	4	B	
−12°4523	16 24.7	−12 25	9.8	dM5	2	− 4	2	C	
36 Oph C	17 10.1	−26 24	6.7	dK8	2*	0	1	A	3
−8°4501	17 42.0	− 8 44	10.8	sdF8	2	+ 91	1	A	
μ Her BC	17 42.5	+27 47	9.8	dM4	2	− 20	5	D	4
Barnard's star	17 52.9	+ 4 25	*9.4*	dM5+	3	−111	5	B	5
−13°4807 AB	17 53.0	−13 04	9.4	sdG5	2	+198	2	B	6
−3°4233	17 59.8	− 3 02	9.2	dM1	2	+ 34	3	C	
−18°4986	18 25.5	−18 58	7.0	dK2	1	− 50	2	D	
+13°3683	18 28.7	+13 03	*10.6*	sdF5	1	+112	11	F	
+51°2402	18 31.6	+51 39	8.6	dK5	2	− 39	3	C	
+45°2743	18 32.4	+45 39	*10.2*	dM0	2	− 28	1	A	
+59°1915 A	18 41.7	+59 29	8.9	dM3+	1	− 4	3	C	7
+59°1915 B	.....	.....	9.7	dM4	1	+ 3	7	C	7
+4°4048	19 12.1	+ 5 02	9.1	dM3	2	+ 35	1	B	
−21°5703	20 17.7	−21 40	8.5	sdG0	1	−178	9	C	8
AC+25°67928	20 20.5	+24 44	10.6	sdF0	2	−319	2	B	
Wolf 1346	20 30.1	+24 44	11.3	wA	2	+ 26	3	C	
−14°5850	20 42.0	−14 47	11.2	dF5	2	0	2	D	
Ross 775	21 24.8	+17 12	10.3	dM4+	3	+ 7	6	F	
−0°4234 A	21 27.0	− 0 13	9.7	dK0	2	− 78	2	B	9
−35°14849	21 27.7	−35 52	10.6	sdF	1	+103	13	F	
+27°4120	21 33.5	+27 16	9.8	dM0	2	− 12	2	C	
+21°4747 A	22 20.0	+22 04	9.0	dK4	2	+ 5	3	D	
−1°4323	22 31.0	− 1 21	10.3	dM0	2	+ 13	1	B	
−15°6290	22 47.9	−14 47	10.2	dM5	2	+ 8	1	B	
−14°6437 AB	23 11.9	−14 22	8.3	sdF8	2*	+ 23	6	A	10
−17°6769	23 27.6	−17 23	*8.5*	dK8	1	+ 3	5	C	
−26°16876 AB	23 56.7	−26 21	8.8	sdA8	2*	+ 36	2	A	11

NOTES TO TABLE 1

1. Since the velocity of this star has been suspected of variability, the individual values are given here:

1943, Aug. 20, 11:38 U.T. ..... $V = +43 \pm 5$ km/sec
1943, Sept. 17, 11:20 U.T. ..... $V = +32 \pm 7$ km/sec
1943, Sept. 17, 12:03 U.T. ..... $V = +30 \pm 7$ km/sec

The first plate has a dispersion of 55 A/mm, and the last two 76 A/mm, at Hγ.

2. The velocity previously published is -9.7 ± 0.8 km/sec.
3. The velocity obtained here (0 ± 1 km/sec) differs somewhat from that given in the Lick *Catalogue of Radial Velocities* (-10 ± 1) but agrees with the velocities of the other components of the system ($V_A = -0.2 \pm 0.5$ km/sec, $V_B = -0.6 \pm 0.3$ km/sec).
4. The velocity of μ Her A is -16.1 ± 0.2 km/sec.
5. BD+4°3561. The previously published velocity is -110 ± 4 km/sec.
6. The large radial velocity is in accordance with Kuiper's suspicion that this star is a subdwarf.
7. Previously published velocities are 0 ± 2 for A and $+7 \pm 3$ km/sec for B.
8. A previously determined velocity is −179 km/sec.
9. The companion is a white dwarf (Kuiper).
10. A previous determination is $+6 \pm 2$ km/sec.
11. A previous determination is $+61 \pm 5$ km/sec.

THE WOLF-RAYET SPECTROSCOPIC BINARY HD 214419*

W. A. HILTNER
Yerkes and McDonald Observatories
Received February 18, 1944

ABSTRACT

The velocity-curve of this Wolf-Rayet spectroscopic binary was obtained from 50 spectrograms taken from November 5 to December 20, 1943. The curve for *N* IV 4058 leads to the following elements: P = 1.6410 days, $\gamma = -75$ km/sec, $K = 295$ km/sec, and $e = 0$ (assumed). The period was established with the help of 20 Ann Arbor spectrograms. Emission of *He* II in the Pickering series suggests a similar solution, except for a shift in the γ-axis to $+180$ km/sec and a small decrease in K. A phase difference is suggested by the velocity measurements, the *He* II emission leading *N* IV 4058 by 0.05 days. The intensity of the emission in this series varies appreciably during a cycle. The line *He* II 4686 gives a velocity-curve entirely different, leading to the following elements: $\gamma = +137$ km/sec, $K = 165$ km/sec, $e = 0.35$, $\omega = 0$, and T = phase 0.41 day. It is suggested that the radial velocities of this emission line represent more than orbital motion. Variations in structure of *He* II 4686 are noted. Thus far no lines of the companion star have been detected. The star has been observed with a Fabry photometer attached to the 40-inch refractor of the Yerkes Observatory; and, from seven nights' observations, a variation of 0.20 mag. is established. The star is brightest when the Wolf-Rayet component is on the far side of the system. No evidence of an eclipse has been detected.

The Wolf-Rayet star, HD 214419,[1] was announced to be a spectroscopic binary from spectrograms obtained at Ann Arbor in 1941.[2] With the dispersion employed (150 A/mm at $H\gamma$) at the time of this discovery, the existence of absorption lines, presumably belonging to the secondary star, could not be established with confidence. Furthermore, structural and intensity variations in *He* II 4686 were suspected, but the evidence was not conclusive. Consequently, in November, 1943, the star was placed on the observing program of the 82-inch reflector of the McDonald Observatory, and Struve obtained a series of 44 spectrograms (dispersion, 40 A/mm at λ 3933) with the quartz Cassegrain spectrograph between November 5 and November 17, 1943. Six additional spectrograms were obtained by the author in December of the same year.

The Wolf-Rayet spectrum is of type WN6, with *He* I, *He* II, *N* III, *N* IV, and *N* V being responsible for nearly all the bands. No spectral features that can be attributed to the companion star have been observed. Some of the emission bands in the Wolf-Rayet star possess well-defined violet absorption edges, especially the Pickering series of *He* II and λ 4603 of *N* V, while other bands, for example, *N* IV 4058, are observed only in emission. The intensity of the emission in the Pickering series varies appreciably during a cycle, being strongest when the Wolf-Rayet is on the far side of the system. This strengthening of the emission appears to be accompanied by a weakening of the violet absorption edges. In contrast, the emission band *N* IV 4058 displays little variation in intensity. It is difficult to determine by visual inspection whether or not *He* II 4686 varies in intensity, since this band, by far the strongest in the photographic region, was usually overexposed, making estimates of intensities impossible. Plates XIII and XIV are reproductions of spectrograms of HD 214419 taken at different phases.

The results of the radial-velocity measurements are listed in Table 1, which records the results of the Ann Arbor spectrograms, and Table 2, which records the measurements of the McDonald spectrograms. Only *He* II 4686 was measured on the Ann Arbor plates,

* *Contributions from the McDonald Observatory, University of Texas*, No. 91.

[1] $\alpha = 22^h32^m.9$, $\delta = +56°23'$ (1900), ptm. mag., 8.92.

[2] Dean B. McLaughlin and W. A. Hiltner, *Pub. A.S.P.*, **53**, 328, 1941.

their primary function being that of yielding a more accurate period for the system than was possible with the McDonald observations alone. Since there are large systematic differences between the velocities derived from various lines, the velocities of *N* IV 4058, *He* II 4686, and the mean of *He* II 4200, 4339, and 4541 of the Pickering series are recorded individually for the McDonald spectrograms. The phases are computed from the formula

$$\text{JD} = 2431037.82 + 1.6410E\,.$$

Zero phase corresponds to the time when the velocity-curve of the Wolf-Rayet star crosses from the negative to the positive side of the γ-axis as determined by *N* IV 4058.

TABLE 1

RADIAL VELOCITIES OF HD 214419, ANN ARBOR

Plate	Date	Phase	Vel. in Km/Sec *He* II 4686	Plate	Date	Phase	Vel. in Km/Sec *He* II 4686
X 15738	1941 Sept. 21.164	0.319	+229	X 16093	1942 July 20.350	0.561	+224
X 15752	23.172	0.686	+ 56	X 16102	21.300	1.511	+ 14
X 15820	Oct. 26.229	0.923	+ 47	X 16105	23.394	0.323	+341
X 15825	28.233	1.286	− 44	X 16107	24.365	1.294	+ 1
X 15826	29.175	0.587	+152	X 16158	Aug. 20.376	0.408	+377
X 15840	Nov. 4.158	0.006	+138	X 16166	21.337	1.369	+ 11
X 15899	25.143	1.299	+ 15	X 16212	Oct. 10.275	0.436	+196
X 15914	27.154	0.028	+184	X 16219	11.222	1.383	+ 52
X 15935	29.140	0.373	+302	X 16229	12.253	0.773	+ 77
X 15948	1941 Dec. 19.040	0.581	+195	X 16233	13.237	0.116	+156
X 16089	1942 July 19.390	1.242	− 77				

A period of 1.6410 days was determined with the help of the Ann Arbor spectrograms. The individual observations of *N* IV 4058, the means of *He* II 4200, 4339, and 4541, and *He* II 4686 are plotted in Figures 1, 2, and 3, respectively. The plot of *N* IV 4058 shows a well-defined velocity-curve with an eccentricity near zero. Assuming $e = 0$, a graphical solution yields the following elements:

$$P = 1.6410 \text{ days}, \qquad e = 0.0 \text{ (assumed)},$$

$$\gamma = -75 \text{ km/sec}, \qquad a \sin i = 6.66 \times 10^6,$$

$$K = 295 \text{ km/sec}, \qquad \frac{m_2^3 \sin^3 i}{(m_1 + m_2)^2} = 4.38\,.$$

The representation of the observations of *N* IV 4058 by the above solution is shown by the continuous curve in Figure 1. The resulting mass function is large, indicating that the system is very massive.

The *He* II lines of the Pickering series have marked absorption edges. The center of the absorption, as well as the emission, was measured whenever possible; and means of the three lines most frequently measured in this series are plotted in Figure 2. The filled circles indicate emission, and the open circles represent measurements of the absorption edges. The line λ 4339 was included in the mean, since it is evident from comparing individual plots of this line and *He* II 4200 and 4541 that $H\gamma$ contributes insignificantly, although emission to the violet of the absorption may infrequently be present. This emission is probably similar to that observed by O. C. Wilson in HD 193576.[3] The

[3] *Ap. J.*, **95**, 404, 1942.

PLATE XIII

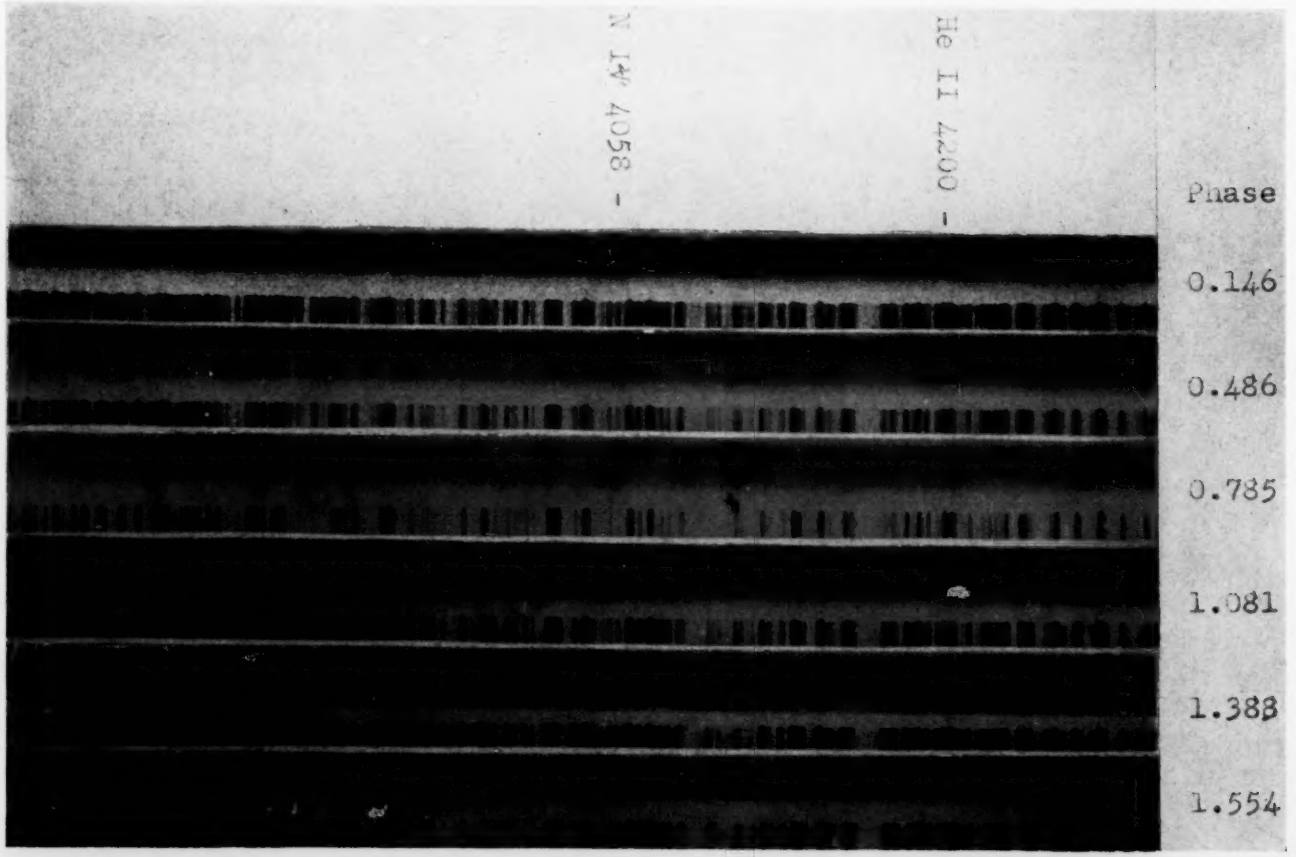

THE SPECTRUM OF HD 214419

PLATE XIV

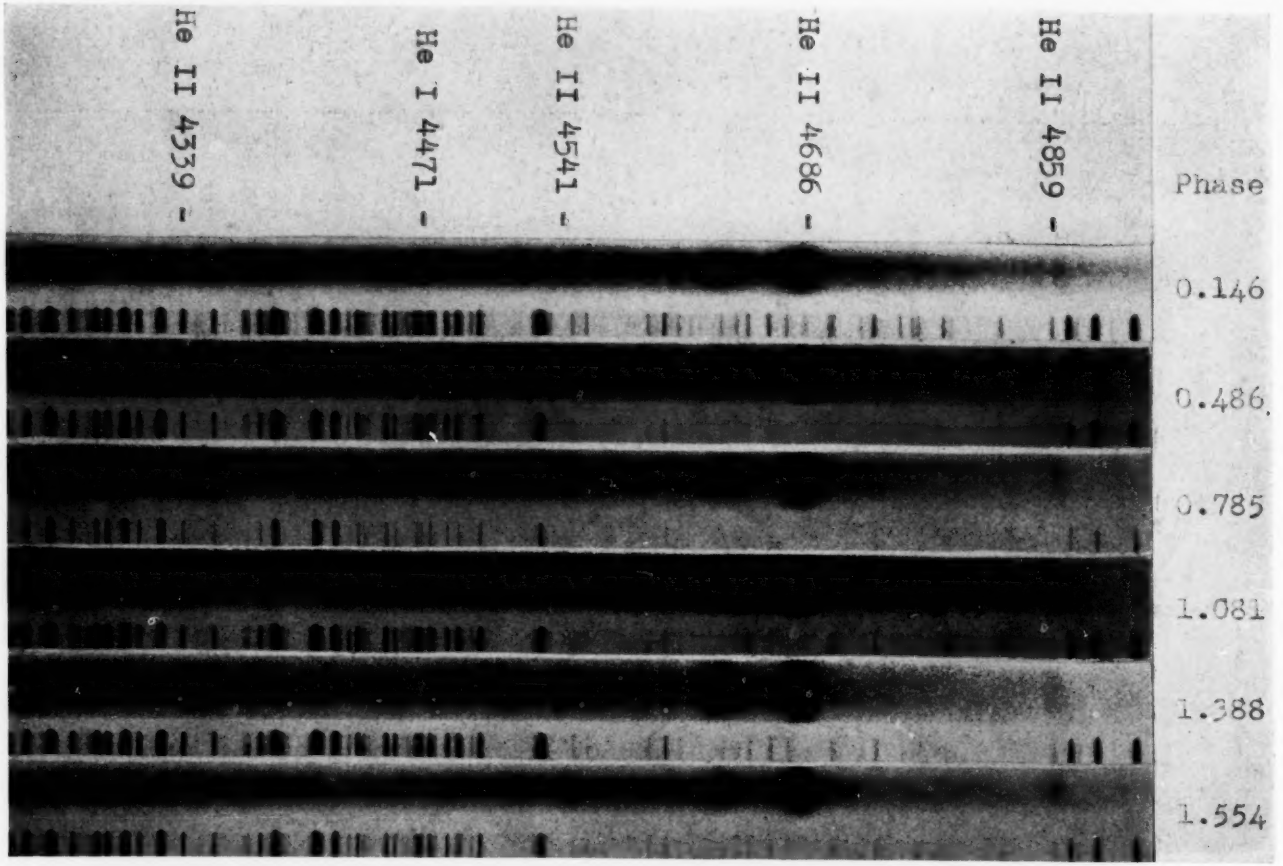

THE SPECTRUM OF HD 214419

TABLE 2

RADIAL VELOCITIES OF HD 214419, McDONALD OBSERVATORY

PLATE	DATE	PHASE	RADIAL VELOCITY IN KM/SEC			
			λ 4058	λ 4686	He II$_A$	He II$_B$
CQ 2524	1943 Nov. 5.092	0.695	+113	+153	− 62	+289
2527	5.262	0.865	−128	+ 73	−362	+131
2533	6.053	0.015	− 69	+ 64	− 99	+294
2552	7.094	1.056	−364	+ 24	−446	− 62
2562	8.127	0.448	+210	+300	− 59	.....
2583	9.102	1.423	−288	− 24	−424	− 69
2584	9.140	1.461	−278	+ 3	−365	+ 84
2589	9.233	1.554	−184	+ 19	−411	+204
2593	9.324	0.004	− 80	+ 95	.....	.....
2608	10.105	0.785	+ 14	+122	−226	+175
2611	10.181	0.861	−132	+113	−386	+120
2614	10.255	0.935	−233	+ 81	−386	+ 33
2617	10.330	1.010	−292	+ 59	−437	− 43
2629	11.147	0.186	+134	+219	− 96	+416
2633	11.233	0.272	+190	+309	− 94	+456
2637	11.333	0.372	+255	+354	− 14	+452
2641	12.042	1.081	−334	+ 28	−427	− 6
2642	12.064	1.103	−342	+ 23	−428	+ 48
2643	12.085	1.124	−337	+ 70	−460	− 23
2644	12.110	1.149	−360	+ 79	−480	− 82
2645	12.128	1.167	−370	+ 77	−484	− 35
2646	12.149	1.188	−367	+ 85	−509	− 83
2647	12.170	1.209	−328	+ 72	−518	− 66
2648	12.191	1.230	−357	+ 63	−495	− 85
2652	12.243	1.282	−360	+ 45	−517	−131
2653	12.264	1.303	−376	+ 58	−482	−108
2657	12.316	1.355	−367	+ 67	−424	− 64
2658	12.338	1.377	−321	+ 67	−545	− 35
2659	12.366	1.405	−298	+ 10	−500	− 23
2667	13.031	0.429	+207	+345	− 90	+442
2668	13.057	0.455	+200	+340	− 90	+413
2669	13.088	0.486	+174	+322	− 64	+474
2670	13.114	0.512	+206	+309	− 64	+470
2671	13.135	0.533	+180	+277	− 11	+396
2674	13.185	0.583	+141	+290	− 10	+361
2675	13.215	0.613	+141	+232	− 38	+332
2676	13.255	0.653	+153	+228	− 72	+293
2686	14.038	1.436	−237	+ 32	−420	+ 19
2697	15.036	0.793	− 32	+ 67	−273	+185
2698	15.062	0.819	− 52	+ 67	−365	+ 95
2700	16.030	0.146	+ 86	+187	− 55	+ 84
2701	16.062	0.178	+118	+187	− 88	+400
2711	17.033	1.149	−361	+ 72	−445	− 28
2712	17.061	1.177	−370	+ 80	−475	− 44
2724	Dec. 19.088	0.384	+210	+370	− 8	.....
2725	19.156	0.452	+226	+352	− 83	+460
2726	19.194	0.490	+226	+330	−108	+434
2728	20.047	1.343	−363	+ 30	−534	+ 38
2729	20.092	1.388	−304	− 23	−494	− 78
2730	20.146	1.442	−263	+ 55	−506	+ 32

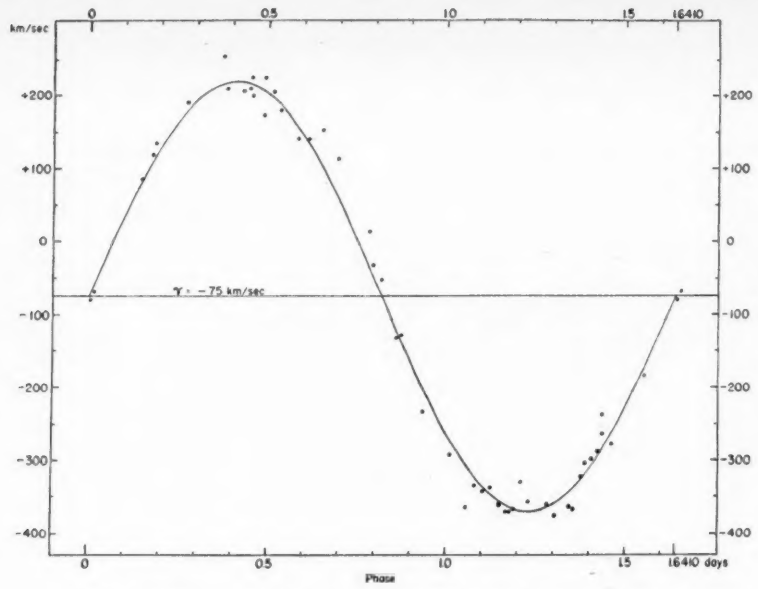

FIG. 1.—Observed velocity-curve of HD 214419 from *N* IV 4058

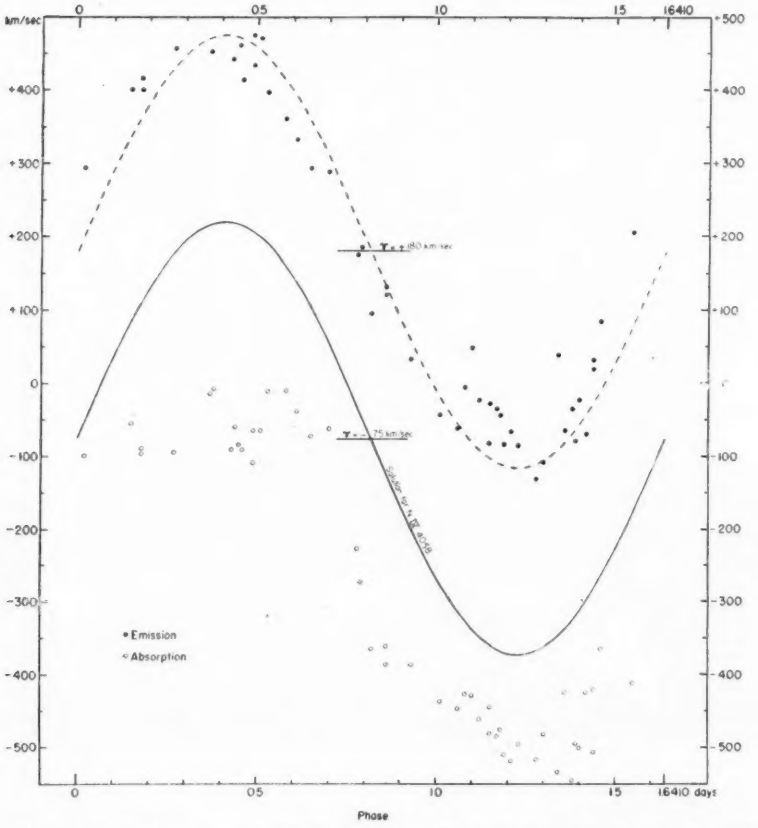

FIG. 2.—Observed velocity-curve of HD 214419 from *He* II of the Pickering series. Filled circles represent emission, and open circles, the violet absorption-edge. The continuous curve is the solution for *N* IV 4058 and the dashed curve is the same, except that the γ-axis is shifted from −75 km/sec to +180 km/sec. Note the difference in phase between *He* II (Pickering) and *N* IV 4058.

continuous curve in Figure 2 represents the solution for *N* IV 4058, and the dashed curve is the same except for a shift in the γ-axis from -75 km/sec to $+180$ km/sec. The latter satisfies the observations except that, in addition to a small decrease in the semi-amplitude, an appreciable difference in phase between *N* IV and *He* II is suggested, the difference amounting to approximately 0.05 days. The explanation for this phenomenon is not clear. The observations do not indicate whether or not a similar shift in phase exists for the violet-absorption edges of the emission bands. It does not seem possible to explain the phase difference in terms of a transit time effect discussed by O. C. Wilson[4] in connection with HD 193576, unless we assume a stratification in which *N* IV is at a much higher level than *He* II, since the band widths are similar to a first approximation. The violet-absorption edges are undoubtedly responsible for the shift in the γ-axis of 255 km/sec.

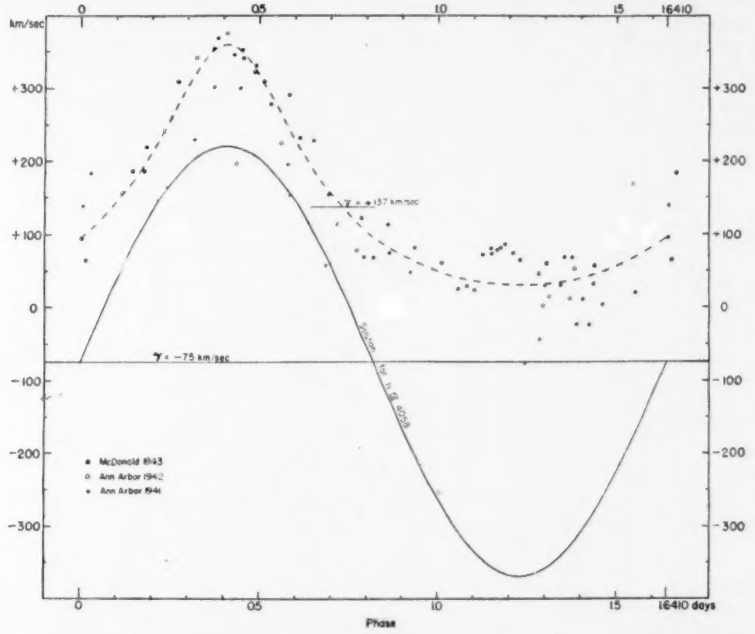

FIG. 3.—Observed velocity-curve of HD 214419 from *He* II 4686. The filled circles represent McDonald observations in 1943; open circles, 1942 Ann Arbor observations; and crosses, 1941 Ann Arbor observations. The continuous curve is the solution for *N* IV 4058, and the dashed curve is the solution for *He* II 4686.

The observations of *He* II 4686 are plotted in Figure 3. The 1941 and 1942 Ann Arbor observations are included with the more numerous 1943 McDonald measures. Again the continuous curve is the solution for *N* IV 4058. Obviously, it is impossible to adjust the *N* IV 4058 solution to satisfy both *N* IV 4058 and *He* II 4686. A rough graphical solution for *He* II 4686 alone yields the following elements

$$P = 1.6410\,, \qquad \omega = 0$$

$$\gamma = +137 \text{ km/sec}\,, \qquad T = \text{Phase } 0.41 \text{ days}\,,$$

$$K = 165 \text{ km/sec}\,, \qquad a \sin i = 2.06 \times 10^6\,.$$

$$e = 0.35\,, \qquad \frac{m_2^3 \sin^3 i}{(m_1 + m_2)^2} = 0.130\,.$$

This solution is represented by the dashed curve in Figure 2.

[4] *Ibid.*, pp. 409–417.

The velocity-curve of *He* II 4686 should be regarded with suspicion, since it is the only line that shows such a variation in velocity. In addition to *N* IV 4058 and *He* II of the Pickering series, *He* I 4471 also indicates an eccentricity near zero, although the amplitude may be smaller than that for *N* IV 4058, probably similar to that for the Pickering *He* II absorption edges. The measures are not sufficiently accurate and numerous to be conclusive and, hence, were not included in Table 2 along with the other measured velocities. An argument of equal weight that the velocity-curve of *He* II 4686 does not represent orbital motion alone is that this line is subject to appreciable variations in structure during a cycle. From phases 0.0–0.8 the band usually appears symmetrical with infrequent indication of shading to the red; but from phases 0.8–1.6 the band is normally shaded to the violet. The measures represented in Figure 3 refer to the "center of gravity." Structural variations were also observed on the Ann Arbor spectrograms.

The lines of *He* I are present in this Wolf-Rayet star both in emission and in absorption. The emission is always very weak and never of sufficient intensity to measure with accuracy. The absorptions of λλ 4471, 4026, and 3889 were measured when possible. The last two are probably blended with *He* II. Although the measures were usually very uncertain because of weakness of the lines and varying intensity, they do prove conclusively that the *He* I absorption normally present belongs to the Wolf-Rayet.

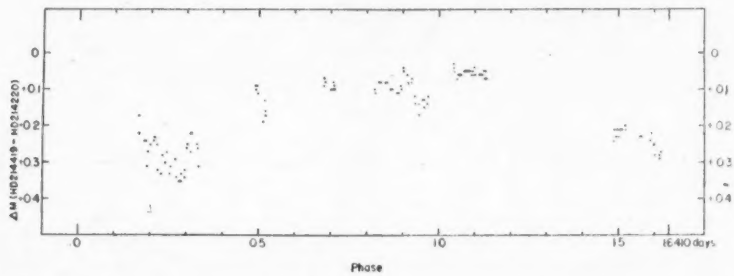

FIG. 4.—Photometric measures of HD 214419. Dots represent individual observations. The Wolf Rayet star is brightest when it is on the far side of the system.

In a behavior thus far unpredictable, the three *He* I lines mentioned previously, or *He* I 3889 alone, may show a relatively sharp component strongly displaced toward the violet (see Pl. XV). For example, on November 8.127, 1943, phase 0.448, a sharp absorption line of *He* I 3889 ($2^3S - 3^3P^0$), displaced by −1100 km/sec, was observed to be moderately strong, although only the component belonging to the Wolf-Rayet star was present at λ 4026 ($2^3P^0 - 5^3D$) and λ 4471 ($2^3P^0 - 4^3D$). This line has not been previously or later observed with certainty. However, all the spectrograms taken on November 13, from phases 0.429–0.653, show a strong, violet-displaced, relatively sharp absorption line of *He* I 4471, 4026, and 3889, in addition to the Wolf-Rayet component. The violet displacement corresponds to −800 km/sec for all three lines. The wave lengths of this component remained constant within the errors of measurements, although the velocity of the Wolf-Rayet star changed from −220 km/sec to −100 km/sec during the interval of the observations. Only one plate was obtained on November 14 (phase 1.436), but the violet component of λ 3889 was still strongly present at the same displacement and was probably sharper than on the previous night, while only the Wolf-Rayet components of λ 4026 and λ 4471 were present. No trace of the violet component of λ 3889 was observed on November 15 (phase 0.793 and 0.819) or on subsequent nights. This behavior strongly suggests that the system is subject to erratic ejection of material of such velocities that we have an enormous change in dilution in an interval of only twenty-four hours.

PLATE XV

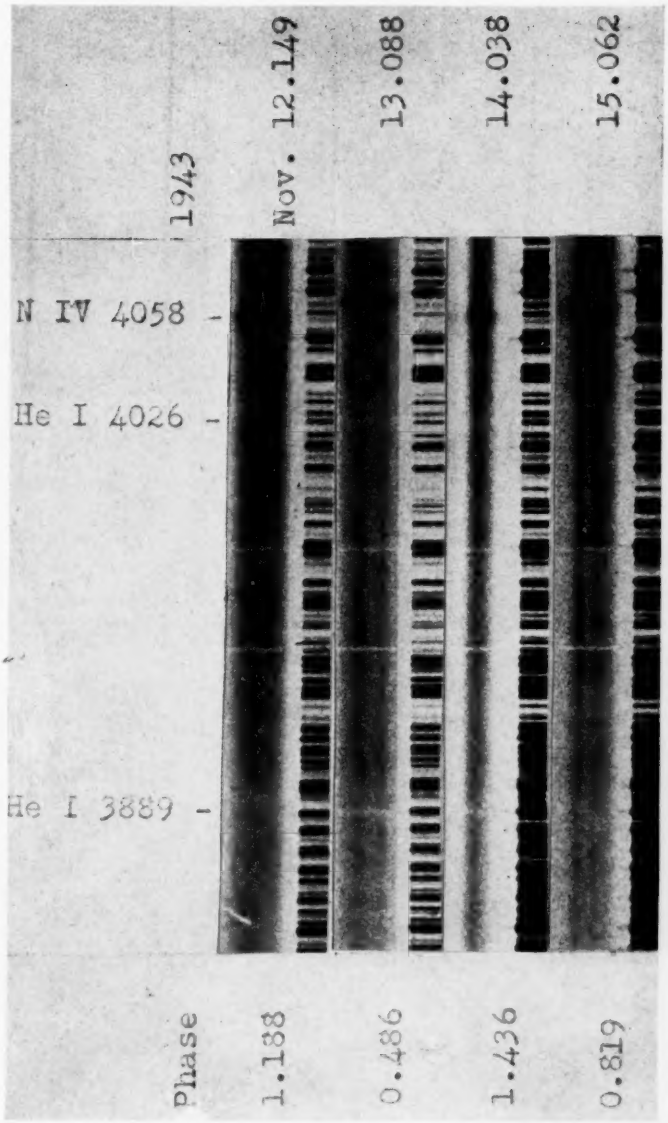

THE SPECTRUM OF HD 214419 ON FOUR CONSECUTIVE NIGHTS

Note the presence of a relatively sharp violet component of *He* I 3889 and 4026 on 1943 Nov. 13, and that on 1943 Nov. 14 only the component of *He* I 3889 is present and at the same displacement. The two sharp lines are interstellar *Ca* II.

Since the amplitude of the velocity-curve is large, HD 214419 was observed for possible light-variations. It is not listed as a known variable. Figure 4 is a plot of the observations thus far obtained on seven nights with a Fabry photometer[5] attached to the 40-inch refractor of the Yerkes Observatory. The dates of the observations and the mean for the night are listed in Table 3. The stars HD 214220 of spectral type A3 and HD 214259 of type A0 were used for comparison stars, the latter serving primarily as a check on the former. These comparison stars were selected because of their proximity to HD 214419, their distances being 11′ and 31′, respectively, and because they are of nearly the same magnitude as the Wolf-Rayet star. The exposure time on Eastman II-0 emulsion was 90 seconds, and exposures of the comparison stars were made at frequent intervals, about every 20 minutes. The plates were calibrated with a tube sensitometer and measured with a Hartmann microphotometer. Although no eclipse is evident, the observations strongly suggest that a variation of approximately 0.20 mag. exists. The variation thus far observed is such that it can be explained qualitatively by a "reflection effect" on the Wolf-Rayet component. It may be recalled that *He* II emission of the Pickering series is much stronger when the Wolf-Rayet star is on the far side of the system.

TABLE 3

PHOTOMETRIC MEASURES OF HD 214419

Date	Phase	ΔM (HD 214419–HD 214220)
1943 Dec. 30.144	1.594	+0.25
Dec. 31.093	0.902	.10
1944 Jan. 1.084	0.252	.28
Jan. 13.015	0.606	.09
Jan. 15.046	1.086	.06
Jan. 21.029	0.505	.13
Jan. 22.026	1.502	+0.22

(Since the preparation of this paper, Dr. Gaposchkin has kindly informed the author of his unpublished photometric observations of HD 214419. The light-curve, according to Dr. Gaposchkin, is of the β Lyrae type, with the two minima of nearly equal depth, approximately 0.35 mag., and with one minimum asymmetrical. Since the contribution by the companion star to the total light is appreciable, it is remarkable that no spectral features of the companion have been observed. A finer-grained and higher-contrast emulsion than Eastman 103a-0 employed in this investigation may possibly reveal some spectral information concerning the companion star. Dr. Gaposchkin published a remark concerning the light-variability of HD 214419 [BD+56°2818] and other Wolf-Rayet stars in *Pub. A.A.S.*, **10**, 250, 1942.)

I wish to express my appreciation to Dr. O. Struve for obtaining nearly all the McDonald spectrograms used in this investigation and for many helpful discussions. I also wish to thank Dr. W. Carl Rufus, acting director of the Observatory of the University of Michigan, for lending the Ann Arbor spectrograms to the author, and to Dr. W. W. Morgan and Dr. G. Van Biesbroeck for generously relinquishing observing time with the 40-inch refractor so that photometric observations might be obtained. Miss G. Peterson kindly reduced a large number of the spectrograms and prepared the figures for publication.

[5] For details concerning this instrument see O. Struve and C. T. Elvey, *Ap. J.*, **83**, 167, 1936.

THE SPECTRUM OF NOVA PUPPIS 1942*

HAROLD F. WEAVER[1]
McDonald Observatory and Cambridge, Mass.
Received February 19, 1944

ABSTRACT

The development of the spectrum of Nova Puppis 1942 is described on the basis of a series of spectrograms obtained at the McDonald Observatory between November, 1942, and May, 1943.

Attaining a maximum brightness of magnitude[2] +0.4 on November 12.0, Nova Puppis[3] 1942 became the fourth brightest nova of the last three hundred years. Its light-curve,[4] while rather peculiarly its own, resembles in some respects the light-curve[4] of Nova T Coronae Borealis 1866. Both of these novae are noteworthy for their rapid decline in brightness after maximum. McLaughlin's "mean relative Δt" unit,[5] the time in days required for the nova to decline through 3.0 magnitudes after maximum light, is, for N Puppis, 6.5 days, for N T Coronae Borealis 1866, 6.0 days.[6] These are the smallest mean relative Δt units recorded. For comparison with other fast novae of the twentieth century, the mean relative Δt unit of N Aquilae[5] 1918 is 7.0 days, of N Lacertae[5] 1936, 8.5 days. For slow novae this unit has a different order of magnitude. For N Herculis 1934[5] the unit is 93 days, for N Pictoris 1925,[5] 150 days.

Perhaps the most unusual feature in the light-curve of N Puppis is its remarkable pre-maximum rise. Harvard plates[7] having a limiting magnitude of 17 fail to show the star in the prenova stage. An independent search of the Franklin-Adams chart on which the nova should appear (April 19, 1912) was made by Pettit.[8] No star was found in the position of the nova, which, in 1912, was therefore fainter than magnitude 14.5, the plate limit. This remarkable rise of 17 magnitudes is considerably greater than the rough average of 11 magnitudes[9] for fast novae and puts the star within the range of the supernovae. The spectrum of N Puppis, however, bears no relationship to the spectra of the supernovae.

Humason and Sanford,[10] using the velocity determined from the interstellar lines, find, by the method of McLaughlin,[11] $M_{max} = -11$, a very high value for galactic novae. If $M_{max} = -11$, the M of the star in the prenova stage was roughly +6. M for N Aquilae 1918 in the prenova stage was, according to Wyse,[12] +3.9. Interstellar absorption, the effect of which should be small, is not included in the estimate of M for N Aquilae.

* *Contributions from the McDonald Observatory, University of Texas*, No. 93.

[1] National Research Fellow, 1942–1943. The author left the Yerkes Observatory before this work was completed to engage in war research.

[2] Mean values are from: (1) L. Campbell, *Pop. Astr.*, **51**, 226, 1943, and unpublished material kindly furnished by Mr. Campbell; (2) E. Pettit, *Pub. A.S.P.*, **55**, 14, 1943; (3) G. P. Kuiper, *Ap. J.*, **97**, 443, 1943; and (4) W. W. Morgan, material kindly furnished in advance of publication.

[3] α (1943.0), 8^h09^m6; δ (1943.0), $-35°11'$.

[4] Campbell, *loc. cit.*

[5] *Ap. J.*, **95**, 432, 1942.

[6] McLaughlin, *Pop. Astr.*, **47**, 539, 1939.

[7] *Sky and Telescope*, **2**, 2, 1943.

[8] *Op. cit.*, p. 19.

[9] McLaughlin, *op. cit.*, p. 545. McLaughlin's value has been rounded off to the nearest whole magnitude.

[10] *Pub. A.S.P.*, **54**, 256, 1942.

[11] *Ap. J.*, **93**, 417, 1942.

[12] *Pub. Lick Obs.*, **14**, 93, 1940.

PLATE XVI

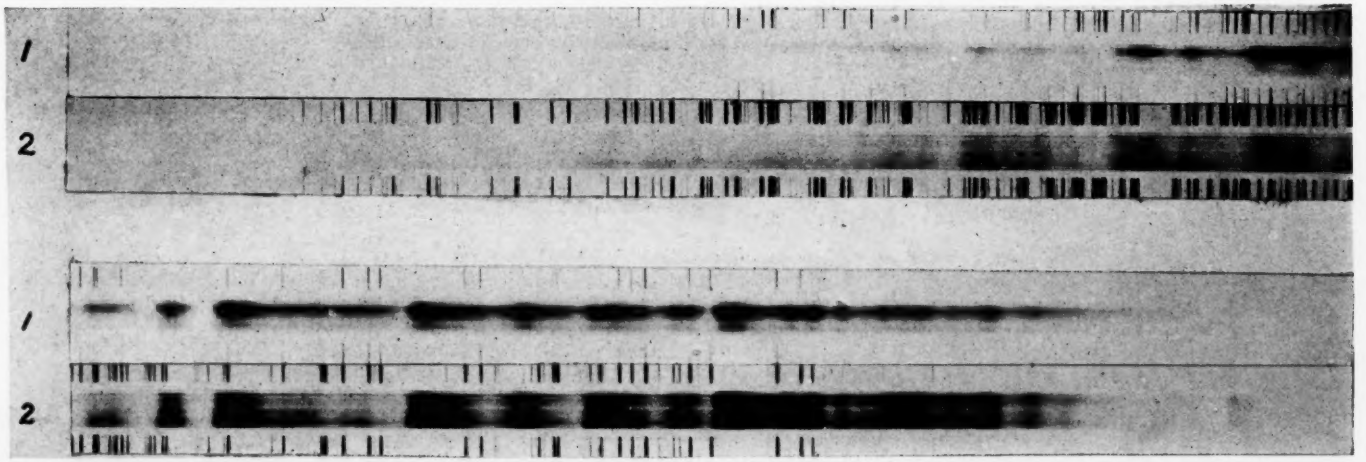

SPECTRA OF NOVA PUPPIS 1942

(1) 1942 November $13^{d}12^{h}40^{m}$ U.T.; (2) 1942 November $14^{d}12^{h}30^{m}$ U.T.

PLATE XVII

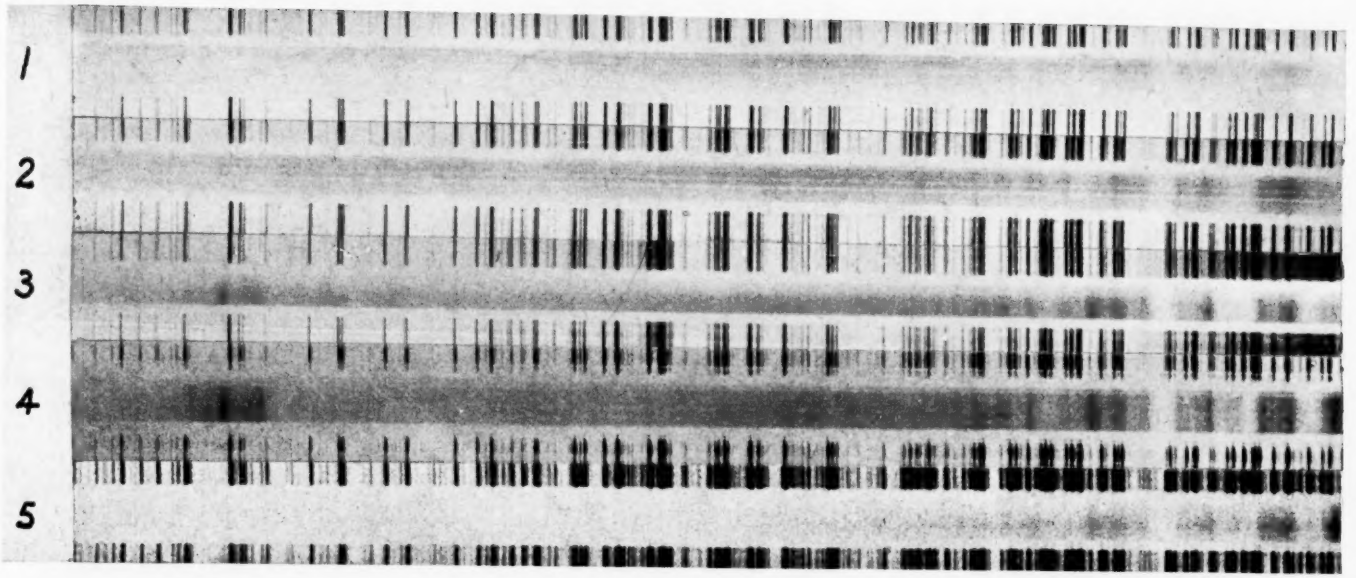

SPECTRA OF NOVA PUPPIS 1942

(1) 1942 November $24^{d}11^{h}55^{m}$ U.T.; (2) 1942 November $26^{d}9^{h}42^{m}$ U.T.; (3) 1942 December 30^{d} $m8^{h}25^{m}$ U.T.; (4) 1943 February $12^{d}5^{h}43^{m}$ U.T.; (5) 1943 March $29^{d}3^{h}57^{m}$ U.T.

While the spectrum of N Puppis is not that of an ordinary fast nova in all details, the general trend of spectral development is not marked by the unusual features of the light-curve and follows the pattern set by the fast novae in general.[5] More particularly, if we say that any specific spectral development occurs at magnitude Δm, where Δm is measured from light-maximum, then $\Delta m > \overline{\Delta m}$, the average Δm for this specific development found by McLaughlin[5] from four fast and three slow novae. For slow novae there is a tendency for Δm to be less than $\overline{\Delta m}$. Analogous statements can be made for N Puppis and fast and slow novae in general in regard to the temporal development of the spectrum, if we measure time in mean relative Δt units and use the time of light-maximum as zero point.

The first spectrograms of N Puppis taken at the McDonald Observatory with the quartz Cassegrain spectrograph and the 500-mm camera[13] were obtained on the mornings of November 13 and 14.

The general character of the spectrum may be seen from the reproductions in Plate XVI. The absorption lines are exceedingly broad and diffuse, with hazy emission borders on their redward sides. From a visual examination of the plates the absorption components in the photographic region appear to be between 10 and 15 A wide. A microphotometer tracing makes it appear that the violet extension of an absorption component is terminated only by the emission component of the next line toward the violet end of the spectrum.

A compilation of measured wave lengths, probable identifications, and certain other data for the spectrum as observed on these dates is made in Table 1. In this table, as well as in others to follow, wave lengths are corrected for the orbital velocity of the earth, and identifications are restricted, in general, to atoms and ions believed to be appreciable contributors to the observed lines. Doubtful identifications are noted with a question mark. Values in parentheses have not been included in the means because of suspected uncertainties in the values so bracketed.

The probable error of a tabulated wave length is of the order of ± 0.9 A in the region of the K line of *Ca* II and increases to perhaps ± 2.5 A at $H\alpha$.

The lines observed in the nova are satisfactorily represented by the strongest lines of *H*, *O* I, [*O* I], *Na* I, *Mg* II, *Si* II, *Ca* I, *Ca* II, *Ti* II, *V* II, *Cr* II, *Mn* II, *Fe* II, *Ni* II, and *Sr* II(?). *Fe* I does not appear to be present to any important degree.

The hydrogen series can be followed with certainty to *H* 14, and more members are undoubtedly present, since there is absorption in the region of *H* 15, *H* 16, etc.; but the lines are not sufficiently well separated to be seen individually, and there are also complications owing to blends and emissions. On November 13, a red emission border was certainly present at $H\delta$, was overpowered by the H line of *Ca* II in the case of $H\epsilon$, and may be present on $H\zeta$; but this last observation is very doubtful. In addition, emission borders are certainly present on the lines of *Ca* II, *Fe* II, and *Ti* II on November 13, and it seems probable that other elements may be present in the emission. The true level of the continuous spectrum is difficult to locate, however, and a more exact statement of elements present in emission is impossible. On November 14 the emissions had become stronger, and it appears that all lines except, perhaps, the faintest, have emissions toward the redward. The emission border of *H* 10 is plainly visible. *H* 11 is completely overpowered by the emission border of the *Ti* II blend measured at 3746 A but otherwise would probably also show an emission border. The disappearance of *H* 11 is, in fact, good evidence of the increase in intensity of emission. Faintly visible on November 13, *H* 11 is quite invisible on plates of November 14, owing to the increased emission of *Ti* II.

From a comparison of line intensities of lines in N Puppis with the intensities of corresponding lines in α Cygni, made in the manner described by Wyse,[14] it appears that

[13] Dispersion, 40 A/mm at λ 3933.

[14] *Op. cit.*

TABLE 1

THE ABSORPTION SPECTRUM OF N PUPPIS 1942
(November 13, 14, 1942)

November 13.5 λ	Δλ	v Km/Sec	November 14.5 λ	Δλ	v Km/Sec	λ, *I* α Cygni*	Laboratory Identification
			3430.8	−12.1	−1060	42.1(7), 44.3(4n)	42.0 *Mn* II (100), 44.3 *Ti* II (30)
			3449.0	−11.3	− 980	60.3(5), (68.7(3))	60.3 *Mn* II (75), (68.7 *Fe* II (8))
			3464.7	− 9.4	− 810	74.1(6)	74.0 *Mn* II (50), 74.2 *Mn* II (40)
			3527.0	(−14)	(−1190)	35.5(2), *45.1(3)*	35.4 *Ti* II (40), 45.1 *V* II (1000)
			3547.0	(− 9)	(− 760)	*56.8(3)*	56.8 *V* II (1500)?
			3563.7			76.8(4), 81.2(4), 85.3(6), 89.5(2),	76.8 *Ni* II (3), 85.3 *Cr* II (60), 85.5 *Cr* II (40)
			3575.8			96.9(2)	89.7 *V* II (1000), 92.0 *V* II (800), 96.1 *Ti* II (60)
			3601.9	−15.6	−1300	13.7(4bn), 24.6(2)	13.2 *Cr* II (20), 24.8 *Ti* II (70)
			3620.9	−10.7	− 890	31.6(6)	31.5 *Cr* II (50), 31.7 *Cr* II (40)
			3635.0	−10.8	− 890	41.2(2), *50.4(1)*	41.3 *Ti* II (100), 50.4 *Cr* II (40)
			3651.9	−10.2	− 840	*59.6(2), 62.1(2), 64.7(2)*	59.8 *Ti* II (60), 62.2 *Ti* II (40), 65.0 *Cr* II (30)
3671.6	−10.7	− 880	3671.2	−11.1	− 910	77.9(4), 85.2(6)	77.7 *Cr* II (40), 77.9 *Cr* II (50), 85.2 *Ti* II (250)
3696.6	−12.9	−1050	3696.4	−13.1	−1060	03.8(10), 06.1(4), 12.1(10), 15.4(4)	03.9 *H* 16, 06.0 *Ca* II (10nr), 12.0 *H* 15, 13.0 *Cr* II (35), 15.5 *V* II (1200)
			3713.1	−11.6	− 940	21.9(10), 27.4(4)	21.9 *H* 14, 27.4 *V* II (1000), 27.4 *Cr* II (40)
3726.5	−12.7	−1020	3726.7	−12.5	−1010	34.4(10), 36.9(4), (41.5(4)), (47.7(4))	34.4 *H* 13, 36.9 *Ca* II (11nr), 37.3 *V* II (800), 41.6 *Ti* II (50), 45.8 *V* II (800)
3746.0	−12.3	− 980	3746.0	−12.3	− 980	50.1(10), 59.4(6), 61.4(6)	50.2 *H* 12, 59.3 *Ti* II (200), 61.3 *Ti* II (200)
3786.0	−11.9	− 940	3786.3	−11.6	− 920	97.9(15)	97.9 *H* 10
3821.5	−13.9	−1090	3821.8	−13.6	−1070	35.3(20)	35.4 *H* 9
3848.7	−16.9	−1320	3853.9	−11.7	− 910	*65.4(2)*	65.6 *Cr* II (75)
3877.0	−12.1	− 940	3874.8	−14.3	−1110	89.1(20)	89.1 *Hζ*
3890.4	−17.1	−1320				00.6(4), 13.6(7)	00.5 *Ti* II (70), 13.5 *Ti* II (60)
3918.5	−15.1	−1160	3917.7	−15.9	−1240	33.6(15)	33.7 *Ca* II (400R)
Interstellar K			Interstellar K				
3953.4	−15.1	−1150	3952.6	−15.9	−1210	68.5(20)	68.5 *Ca* II (350R) (*Hε*)
Interstellar H			Interstellar H				
			3999.0	−12.4	− 930	12.4(4)	(05.7 *V* II (800)), 12.4 *Ti* II (4), 12.5 *Cr* II (30)
Four lines faintly visible but not measured			4012.0	−14.5	−1080	24.5(4), 28.3(3)	24.6 *Fe* II (5), 28.3 *Ti* II (7)
			4039.1	−14.7	−1090	53.8(4)	53.8 *Ti* II (3), —?
			4054.5	−13.0	− 960	67.1(4), (77.6(3))	67.0 *Ni* II (3), (77.7 *Sr* II (400r))
4087.8	−14.0	−1030	4087.3	−14.5	−1060	01.7(20)	01.8 *Hδ*
4159.7	−14.0	−1010	4152.1 v.e.	(−21)	(−1520)	63.6(4), 73.5(8), 78.9(8)	63.7 *Ti* II (40), 71.9 *Ti* II (30), 73.5 *Fe* II (8), 78.9 *Fe* II (8)

* Wave lengths and intensities are from Wyse, *Lick Obs. Bull.*, **18,** 129, 1938, unless given in italics. Wave lengths and intensities in italics are not in Wyse's table and are from Struve, *Ap. J.*, **90,** 699, 1939.

TABLE 1—*Continued*

November 13.5 λ	Δλ	v Km/Sec	November 14.5 λ	Δλ	v Km/Sec	λ, *I* α Cygni	Laboratory Identification
4219.4	−13.8	− 980	4215.5 v.e.	(−17.7)	(−1260)	27.0(1), 33.1(12)	(15.5 *Sr* II (300r)), 26.7 *Ca* I (500), 33.2 *Fe* II (11)
4283.5	−13.4	− 940	4280.3	(−16.6)	(−1160)	90.3(4), 94.1(4), 96.5(4), 00.0(4), 03.3(4–5)	90.2 *Ti* II (50), 94.1 *Ti* II (40), 96.6 *Fe* II (6), 00.1 *Ti* II (60), 03.2 *Fe* II (8)
4324.8	−15.7	−1090	4321.7	−18.8	−1300	40.5(20)	40.5 *Hγ*, (51.8 *Fe* II (9))
4365.1?	−20.3	−1400	.....	.....	.....	85.4(5)	85.4 *Fe* II (7)
4375.2	−15.5	−1060	4378.1 br. bl.	(−14)	(− 960)	90.7(3n)	90.6 *Mg* II (10), —?
4384.2?	−12.6	− 860	.....	.....	.....	95.0(5), 99.8(3)	95.0 *Ti* II (60), 99.8 *Ti* II (35)
4407.1	− 9.7	− 660	4403.8	−13.0	− 890	16.9(5)	16.8 *Fe* II (7)
4432.2	−14.5	− 980	4430.9	−15.8	−1070	43.8(4)	43.8 *Ti* II (50), 49.6 *Ti* II (60)
4456.2	−14.1	− 950	4453.5	−16.8	−1130	68.5(4)	68.5 *Ti* II (50), 72.0 *Ti* II (50n)
4470.2	−14.7	− 990	4471.7	−13.2	− 890	81.3(12), 89.2(3–4), 91.4(4)	81.1, 81.3 *Mg* II (100), 89.2 *Fe* II (4), 91.4 *Fe* II (5)
4493.3	−12.1	− 810	4491.9	−13.5	− 900	01.3(3–4), 08.3(5)	01.3 *Ti* II (40), 08.3 *Fe* II (8)
4509.3	−10.1	− 670	4507.3	−12.1	− 800	15.4(5), 20.2(4), 22.7(5)	15.3 *Fe* II (7), 20.2 *Fe* II (7), 22.6 *Fe* II (6)
4536.8	−16.6	−1100	4536.7	−16.7	−1110	49.5(12), 56.0(6), 58.7(6)	49.5 *Fe* II (10), 49.6 *Ti* II (60n), 55.9 *Fe* II (8), 58.7 *Cr* II (100)
4569.3	−16.0	−1050	4565.3	−20.0	−1310	83.9(8), 88.2(3–4)	83.2 *Fe* II (11), 88.2 *Cr* II (75)
4609.8	.....	.....	4607.4	(−21.9)	(−1450)	29.3(4)	29.3 *Fe* II (7)
.....	.....	.....	4648.1	(−20.4)	(−1300)	66.8(2–3), 70.2(2)	66.8 *Fe* II (2), 70.2 *Fe* II (0)
.....	.....	.....	4717.9	−14.8	− 940	31.5(3–4)	31.4 *Fe* II (3), 34.1 *Fe* II (3)
.....	.....	.....	4753.1	(−24.9)	(−1570)	79.9(2)	78.0 *Ti* II (1), —?
.....	.....	.....	4799.5	−16.6	−1040	05.1(6), 24.4(8)	05.1 *Ti* II (2), 24.1 *Cr* II (75)
.....	.....	.....	4839.1	−22.2	−1380	61.3(20)	61.3 *Hβ*
.....	.....	.....	4903.9	−20.0	−1220	24.1(10)	23.9 *Fe* II (12)
.....	.....	.....	4998.8	−19.6	−1180	18.4(10)	18.4 *Fe* II (12)
.....	.....	.....	5148.7 br.	−20.3	−1180	69.0(10)	69.0 *Fe* II (12)
.....	.....	.....	5216.0	−20.5	−1170	34.7(6), 37.4(5)	34.6 *Fe* II (7), 37.3 *Cr* II (75)
.....	.....	.....	5259.0	−17.0	− 970	75.8(8)	76.0 *Fe* II (7)
.....	.....	.....	5297.4	−19.2	−1090	16.7(8)	16.6 *Fe* II (8)
.....	.....	.....	5350.1	−12.9	− 720	62.9(5)	62.9 *Fe* II (5)
.....	.....	.....	5869.1	−24.2	−1240	89.9(15), 95.9(12)	90.0 *Na* I (8R), 95.9 *Na* I (10R)
.....	.....	.....	6133.6†	−23.5	.....	56.1(2), 58.1(2)	56.0 *O* I (7), 56.8 *O* I (8), 58.2 *O* I (10)
.....	.....	.....	6216.2†	−26.4	.....	38.5(5), 47.6(5)	38.4 *Fe* II (1), 47.6 *Fe* II (3)
.....	.....	.....	6278.4†	.....	.....	.....	Space between emission components of *Fe* II 6216.2 and [*O* I] 6300, which is a faint emission band
.....	.....	.....	6333.0†	−24.9	.....	47.1(12), 71.5(10)	47.1 *Si* II (10), 71.4 *Si* II (8)
.....	.....	.....	6397.6†	−19.3	.....	16.9(3), (32.8(2))	16.9 *Fe* II (1), (32.7 *Fe* II)
.....	.....	.....	6432.7†	−23.7	.....	56.6(6)	56.4 *Fe* II (3), (*O* I)?
.....	.....	.....	6531.3†	−31.5	.....	*Hα*	62.8 *Hα*

† It is not certain that these measures refer to true absorption lines. It seems likely that they apply to the space between emission components (which are plainly visible) or to an area adjacent to an emission line which has appeared light by contrast. The identifications, of course, are valid for the emission lines.

the excitation temperature of N Puppis was lower than that of α Cygni during the time at which these plates were taken. In general, those lines in the nova having lower excitation potentials of less than approximately 2 e.v. are strengthened relative to those lines whose lower excitation potentials lie above 2 e.v., when compared to α Cygni. This is a situation quite similar to the one found for N Aquilae 1918 by Wyse,[14] who states that in the case of N Aquilae, however, there are certain departures from this rule which appear to be real. *Mg* II λ 4481, lower E.P. = 8.8 e.v., and *Fe* II λ 4233, lower E.P. = 2.6 e.v., are stronger than might be expected, judging from their excitation potentials. In the spectrum of N Puppis, the *Mg* II line seems normally weakened, but the *Fe* II line at λ 4233 is quite strong and exhibits the same discrepancy found in N Aquilae. In addition, it appears that the *Fe* II line at λ 4173, having the same lower level as λ 4233, is also strong in N Puppis. It would be of interest to check the intensity of this line in N Aquilae.

It is doubtful, however, that significant results can be obtained from a study of line intensities in a nova if the lines are studied in groups, the members of which are alike only in having similar lower excitation potentials. Fluorescence phenomena and the dilution of radiation in the expanding nova shell are factors of major importance, as Struve has shown in his study of N Herculis 1934.[15]

In N Herculis, McLaughlin's absorption II was present from the end of December until the latter part of March. The lines were strong and sharp, and no violent changes took place in them. Struve states[16] in regard to *Mg* II λ 4481:

> While the spectrum, as a whole, changed very little in appearance during the latter part of December and all of January, the *Mg* II line, which was at first exceedingly strong, rapidly faded, so that by January 5 it was quite inconspicuous and by January 11 it had completely disappeared.

This description makes it clear that considerations of line intensities should involve, besides the excitation potentials, a study of the types of levels involved in the transitions of the observed lines, as well as the relaxation times of the various lines in a given expanding shell. It is possible that the *Mg* II "anomaly" might not have appeared in N Aquilae if Wyse had determined the excitation temperature again a few days after his first determination was made. On the other hand, it is possible that it might have appeared in N Puppis if the star had been examined a day earlier. McLaughlin[17] gives an estimate of the velocity of *Mg* II for November 12. Since the *Mg* II line at λ 4481 is very faint and presumably blended on November 13.5, it is possible that *Mg* II was stronger on November 12.

Likewise, the intensity of the *Fe* II lines in both stars is not surprising. The lines studied are more intense than might be anticipated for two reasons: (1) these particular *Fe* II lines have metastable lower levels, and these are overpopulated relative to the nonmetastable levels, because of the dilution of the radiation in the nova shell; (2) the lines under consideration arise from low-lying levels, which are populated in preference to higher levels. It is possible that *Fe* II lines, other than the one specifically mentioned by Wyse, were also somewhat strong in N Aquilae. Such a possibility seems to be distinctly probable for N Puppis, but the diffuse character of the lines, together with the considerable amount of blending present, makes a detailed study of line intensities difficult, if not impossible.

The radial velocities obtained from the absorption lines in N Puppis are given in Table 2.

The velocities of November 13.5 are in good agreement with the estimates of velocity for the morning of November 12 made by McLaughlin:[17] hydrogen, −1100 km/sec; *Fe* II and *Ti* II, −900 km/sec; *Mg* II, −750 km/sec. If the line measured at λ 4471 is at-

[15] *Proc. Amer. Phil. Soc.*, **81**, 211, 1939. [16] *Ibid.*, p. 225.

[17] *Harvard Announcement Cards*, No. 639, November 14, 1942.

tributed solely to *Mg* II, there is also agreement as to the velocity of *Mg* II. It seems probable, however, that the measured line is a blend of *Mg* II and two *Fe* II lines.

McLaughlin states that the *H* lines were "just suspected double" on November 12. This observation cannot be confirmed from the McDonald plates of November 13.5, but the lines are very diffuse, and the dispersion used may be such that it would prevent the making of such an observation. Humason and Sanford[18] state that on November 13 *Hα* appeared to have increased its displacement toward the violet—a fact which may indicate the further appearance of the component suggested by McLaughlin a day earlier.

In order to check the reality of the differences in velocity obtained for *H* on the two dates, a third plate taken on November 14 was measured. This plate was overexposed and shows only the deeper parts of the stronger absorption lines. Four *H* lines yielded a velocity of −1165 km/sec.

The structure of the absorption lines appears to be rather different on the two dates. On the plates of November 14 the strengthening emissions appear to have cut into the red edges of the absorption lines slightly more than on the previous day. At the same time the absorption components appear to have expanded somewhat toward the violet, and the contour of the stronger absorption lines is more flattened in the deeper parts

TABLE 2

RADIAL VELOCITIES OF N PUPPIS

	Nov. 13^d5 U.T.	Nov. 14^d5 U.T.
All lines measured	−1010 km/sec (27)*	−1020 km/sec (43)
H lines	−1010 km/sec (5)	−1140 km/sec (6)
Fe II–*Ti* II lines	− 930 km/sec (9)	−1070 km/sec (18)

* The number in parentheses indicates the number of lines included in the mean.

than on the previous morning. The general appearance of the lines strongly suggests a violet component accompanying the strongest lines, that is, the lines of *H*, *Ca* II, *Fe* II, and *Ti* II. Tentative measures of both spectrograms and microphotometer tracings place this suspected component about 1000 km/sec to the violet of the corresponding line in the principal spectrum. It is possible that this is the component suspected by McLaughlin on November 12 and that it was not sufficiently strong to show on the McDonald spectrograms of November 13. These suspected components, which would explain the velocity differences on the two days very satisfactorily, fit well with the criteria given by McLaughlin[19] for the "diffuse enhanced absorption."

Unfortunately, no spectrograms of N Puppis were taken at the McDonald Observatory during the next eight nights, and further information regarding the development, or even the existence, of these suspected components must await the discussion of a more complete set of observations.

The differences in velocity exhibited by different atoms seem securely established and are suggestive of stratification in the nova shells. It is not impossible, however, that the measurements have been systematically influenced by the emissions which vary in intensity rather systematically with *H*, *Fe* II, *Ti* II, etc. This explanation is analogous to that of Merrill[20] for the difference in the velocities determined from forbidden and permitted emission lines of the same element.

Measures of the interstellar H and K lines of *Ca* II on three plates yield a velocity of +26.1 km/sec. Humason and Sanford[21] found a velocity of +23.8 km/sec from the interstellar H and K lines of *Ca* II, λ 4226 of *Ca* I, λ 4300 of *CH*, and D 1 and D 2 of *Na* I. They

[18] *Op. cit.*, p. 257.

[19] *Pub. U. Michigan Obs.*, **8**, No. 12, 156, 1943.

[20] *Mt. W. Contr.*, No. 530, p. 18; *Ap. J.*, **82**, 430, 1935.

[21] *Op. cit.*, p. 257.

also observed two weak components to the redward of the strong principal interstellar H and K lines. The velocities measured for those weak components are +44.1 km/sec and +58.2 km/sec. These weak components are not visible as such on the McDonald spectrograms.

By November 23.5, the date of the next McDonald observation, the spectrum (see Strip 1, Pls. XVII and XVIII) had become one composed primarily of emissions. Absorption components seem to be confined to the lines of *H*, *Ca* II, and *Na* I. There is a moderately strong continuous spectrum.

The following elements appeared in the spectrum during the period November 23.5–26.5: *H*, *He* I, *He* II, *C* I(?), *C* II, *N* II, [*N* II], *N* III(?), *O* I, [*O* I], *O* II, *Si* II, [*S* II](?), *Ca* II, *Fe* II, and possibly the unidentified lines found in N Aquilae 1918 at λ 6001±, λ 6009± by Wyse.[12]

The Balmer series can be traced as far as *H* 18, and the Balmer continuum is strong. The *He* I triplets are stronger than the corresponding singlets. *He* II λ 4686 first appeared on plates taken November 25.5. It was definitely not present on November 24.5. The structure of this line is different from that of the other lines in general and consists of two fairly narrow maxima, each approximately 3–4 A wide, with centers separated by approximately 17 A. The violet component is definitely stronger than the red one and is also probably more sharply defined at the edges. This same structure seems to be shared by *He* I, though not in such a pronounced form, and possibly by [*O* I] also. The emission bands in general have widths corresponding to 1500 km/sec. This is probably an upper limit. There is undoubtedly a photographic density effect involved to some degree in the measures of width. The structure of a band may be seen in the reproductions. At the violet side of a band there is a pronounced sharp maximum, then a rather shallow minimum extending slightly to the redward of the middle of the band, and then a broad maximum. Within the broad minimum there are three narrow emission minima visible on the McDonald plates. The violetward and redward minima are each about 90 km/sec wide and are displaced from the middle component by amounts equivalent to 330 km/sec and 300 km/sec, respectively. The violet component is about 270 km/sec wide and is displaced to the violet of the normal position of the line by about −20 km/sec. This agrees generally with the description given by Humason and Sanford,[22] who state: "The emission band at $H\gamma$ appeared to have three absorption components within it, the middle one approximately in the undisplaced position for $H\gamma$ and the other two about 5 A on either side." The observation applies, presumably, to November 15.

Again, in discussing observations of emission lines of N Puppis made with the 100-inch coudé spectrograph on April 19, 1943, Sanford[23] remarks:

> These lines are interesting because their densities are far from uniform throughout their widths, minima resembling wide absorption lines being conspicuous in lines with proper exposure. The positions of these minima are expressed by the following Doppler shifts:
>
> | | |
> |---|---|
> | −340 km/sec | +220 km/sec |
> | − 75 | +305 |
> | + 15 | +420 |
> | +145 | +495 |
>
> It is probable that the minima are the results of irregularities in the matter ejected from the star, for they appear in forbidden as well as permitted lines.

Once more referring to the spectrum as seen in November, the K line of *Ca* II has a width of approximately 1350 km/sec, approximately 91 per cent of the width of the other lines. Except for the strong, sharp, interstellar K line, it is quite devoid of any internal structure. These two facts suggest a stratification for *Ca* II which differs from the other elements, such as *H*.

[22] *Op. cit.*, p. 257.

[23] *Pub. A.S.P.*, **55**, 196, 1943.

PLATE XVIII

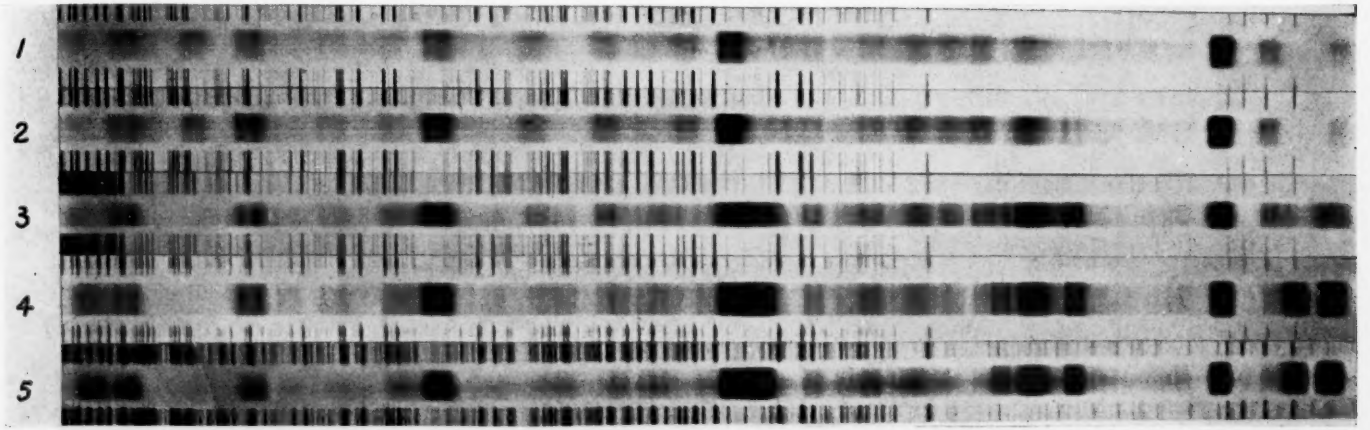

SPECTRA OF NOVA PUPPIS 1942

(1) 1942 November $24^d11^h55^m$ U.T.; (2) 1942 November $26^d9^h42^m$ U.T.; (3) 1942 December $30^d8^h25^m$ U.T.; (4) 1943 February $12^d5^h43^m$ U.T.; ()5 1943 March $29^d3^h57^m$ U.T.

PLATE XIX

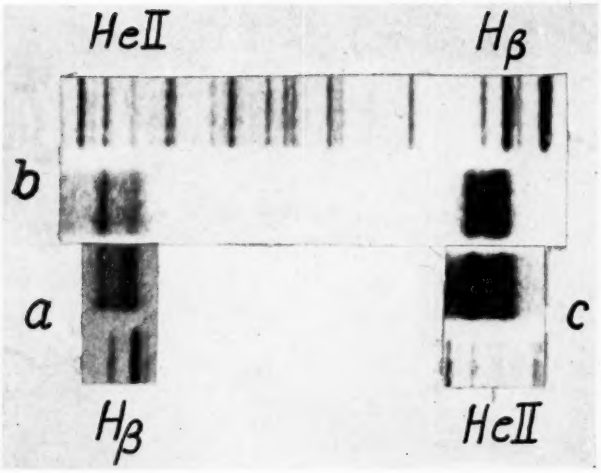

COMPARISON OF LINE STRUCTURE OF *He* II λ 4686 AND *Hβ* ON DECEMBER 22, 1942

Exposure times: (*a*) 3^{m}, (*b*) 8^{m}, (*c*) 18^{m}

C I.—There is a very faint emission extending from λ 4756 to λ 4782. It may be tentatively represented by the group of *C* I lines between λ 4762 and λ 4782, which are identified as a blend in N Cygni 1920 by Baldwin.[24] The identification needs confirmation.

[*N II*].—The transition $^1D - {}^1S$ at λ 5755 is faintly visible.

N III.—The strong fluorescence line λ 4640.64 is faintly visible on November 26.

[*O I.*]—The three forbidden transitions in the region observed—$^3P_1 - {}^1D$, λ 6364, $^3P_2 - {}^3D$, λ 6300, and $^1D - {}^1S$, λ 5577—are all present. The line at λ 6300 is remarkably strong, surpassing in intensity all lines observed to the redward of *Hβ* with the exception of *Hα*.

[*S II*].—The $^4S - {}^2P_{\frac{3}{2}}$ and $^4S - {}^2P_{\frac{1}{2}}$ transitions at λ 4076.5 and λ 4068.5 are probably faintly present, though blended with *O* II.

After a lapse in time of nearly a month, the nova was again observed during the period December 22, 1942, to January 1, 1943. During the interval of no observations the forbidden lines of *O* I, *N* II, and *S* II had increased in strength, and new lines of *O* III, *N* III, [*Ne* III], and [*Fe* II] had appeared. The *He* II lines had strengthened; Bowen's fluorescence mechanism had become of great importance. The K line of *Ca* II had decreased in strength. It is just visible on a strongly exposed plate of December 30. The general development can be seen in Plates XVII and XVIII.

Wave lengths and identifications for this period are given in Table 3. In addition to the lines listed, the fluorescent lines of *O* III at λ 3444.1 and λ 3749.9 can be identified by inspection. Both are strong. The violet emission maximum of λ 3444 is especially marked. Faint, unidentified emission lines of intensity approximately one-half to one-third that of *O* III λ 3444 appear at 3434 A and 3467 A. No effort has been made to make measures in the crowded region of *H* lines for $\lambda < 3800$ A, although a number of fluorescent *O* III lines are located in this region of the spectrum.

The fluorescent *N* III lines in the λ 4640 region are very prominent. Their structure follows that of *He* II λ 4686 precisely, as far as can be determined with the existing blending of *N* II, *N* III, and *O* II in this crowded region. The main differences between the *He* II lines and the "normal" lines (as exemplified by *H*) are (1) the rather dark area between the violet and red maxima of *H* and the lack of darkening between the maxima of *He* and (2) the rather broader red maximum of *H*, compared to *He*, as seen on any one plate. This last is, however, probably an illusion, at least in part. On December 22, three plates of N Puppis were taken; the exposure times are: (*a*) 3^m, (*b*) 8^m, (*c*) 18^m. The intensity of the *He* II line on *b* is quite comparable to the intensity of *Hβ* on *a*. A comparison of these plates brings out the intensity differences of the red and violet components very well. The intensity of *He* II on *c* is quite comparable to the intensity of *Hβ* on *b*. A comparison of these brings out the similarities in widths of maxima. These comparisons are exhibited in Plate XIX. It is probable that the only real difference in the internal structure of *He* and *H* lines is the difference in intensity of violet and red components. The three emission minima, mentioned in the previous description of line structure, are not observed in λ 4686. If they are present, they are too faint to be seen on the McDonald plates. The widths of the lines at this period correspond to approximately 1500 km/sec, the same value found in November.

In addition to *He* II λ 4686, the $4^2F^0 - m^2G$, etc., series of *He* II is present, at least as far as $m = 19$, and possibly more members are present. Blends make a precise determination of the series extent difficult. The observed *He* I series has not changed appreciably from November 26.

The [*O* III] lines had all appeared before December 22 and are easily visible on a spectrogram taken that morning. *O* III lines are also prominent. It is just possible that the *O* IV lines at λ 4783.4 and λ 4798.3 are present, but the observation is a questionable one.

[24] *Pub. U. Michigan Obs.*, **8**, No. 5, 1940.

TABLE 3

EMISSION SPECTRUM OF NOVA PUPPIS 1942

DECEMBER 22–JANUARY 1				FEBRUARY 23			
Feature	λ	*I*	Identification	Feature	λ	*I*	Identification
v.e.	3789.0			v.e. max	2752.2		3750.2 *H* 12
v. max	3791.8	2–3	3797.9 *H* 10	e	3759.1	2	
r. max	3805.2		3813.5 *He* II	e	3762.3		3759.9 *O* III (9)
r.e.	3808.7	1		e	3769.2	2	3770.6 *H* 11
r.e.	3820.4			r.e.	3778.7		
v.e.	3825.5			v.e.	3791.0		
v. max	3828.8			r.e. max	3792.7		
min	3833.4	3	3835.4 *H* 9	min	3793.9		
r. max	3841.5			min	3797.7	2	3797.9 *H* 10
r.e.	3846.2			min	3801.6		
r.e. max	3854.8			e. max	3804.6		
max	3856.6			e. max	3806.7	1	3913.5 *He* II
e. max	3859.2	1–2	3862.6 *Si* II (6), 3856.0 *Si* II (8), 3858.1 *He* II, 3868.7 [*Ne* III]	r.e.	3820.0		
max	3861.5			v.e.	3827.3		
e. max	3863.2			e. max	3830.2		
r.e. band	3872.0			min	3830.9		
v.e.	(3882.0)			min	3835.0	3	3835.4 *H* 9
v. max	3882.6			min	3838.8		
min	3888.2	4	3889.1 *H* 8, 3888.6 *He* I (10)	e. max	3840.5		
r. max	3895.6			r.e.	3843.3		
r.e.	3903.1						
v.e.	3917.6			ext. from	3848±		
Interstellar K		0–1	3938.3 *Fe* II (2), 3935.9 *Fe* II (6), 3933.7 *Ca* II (K) (400R)	v.e.	3855.8		
r.e.	3942.0			v.e. max	3861.1		3856.0 *Si* II (8), 3858.1 *He* II
				r.e. of above max	3863.1		3862.6 *Si* II (6)
v.e.	3956.6			v.e. max	3864.1	3	
v. max	3963.8			r.e. of above max	3866.9		3868.7 [*Ne* III]
min	2968.2	4	3970.1 *He*, 3961.6 *O* III (8)	v.e. sharp max	3869.7		
r. max	3976.1			r.e. of above max	3871.3		
r.e.	2982.5			v.e. flat min	3877.0		
v.e.	3985.9			r.e. of above min	3881.9		
v. max	3988.4			r.e. of above max	3884.0	4	3889.1 *H* 8, 3888.6 *He* I (10)
min	3993.3	1–2	3995.0 *N* II (10)	v.e. max	3890.1		
r. max	4000.6			r.e.	3897.8		
r.e.	4007.4			v.e.	3960.8		
v.e.	4016.4			e. max	3964.5		
v. max	4019.8			min	3965.5	6	3970.1 *He*, 3967.5 [*Ne* III], 3961.6 *O* III (8)
min	4025.0	1–2	4024.6 *Fe* II (5), 4026.2 *He* I (5)	min	3969.4		
r. max	4032.1			min	3973.5		
r.e.	4037.6		4041.3 *N* II (5)	r.e.	3979.1		
a sharp max	4047.7						

TABLE 3—*Continued*

TABLE 3—*Continued*

December 22–January 1				February 23			
Feature	λ	*I*	Identification	Feature	λ	*I*	Identification
v.e.	4059.6			v.e.	3987.0		
v.e. of $H\delta$	4085±	3	4068.6 [*S* II], 4076.2 [*S* II], 4072.2 *O* II (8), 4075.9 *O* II (10)	e. max	3989.6	1	3995.0 *N* II (10)
v. max	4096±			e. max	3999.7		
min	4100±	6	4101.8 $H\delta$, 4097.3 *N* III (10), 4103.4 *N* III (9)	r.e.	4005.0		
r. max	4107±						
r.e.	4118.3	0(?)	4120.8 *He* I (3), 4124.8 *Fe* II (1)(?), 4128.7 *Fe* II (3)(?),	v.e.	4018.2		
ext. to	4130±		4122.6 *Fe* II (4)(?)	e. max	4021.0	1	4026.2 *He* I (5), (4025.6 *He* II)
				e.	4029.5		
v.e.	4135.1	1	4143.8 *He* I (2)	e.	4037.7	0	4041.3 *N* II (5)
r.e.	4157.0			v.e.	4049.0		
v.e.	4168.1						
v. max	4172.1			v.e.	4062.0	4	4068.6 [*S* II], 4076.2[*S* II], 4075.9 *O* II (10), 4072.2 *O* II (8),
min	4176.4	3–2	4173.5 *Fe* II (8), 4178.9 *Fe* II (8)	e.	4088.9	>10	4068.9 *Ca* II (7), 4070.4 *C* III (8)
r. max	4182.7			r.e.	4112.9	<0	4101.8 $H\delta$, 4097.3 *N* III (10), 4103.4 *N* III (9)
r.e.	4187.6			ext. to	4128±		4120.8 *He* I (3), 4124.8 *Fe* II (1)(?), 4218.7 *Fe* II (3)(?)
v.e.	4191.1		4185.5 *O* II (8), 4189.8 *O* II (10)	v.e.	4135±	0–1	4143.8 *He* I (2)
v. max	4193.2			r.e.	4152±		
min	4199.8	1–2	4199.9 *He* II, 4195.7 *N* III (5), 4200.0 *N* III (6)	v.e.	4169.8		
r. max	4206.3			e.	4179.2	2	4173.5 [*Fe* II](8),
r.e.	4208.9			e.	4186.6	2	4178.9 *Fe* II (8)
				e.	4191.7		4195.7 *N* III (5) 4187.1 *C* III (10), 4185.5 *O* II (8),
v.e.	4224.2			e.	4198.0	2	4199.9 *He* II 4189.8 *O* II (10)
r.e. of v. max	4227.8			r.e.	4209.3		4200.0 *N* III (6)
min	4234±	4	4233.2 *Fe* II (11), 4237.0 *N* II (6), 4241.8 *N* II (8)				
r. max	4238±			v.e.	4225.2		
r.e.	4242.2		4244.0 [*Fe* II]	e.	4235.5	1	4233.2 *Fe* II (11)
v.e. min	4253.5			e.	4241.1	1–2	4244.0 [*Fe* II], 4237.0 *N* II (6), 4241.8 *N* II (8)
r.e. min	4259.3			e.	4251.6		
r.e. sharp max	4261.8		4267.0 *C* II (8), 4267.3 *C* II (10), 4258.2 *Fe* II (3)(?)				
r.e. min	4268.8			v.e.	4258.9		
v.e. max	4279.0		4276.8 [*Fe* II], 4273.3 *Fe* II (3)(?)	e.	4268.9	1	4267.0 *C* II (8), 4267.3 *C* II (10)
r.e. max	4285.5			e.	4275.8	4	4276.8 [*Fe* II]
v.e. max	4293.9	2–3	4287.3 [*Fe* II]	e.	4281.0	2	4273.3 *Fe* II (3)(?) 4287.4 [*Fe* II]
r.e. max	4297.9		4296.6 *Fe* II (6)	r.e.	4297.1		
v.e. max	4308.7		4303.2 *Fe* II (8)				
r.e. max	4314.4			v.e.	4309.8	3	4303.2 *Fe* II (8)
				e.	4329.5	>10	4340.5 $H\gamma$, 4363.2 [*O* III]
v.e.	4323±			r.e.	4381.5		
v. max	(4333)						
min	(4338)	9	4340.5 $H\gamma$	v.e.	4406.9		
r. max	(4346)			e. max	4412.1	2	4413.8 [*Fe* II], 4416.3 [*Fe* II], 4416.8 *Fe* II (7), 4414.9 *O* II (10),
narrow max	(4348)		4351.8 *Fe* II (9)	e. max	4419.6		4417.0 *O* II (8)
r.e. max	(4350)			r.e.	4426.2		
v.e. broad min	(4360)		4363.2 [*O* III] 4359.1 [*Fe* II](?)				
broad min	(4367)	7	4369.4 *Fe* II (2)	v.e.	4439.2	2	4447.0 *N* II (10), 4452.1 [*Fe* II]
ft. r. max	(4373)			e.	4462.7		
r.e.	4394.6		4379.1 *N* III (10n), 4385.4 *Fe* II (7)	e. max	4466.3		4458.0 [*Fe* II]
				min	4467.1	4	4471.5 *He* I (5)
				min	4470.6		
				min	4476.3		
				r.e. max	4480		

TABLE 3—*Continued*

Feature	λ	*I*	Identification
December 22–January 1			
v.e	4405.0		
v. max	4409.0		
min	4414.8	3	4416.8 *Fe* II (7), 4414.9 *O* II (10), 4417.0 *O* II (8), 4413.8 [*Fe* II], 4416.3 [*Fe* II]
r. max	4422.1		
r.e.	4427.7		
v.e.	4436.0		4447.0 *N* II (10), 4452.0 [*Fe* II](?)
v.e. max	4462.4	2–3	4458.0 [*Fe* II]
r.e. max	4467.0		
v.e. max	4477.3	3	4471.5 *He* I (5)
r.e. max	4485.2		
v.e.	4492±		
v.e. max	4507.8	4	4508.3 *Fe* II (8), 4491.4 *Fe* II (5), 4489.2 *Fe* II (4) 4515.3 *Fe* II (7), 4520.2 *Fe* II (7), 4522.6 *Fe* II (9)
r.e. max	4531.9		
v.e.	4541.0		
v.e. general max	4547.1		
r.e. sharp max	(4550)	3–4	4549.5 *Fe* II (10) 4555.9 *Fe* II (8)
r.e. general max	4556.8		
r.e.	4566.5		
v.e.	4574.9		
v. max	(4578.4)		
broad min	(4586.0)		4583.8 *Fe* II (11)
ft. max	(4590.4)	4	
ft. min	(4593.5)		4591.0 *O* II (9), 4596.2 *O* II (8)
ft. max	(4596.7)		
r.e.	4599.1		
v.e. max	4608.2		4603 *N* V, 4620.5 *Fe* II (3)(?)
max	4615.1		
r.e.	4620.9		
ft. max	(4627)		
ft. min	(4628)	3	4629.3 *Fe* II (7)
sharp max	(4633)		4634.2 *N* III (8), 4640.6 *N* III (10)
r.e. of above max	(4634.7)		
r.e.	(4653)	4	
v.e. max	4675.2		
max	(4678)		
r.e. of above max	(4680)		
min	(4685)	5–6	4685.8 *He* II
v.e. max	(4689)		
max	(4693)		
r.e. of above max	4698.3		
haze ext. to	4739±	1–2	4713.1 *He* I, 4728.1 [*Fe* II](??)
v.e.	4805±		
r.e.	4825±	1–0	4814.6 [*Fe* II]

Feature	λ	*I*	Identification
February 23			
v.e. ft. isolated	4490.6		4491.4 *Fe* II (5)(?)
r.e. max	4493.1		
v.e.	4499.4	2	4508.3 *Fe* II (8)
v.e. max	4511.7	4	4515.3 *Fe* II (7), 4520.2 *Fe* II (7), 4522.6 *Fe* II (9)
r.e. above max	4528.7		
v.e. max	4534.1		
r.e. above max	4535.9		
v.e. max	4542.1	2	4541.6 *He* II
v.e. sh. sup. max	4546.6		4549.5 *Fe* II (10) 4555.9 *Fe* II (8)
r.e. sh. sup. max	4549.9		
r.e. band	4563.0		
v.e.	4575.8	2	4583.8 *Fe* II (11)
e. max	4596.5		
e. max suspect	4598.4	5	4603 *N* V
e. max triple	4610.8		
r.e. min	4615.4		
v.e.	4623.2	Burnt	4634.2 *N* III (9), 4640.6 *N* III (10)
r.e.	4659.6	out	
v.e.	4675.6	Burnt	4685.8 *He* II,
r.e.	4698.5	out	4728.1 [*Fe* II](?), 4713.1 *He* I
haze ext. to	4734±	0<0	
v.e.	4805	0	4814.6 [*Fe* II]
r.e.	4825		
v.e.	4848.4	Burnt	4861.3 *Hβ*
r.e.	4877.4	out	
v.e.	4916.3	1–2	4923.9 *Fe* II (12), 4921.9 *He* I (4)
e.	4941.6	Burnt	4959.5 [O III]
r.e.	4977.5	out	
v.e.	4988.1	Burnt	5006.8 [*O* III], 5015.7 *He* I (6), 5018.4 *Fe* II (12), 5001.1 *N* II (7), 5001.3 *N* II (7), 5005.1 *N* II (10), 5007.3 *N* II (7)
r.e.	5027.7	out	
February 8 (1 weak plate) (intensity scale differs from above scale)			
v.e.	5149.0		
e.	5159.6	1	5158.0 [*Fe* II], 5158.8 [*Fe* II]
e.	5168.5	3	5169.0 *Fe* II (12)
e.	5180.7	1–2	5182.0 [*Fe* II] +——(?)
r.e.	5193.2		

TABLE 3—*Continued*

TABLE 3—*Continued*

Feature	λ	*I*	Identification
December 22–January 1			
v.e.	4841		
v. max	(4854)	10	4861.3 *Hβ*
min	(4860)		
r. max	(4869)		
r.e.	4884		
v.e.	4913.3		
v. max	4917.4		
min	4922.7	4	4923.9 *Fe* II (12), 4921.9 *He* I (4)
r. max	4933.0		
r.e.	4937.8	2–3	4959.5 [*O* III]+——(?)
ext. to	4960±		
v.e.	4980.2		5001.1 *N* II (7), 5001.3 *N* II (7) 5005.1 *N* II (10), 5007.3 *N* II (7)
v. max	(4995)		
min	(5006)	3	
r. max	(5019)		5018.4 *Fe* II (12), 5015.7 *He* I (6) 5006.8 [*O* III]
r.e.	5036.7		
December 23 (1 weak plate) (intensity scale differs from above scale)			
v.e.	5161.2	0–1	5169.0 *Fe* II (12) 5175.9 *N* II (3), 5179.5 *N* II (5)
e.	5181.7	<0	
r.e.	5192.9		
v.e.	5217.6	<0	5234.6 *Fe* II (7)
r.e.	5237.8		
v.e.	5270.0	0	5276.0 *Fe* II (7)
r.e.	5287.7		
v.e.	5307.8	0	5316.6 *Fe* II (8)
r.e.	5330.0		
v.e.	5565.6	<0	5577 [*O* II]
r.e.	5589.9		
v.e.	5738.3	2	5754.8 [*N* II]
r.e.	5772.0		
v.e.	5862.2	1	5875.6 *He* I (10)
r.e.	5889.6		
v.e.	5988.2	0	6001±, 6009± *N A*, 1918
r.e.	6017.2		
v.e.	6288.5	6	6302 [*O* I]
r.e.	6314.5		
v.e.	6352.7	2	6364 [*O* I]
r.e.	6379.3		
v.e.	6537.7	50	6562.8 *Hα*
r.e.	6600.8		

Feature	λ	*I*	Identification
February 23			
v.e.	5220	0<0	5234.6 *Fe* II (7)
r.e.	5244		
v.e.	5254.0		
e.	5265.0	0	5261.6 [*Fe* II], 5264.8 *Fe* II (2)?
e.	5272.4	2–3	5273.4 [*Fe* II], 5276.0 *Fe* II (7) 5284.1 *Fe* II (3) +——(?)
v.e. max	5282.1		
r.e. max	5285.3	2–3	
v.e. max	5299.9		
r.e. max	5302.6		
v.e. max	5307.3		
r.e. max	5310.0	2–3	5316.6 *Fe* II (8)
v.e. max	5323.9		
r.e. max	5330.1	2–3	5333.7 [*Fe* II]+——(?)
r.e.	5346.2		
v.e.	5366.7	0<0	5376.5 [*Fe* II]
r.e.	5387.3		
v.e.	5401.9		
r.e. max	5406.2	2	5411.6 *He* II
v.e. max	5419.6		
r.e.	5423.6		

The [*Ne* III] line at 3868.7 A is visible on a strongly exposed spectrogram taken on December 30, and it is possible that it is very faintly present on a plate taken on December 25.

N V.—The line listed in Table 3 as having "v.e. max 4608.2, max 4615.1," made its appearance between November 26 and December 22, when it was a reasonably strong line. In appearance it resembled *He* II λ 4686. More accurate measures of its position on a plate of higher dispersion[25] taken when it was a strong line, combined with numerous measures made on CQ plates, place it at 4604.8 A. The line is probably identical with the unidentified line in N Aquilae 1918 listed by Wyse[26] at 4604.3 A, and by Lundt[27] at 4603.9 A. Wyse attributed the line in N Aquilae in part, at least tentatively, to *N* v λ 4603.2 (predicted); but he remarked that the *N* v line which should accompany it at λ 4620 was never more than just suspected. Lunt has no record of observing λ 4620. A similar situation obtains in the spectrum of N Puppis. The line at λ 4604.8 attained considerable intensity, but I cannot say with certainty that λ 4620 was ever visible. The red component of λ 4620 would be rather badly blended, but the violet component should be visible through the red component of λ 4604, provided it attained its theoretical intensity—about one-half that of λ 4604. Actually, if λ 4620 appeared in N Puppis, it must have been much less intense than would be anticipated by theory. In spite of this intensity discrepancy, it is difficult to identify the line at λ 4604.8 as anything other than *N* v.

Nitrogen flaring, if it occurred at all in N Puppis, was certainly not of importance. Strongly exposed plates taken during the last of December and the first part of January suggest greater darkening in the region of λ 4640 A than seems possible on the basis of superposition of the many *O* II and *N* II lines in this rich region, but at no time has the case been clearly in favor of flaring. The CG plates taken in February seem to bear evidence against the flaring, since in the places of greatest darkening the lines of *O* II and *N* II have actually been measured. The CQ plates taken at nearly the same time in February as the CG plates, however, are practically identical with the December plates in the immediate vicinity of λ 4640.

The most unusual feature in the spectrum of N Puppis is the occurrence of [*Fe* II]. So far as I know, the lines of [*Fe* II] have been found previously only in the spectra of slow novae, such as N Aquila 1925, N Pictoris 1925, N Ophiuchi 1933, and N Herculis 1934. Their existence in the spectra of fast novae was, however, predicted by Edlén during the discussion which followed his paper[28] at the conference on novae and white dwarfs held in Paris in 1939. He suggested that [*Fe* II] had not been found in fast novae up to that time because of observational difficulties.

It is extremely unfortunate that in N Puppis nearly all the [*Fe* II] lines occur in blends. Owing to this blending, even though the presence of the line is certain, it is often impossible to make a valid estimate of the line intensity. Lines observed and lines probably present, though badly blended, are listed in Table 4.

The leading lines of [*Fe* III] were searched for but not found. The strongest [*Fe* III] line is situated at λ 4658.05, in a very unfavorable region, since it is between *N* III, λ 4640, and *He* II, λ 4686, a part of the spectrum which is very dark because of the crowding of *O* II and *N* II lines. A reasonably strong line should have been found, however, if present. The second strongest line of [*Fe* III], located at λ 5270.41, is much more favorably situated. An excellent, but not too strongly exposed, spectrogram taken on February 8 (no spectrogram suitable for a search of this region was made in December or January) revealed many [*Fe* II] lines but no trace of [*Fe* III] in the 5270 A region. It is most unfortunate that no strongly exposed spectrograms of the visual region during the months later

[25] Cassegrain spectrograph with glass prisms and 500-mm camera. Dispersion 20 A/mm at λ 3933. Plates designated by the symbol "CG."

[26] *Op. cit.*, p. 29. [27] *M.N.*, **80**, 530, 1920. [28] Unpublished.

than November exist in the McDonald collection. It seems highly probable that if any fast nova were to show lines of [*Fe* III], N Puppis would be a very likely object to do so. A study of its spectrum made as soon as possible during the next observing season would undoubtedly prove to be fruitful.

Spectral changes during 1943 were fairly slow but continuously toward a more complete nebular spectrum, as may be seen in Plates XVII and XVIII. Measures of an excellent plate taken on February 23.2 are given in Table 3 for comparison with the December 30 measures.

The primary changes between December 30 and March 29 are: (1) a considerable weakening of the *Fe* II lines; (2) a strengthening of the forbidden lines of *O* III and *Ne* III, and the line at λ 4604.8 tentatively identified as *N* V; on March 29 this line was one-third as intense as *He* II, λ 4686; (3) the possible appearance of [*Ne* V] during the last of January or first of February. A very faint line suspected at λ 3424± may be the [*Ne* V] line at λ 3425.8. The [*Ne* III] line at λ 3868 was very slightly more intense than $H\zeta$ on March 29. There is some indication that the line at λ 4200, which is attributed to *He* II and *N* III, may have become slightly stronger than it was in December. No change is apparent in the [*Fe* II] lines. The slow change in spectrum, together with the slow change of light after mid-December, points to a long relaxation time for the condition of the nova at that time.

TABLE 4

[*Fe* II] LINES IN N PUPPIS

Transition		λ Pred.	Int.*	Transition		λ Pred.	Int.*
a^6D-b^4P	$3\frac{1}{2}-2\frac{1}{2}$	4889.63	*P*	a^4F-a^4H	$4\frac{1}{2}-6\frac{1}{2}$	5158.81	(1)bl
	$2\frac{1}{2}-1\frac{1}{2}$	4728.07	0<0		$3\frac{1}{2}-5\frac{1}{2}$	5261.62	0
	$1\frac{1}{2}-\frac{1}{2}$	4639.68	bl		$2\frac{1}{2}-4\frac{1}{2}$	5333.66	0–1
a^6D-b^4F	$4\frac{1}{2}-4\frac{1}{2}$	4416.28	bl		$1\frac{1}{2}-3\frac{1}{2}$	5376.48	0<0
	$3\frac{1}{2}-4\frac{1}{2}$	4492.64	*P*?bl	a^4F-b^4F	$4\frac{1}{2}-4\frac{1}{2}$	4814.56	0
	$3\frac{1}{2}-3\frac{1}{2}$	4457.95	bl				
	$2\frac{1}{2}-2\frac{1}{2}$	4188.75	bl	a^4F-a^4G	$4\frac{1}{2}-5\frac{1}{2}$	4243.98	0–1
					$3\frac{1}{2}-5\frac{1}{2}$	4346.86	*P*?bl
a^6D-a^6S	$4\frac{1}{2}-2\frac{1}{2}$	4287.41	0–1		$3\frac{1}{2}-4\frac{1}{2}$	4276.84	0–1
	$3\frac{1}{2}-2\frac{1}{2}$	4359.34	bl		$2\frac{1}{2}-4\frac{1}{2}$	4352.79	*P*?bl
	$2\frac{1}{2}-2\frac{1}{2}$	4413.78	bl		$3\frac{1}{2}-3\frac{1}{2}$	4244.82	*P*?bl
	$1\frac{1}{2}-2\frac{1}{2}$	4452.11	*P*?bl		$2\frac{1}{2}-3\frac{1}{2}$	4319.63	*P*?bl
					$2\frac{1}{2}-2\frac{1}{2}$	4305.90	*P*?bl
a^4F-b^4P	$4\frac{1}{2}-2\frac{1}{2}$	5273.38	bl		$1\frac{1}{2}-2\frac{1}{2}$	4358.38	*P*?bl
	$3\frac{1}{2}-1\frac{1}{2}$	5158.02	(1)bl				
	$1\frac{1}{2}-\frac{1}{2}$	5181.97	*P*?				

* *P* signifies that the line is very probably present. It is quite certainly seen but not separately measured.
P? signifies that the line is probably present, but is badly blended. Lines so designated are not always seen but are probably present, since other weaker and stronger members of the same multiplet are present.
The entry "bl" signifies blend.
Intensities, when given, refer to the [*Fe* II] line.
Wave lengths greater than λ 4900 are taken from a higher-dispersion plate of February 8.2 days. The other wave lengths are from December 30 days. The intensity scale for λ > 4900 differs from the intensity scale for λ < 4900.

There is no apparent change in line structure discernible, but the available plates are not of the best quality for such observations, and slight changes would not be detected. From the CG plates of February, a line width equivalent to 1200 km/sec was obtained. This value differs rather considerably from the value of 1500 km/sec given for the November and December determinations. Comparisons of CQ plates taken in December and May—plates which were of excellent density for this purpose—showed no difference in line width for the two dates. The difference in the two measured values for line width is undoubtedly due to a photographic density effect. The value 1200 km/sec is probably the

more accurate one. The higher figure, as has been previously stated, should be regarded as an upper limit.

The last McDonald plate was taken under very unfavorable conditions on May 10 and is considerably underexposed. At that time the most prominent lines in the photographic region of the spectrum were λ 5007 and λ 4363 of [*O* III]. The relative intensities observed are:

$$\lambda\,5007\ [O\,\text{III}] = \lambda\,4363\ [O\,\text{III}]\,, \qquad \lambda\,4959\ [O\,\text{III}] = H\beta = \tfrac{1}{4}\lambda\,5007\ [O\,\text{III}]\,,$$

$$4640\ N\,\text{III (bl)} = \lambda\,4686\ He\,\text{II}\,, \qquad \lambda\,4686\ He\,\text{II} = \tfrac{1}{3}H\beta\,.$$

It is a pleasure to thank Dr. Otto Struve for affording me the use of the Yerkes and McDonald observatories' equipment and to thank the various members of the staffs of those observatories, who have allowed me to use their plates—Dr. O. Struve, Dr. G. P. Kuiper, Dr. P. Swings, Dr. D. M. Popper, Dr. J. Titus, and Dr. W. W. Morgan. It is an especial pleasure to thank Dr. P. Swings for reading the manuscript of this paper and making several suggestions for its improvement.

November 1943

THE SPECTRUM OF RX CASSIOPEIAE*

O. STRUVE
McDonald and Yerkes Observatories
Received March 20, 1944

ABSTRACT

The spectrum of the eclipsing variable RX Cas is composite, consisting of a gG3 component and a gA5e component. The two spectra are roughly of the same intensity at λ 4000. Assuming that the temperatures are 5000° and 8000°, the ratio of the radii $k = 0.257$. The emission lines show the effect of eclipse, and the entire system resembles that of SX Cas. The velocity-curves from the lines of the G3 star give a symmetrical curve with $P = 32.315$ days, $\gamma = -24$ km/sec, $K = 36$ km/sec, $e = 0.00$, $T =$ phase of passage through γ velocity $= 30.3$ days, $a \sin i = 1.6 \times 10^7$ km, and $f(m) = 0.16\odot$. This star is in front during the principal eclipse. The A5 star gives the velocity-curve of that component which is being eclipsed at principal eclipse: $\gamma = -3$ km/sec, $K = 34$ km/sec, $e = 0.18$, $\omega = 37°$, and $T =$ phase of periastron passage $= 30.3$ days. The difference in γ of the two curves is notable, perhaps also the larger eccentricity of the A5 star's curve. These discrepancies must be due to a distortion of the latter curve by absorption lines formed in the gaseous streams around the A5 star. These phenomena are similar to those observed in SX Cas. The radial velocities obtained from the *H* absorption lines show no periodic oscillation. A rediscussion of the light-curve of RX Cas, using a series of observations by Martinoff, in conjunction with the spectrographic data, leads to the conclusion that the eclipse may be nearly grazing. The principal photometric elements are: $k = 0.257$, $a_0 = 1.00$, ellipticity constant $\epsilon \sin i = 0.7$, duration of photometric eclipse $= 4.3$ days, duration of entire eclipse of gaseous streams $= 5.8$ days, inclination $i = 75°$, $a_0 = 0.50$, $a_A = 0.13$, $L_0 = 0.67$ (in visual light), and $L_A = 0.33$ (in visual light). The remarkable similarity of RX Cas and SX Cas is disturbed only by the fact that in the former the total light of the G star predominates at all phases and in all spectral regions except the extreme violet, while in the latter the light of the A star predominates in all accessible spectral regions and at all phases except near principal mid-eclipse. Because of the distorted character of the velocity-curves of the A stars in both systems we have no information concerning the mass ratios.

I. THE PROBLEM

In a recent study of the spectrum of the eclipsing variable SX Cassiopeiae[1] I reached the conclusion that the hotter component of the system, whose type is gA6, is surrounded by a stream of gas which passes from the cooler, but probably more massive, gG6 component toward the A6 component and flows along the following side of the latter; on the far side of the A6 star the stream splits in two: a part escapes into space as an expanding cloud or shell, while the rest continues to flow around the A6 star and ultimately returns to the G6 star. The stream of gas produces emission lines as well as absorption lines. The former show eclipses before and after the photometric eclipse, while the latter blend with the lines of the A6 star and give rise to a large distortion of the velocity-curve, making it very unsymmetrical and producing a set of spurious orbital elements with a large eccentricity which contradicts the value of $e \cos \omega$ obtained from the light-curve. The stream is concentrated toward the orbital plane. Its height above the surface of the A6 star is approximately equal to the diameter of this star.

This picture has, of course, been inspired by earlier work on β Lyrae, where the observations led to a similar interpretation. Moreover, in the case of β Lyr, Kuiper developed a satisfactory dynamical theory to account for the existence of the gaseous stream. In the case of SX Cas, such a theory is still lacking. But every step of the discussion was supported by strong observational evidence. Hence, it is now possible to emphasize two points which have not been sufficiently appreciated in the past:

* *Contributions from the McDonald Observatory, University of Texas*, No. 94.

[1] *Ap. J.*, 99, 89, 1944.

a) The existence of vast streams of gas which produce strong absorption lines compels us to alter our views concerning the structure of some stellar atmospheres. Apparently, such streams can exist without producing any very large continuous absorption; otherwise the photometric eclipse would more nearly coincide with the eclipses of the bright hydrogen components. An optical depth of $\tau = 0.1$ may not be noticeable in the integrated light but may, in the presence of turbulence, lead to strong absorption lines. The point I want to make is this: Many phenomena of stellar absorption lines must be attributed to layers which are more comparable to the solar chromosphere or its prominences than to the regular solar reversing layer. This is especially important when we consider the support of a reversing layer. It is customary to make use of the equation of hydrostatic equilibrium[2]

$$\frac{dP}{d\tau} = \frac{g}{\kappa}$$

and to allow in the value of g for the effect of radiation pressure. This procedure leads to satisfactory results for the solar reversing layer and probably also for those main-sequence stars which do not possess absorbing shells. Supergiants, on the other hand, and shells cannot be treated in this manner; and the structure of an atmosphere obtained in this way is not in agreement with the observed features of the spectrum.

b) The existence of bright hydrogen lines in SX Cas is interesting in view of the fact that the exciting star has a spectrum of type gA6. The emission lines are fairly strong and resemble those observed in ordinary Be stars. Hence, it would appear that a straightforward application of the Zanstra theory would lead to a temperature that is not compatible with spectral type A6. Either the assumptions which underlie the Zanstra theory are not applicable to stars like SX Cas, or the spectral type is not a dependable measure of the available amount of ultraviolet radiation above the Lyman limit.

Among the known eclipsing binaries, there is one, RX Cas, which bears a certain resemblance to SX Cas. Hence, I have chosen it for study at the McDonald Observatory and have obtained a series of 35 spectrograms with the quartz Cassegrain spectrograph attached to the 82-inch reflector. The dispersion of all spectrograms is 40 A/mm at λ 3933.

The variability in light of RX Cas[3] was discovered in 1904 by Mme L. Ceraski at the Moscow Observatory.[4] Two years later S. Blažko,[5] also at Moscow, found that the variable belongs to the Algol type and that the principal minima are represented by the formula

$$\text{Min.} = 2416250.9 + 32.315E\,. \qquad (1)$$

Blažko also observed a series of secondary minima but was unable to represent them by means of this or any other formula. This uncertainty led to the suspicion, which has persisted almost to the present time, that RX Cas may be a variable of the RV Tauri type. However, a long series of photometric observations by Wendell[6] left no doubt that the star is an eclipsing variable and that the light-curve is one of the β Lyr type. In 1913 H. Shapley[7] derived the elements of the photometric orbit with the help of Wendell's observations. He assigned RX Cas to his stars of the "third grade," which had been observed insufficiently. As a matter of fact, Wendell's light-curve, which was reproduced by Shapley,[8] shows a large amount of scatter and perhaps some asymmetry in the sense that the star is brighter at phase 8 days (after principal minimum) than at phase 24 days (pre-

[2] Unsöld, *Physik der Sternatmosphären*, p. 142, Berlin, 1938.

[3] BD+67°244, $\alpha = 2^h58^m.8$, $\delta = +67°11'$ (1900).

[4] *A.N.*, **164**, 218, 1904.

[5] *A.N.*, **172**, 57, 1906 (star 6, 1904).

[6] *Harvard Ann.*, **69**, 144, 1913.

[7] *Ap. J.*, **38**, 158, 1913; *Contr. Princeton Obs.*, No. 3, 1915.

[8] *Ap. J.*, **42**, 275, 1915.

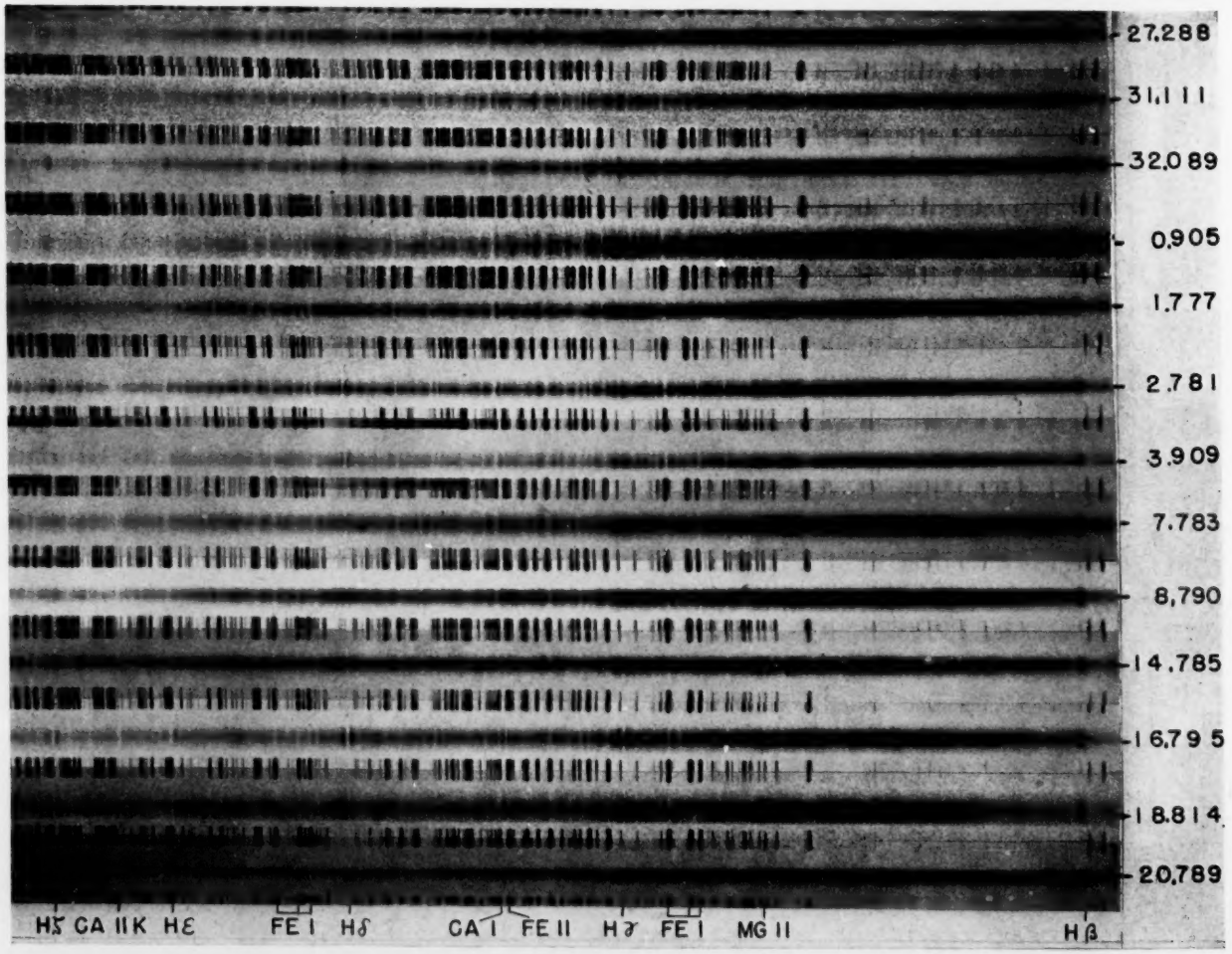

SPECTRA OF RX CASSIOPEIAE

Notice the disappearance of the violet hydrogen emissions at phases 31 and 32 days and the weakening of the red emissions at phase 2 days. This effect is attributed to the eclipse of a stream of hydrogen gas by the G-type component of the binary. Notice also the weakening of *Fe* II 4233 at phase 8 days and the simultaneous weakening of the central *H* absorption cores.

ceding principal minimum). However, the accidental errors are so large that Shapley had to ignore this effect. The secondary minimum of Wendell's light-curve falls almost exactly halfway between successive principal minima, so that

$$e \cos \omega = 0 .$$

The elements as determined by Shapley are:

P	= 32.316 days
Magnitude at maximum	= 8.66
Spectrum	= K0
Principal range	= 0.69 mag.
Secondary range	= 0.55 mag.
Semiduration	= 2.58 days (darkened)
Character of eclipse	= partial with stars equal
α_0 (fraction of area of smaller star eclipsed at principal mid-eclipse)	= 0.61
L_b	= 0.57
L_f	= 0.43
r_b	= $0.28a$ = $14.8r\odot$
r_f	= $0.28a$ = $14.8r\odot$
$\cos i$	= 0.161
J_b/J_f	= 1.3
ρ_b	= $0.0005\rho\odot$
ρ_f	= $0.0004\rho\odot$

In recent years the star has been observed very little; the last complete light-curve known to me is one by D. J. Martinoff[9] covering the years 1925–1929. He finds little or no asymmetry in the light-curve. As drawn by him, the curve suggests a small positive value of

$$t_2 - t_1 - \frac{P}{2} = 0.84 \text{ day} ,$$

but this may not be real. If it were real, we should have approximately

$$e \cos \omega = \frac{\pi\left(t_2 - t_1 - \frac{P}{2}\right)}{P(1 + \operatorname{cosec}^2 i)} = 0.08 ,$$

so that, in all probability, $e < 0.1$. At least, we are certain that Wendell's observations require a smaller value for $t_2 - t_1 - P/2$, possibly even one of negative sign.

The period, according to Martinoff, is very close to Blažko's value. His epoch is 2425492.93, which gives, with $P = 32.315$, O − C = −0.06 day, when $E = 286$. Accordingly, Blažko's elements required no correction as late as in 1929.

The spectrum of RX Cas has been observed at Mount Wilson by Adams and Joy.[10] The H lines were found to be bright, with the centers reversed and with the red edges stronger than the violet. The type was G3p, and the velocity changed by 11 km/sec between maximum light and minimum light. The spectrum of only one component was seen, and "the characteristics of the Cepheid spectrum are shown in the intensity of the enhanced lines."

The great length of the period of RX Cas and the presence in its spectrum of bright lines of H constitute an interesting resemblance to SX Cas. But, whereas the spectral type of SX Cas at maximum light is gA6, that of RX Cas is G3p. The questions arise whether the bright lines are excited by the G-type star and whether the velocity-curve presents the same kind of distortion as the velocity-curve of SX Cas.

[9] *Trav. Obs. U. de Kazan*, No. 26, p. 18, 1930.

[10] *Pub. A.S.P.*, **31**, 308, 1919; *Pub. A.A.S.*, **4**, 138, 1920.

II. THE OBSERVATIONS

The 35 spectrograms were obtained during two consecutive cycles of the variable in January, February, and March, 1944. The weather conditions were, on the whole, rather unfavorable; and on many nights the exposures were unduly long in order to compensate for loss of light by clouds or by poor seeing. Under good conditions the exposure time was 90 minutes, with a slit width of 0.07 mm. This is reduced to 0.037 mm by the camera. Because of the reddish color of the variable, it was not a particularly easy object for the 500-mm camera of our two-prism quartz spectrograph. Nevertheless, it seemed best to use this camera, rather than one of shorter focal length, because the definition given by it is very fine, especially in the violet region.

The distribution of our observations (many of which were very kindly obtained for me by Drs. Helen Steel, Carlos U. Cesco, and Jorge Sahade) is shown in Figure 1, where the times of the mid-exposures are plotted on the light-curve of Martinoff. Both the light-curve and the phases of the spectrograms were computed with Blažko's elements (eq. 1).

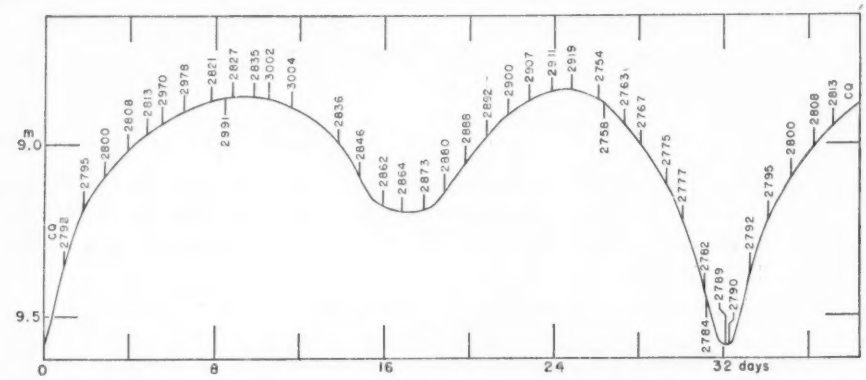

FIG. 1.—The light-curve of RX Cassiopeiae according to Martinoff, with the numbers of the spectrograms in their respective phases.

In order to obtain a rough test of the light-curve, the spectrographic observers have made approximate estimates of the brightness of RX Cas during some of the exposures, using for this purpose the 6-inch finder of the 82-inch telescope. The comparison stars were BD+66°242 (mag. 7.8) and BD+66°243 (mag. 9.8). The estimates are given in Table 1. These estimates place the principal minimum somewhat less than 1 day later than Martinoff's curve would predict, and the secondary minimum almost 1 day earlier. These discrepancies are so small that they cannot be regarded as certain. We shall therefore use the phases which result from Blažko's elements. It must be remembered, however, that the observations of other observers show a large scatter. It is possible, therefore, that the individual curves do not exactly repeat themselves. Such a conclusion was also reached by Dugan in regard to SX Cas.

III. THE SPECTRUM

The spectrum is of type gG3, exactly as found at Mount Wilson; and the absolute magnitude criteria show that the luminosity is very great. For example, the *Sr* II lines are very strong. The *H* lines consist of two bright components of considerable total width, with a sharp reversal approximately in the middle. Of particular interest, however, is the fact that the spectrum is composite. The line *Ca* II K is narrow and sharp, corresponding approximately to spectral type A2 or A5. On a few plates this sharp line appears as a core upon a shallow and very broad line, which must belong to the G3 star.

The entire ultraviolet region is characterized by a fairly strong continuum, upon which one can distinguish numerous *H* lines in emission and absorption and a large number of strong and sharp absorption lines which resemble spectral type A5, probably with supergiant characteristics. On the red side of *Ca* II K the spectrum of the G3 star predominates, although a few of the strongest *Fe* II (and perhaps *Ti* II) lines appear to belong to the A star.

This interesting result shows, beyond doubt, that we are concerned with a system consisting of a G3 and an A2 or A5 star, exactly as in the case of SX Cas. But, while in the latter the total light of the A star predominated at all phases, except those of principal eclipse, the spectrum of RX Cas is dominated at all times by the light of the G3 star, except in the ultraviolet region.

The question arises whether the G3 star or the early-type star—which we shall designate as the "A5 star"—is eclipsed at principal minimum. The following section, on the velocity-curve, will give us a final answer to this question. In the meantime we may point out that the G3-star spectrum undergoes no appreciable change during the principal

TABLE 1

ESTIMATED VISUAL MAGNITUDES OF RX CASSIOPEIAE

Date	Phase	Mag.	Date	Phase	Mag.
1944, Jan. 25	31.2	8.9	1944, Feb. 13	17.8	9.2
26	32.1	9.3	14	18.8	9.0
27	0.9	10.0	15	19.8	9.0
28	1.8	9.1	16	20.8	8.8
29	2.7	9.0	17	21.8	9.2
31	4.8	9.0	19	23.8	8.8
			20	24.8	9.0
Feb. 3	7.8	8.8			
4	8.8	8.7	Mar. 4	5.5	8.7
9	13.8	8.9	5	6.5	8.6
10	14.8	9.2	7	8.5	8.6
11	15.9	9.4	9	10.5	9.0
12	16.8	9.2	10	11.6	8.9

eclipse. I believe that the A5 spectral features may be somewhat weakened at principal mid-eclipse. The continuous spectrum on the violet side of λ 3933 is, however, at all phases visible, and the narrow line of *Ca* II K does not disappear. As Shapley has pointed out, the eclipse may be partial, and the spectra of both components remain visible. Nevertheless, the balance of the argument is in favor of an eclipse of the A5 star by the G3 star, and this conclusion will later be confirmed by the radial velocities.

There is a pronounced strengthening of the violet continuous spectrum and of the absorption lines of middle or late class A at secondary mid-eclipse. Hence, at and near phase 16 days the A star is in front, and part of the light of the G3 star is eclipsed. But here, too, the absorption lines of the G3 star never completely disappear; they are only slightly reduced in intensity, so that the secondary eclipse is partial, or annular.

According to Shapley, the duration of the entire eclipse is 5.16 days. Hence, on our system of phases, the principal eclipse begins at phase 29.74 days, reaches its central point at phase 32.32 = 0.00 days, and ends at phase 2.58. If my photometric estimates are correct, the deepest point of the light-curve occurred at phase 0.75 day, and the beginning and end were shifted accordingly.

During the interval of the eclipse there occurred some remarkable changes in the intensities and the structure of the *H* lines. At phase 28.1 days the *H* lines had their normal appearance. *Hβ* and *Hδ* were double bright lines, with the red component slightly the

stronger. At $H\gamma$ the violet emission component looks abnormally weak, probably because it is blended with a strong line of *Ti* II; but this phenomenon is not conspicuous at other phases outside of eclipse. The higher members of the Balmer series are visible and exhibit some complexity of structure because of blending with strong absorption lines. At phase 29.3 days the red components of the *H* emission lines are relatively enhanced. This is slightly more pronounced at phase 30.1 days and still more at phase 31.1 days. At phase 31.2 days the red emission components are from five to ten times stronger (in energy) than the violet components and are much stronger, relative to the continuous spectrum, than outside of eclipse. At phases 32.1 and 32.2 days the violet emission components are completely gone, and the red components are very strong. Their maximum intensities, relative to the continuous spectrum, must have increased by a factor of 2 or 3. The absorption cores, which are normally central, are now visible as weak, sharp lines on the violet sides of the red emission components. At phase 0.9 day the emission lines are again double, with approximately equal components and with weak absorption cores between them. The maximum intensities of the emission components are now about the same as, or slightly weaker than, outside of eclipse. At phase 1.8 days the violet emission components are stronger than the red components, and at the same time their maximum intensities are somewhat increased with respect to the continuous spectrum. But this phenomenon is not as striking as the opposite phenomenon at phases 32.1 and 32.2 days. At phase 2.8 days the *H* lines have nearly resumed their normal appearance: they consist of two approximately equal emission components separated by a fairly strong, sharp absorption core. The total intensities of the bright *H* lines at this phase are still somewhat greater than normal. At phase 3.9 days even this is gone, and the *H* lines are now exactly as they were at phase 28.1 days.

The succession of changes in the *H* lines during the principal eclipse is very similar to that observed in SX Cas.[11] There can be no doubt that the G3 star eclipses a stream of approaching gas prior to mid-eclipse and a stream of receding gas after mid-eclipse. At phase 0.9 day the two streams are approximately symmetrically obscured by the G3 star. At this phase the two emission components are almost equal in intensity, and their maximum intensities are relatively weaker than at phases 31 and 32 days for the red component or at phase 1.8 days for the violet component. If we remember that at phase 0.9 day the total light of the star was less than one-half that outside of eclipse, we may conclude that at this phase the G3 star cuts down more than one-half of the total light of the emitting nebulosity.

We have no very definite indication of the shape of this nebulosity. But the facts that before and after principal eclipse the emission lines are double and that they are also double at the central phase of 0.9 day suggest that we are dealing with a stream in the orbital plane of the binary. A rotating spherical shell without self-absorption produces a line whose contour is given by[12]

$$A\,(x) = \text{const}\,\frac{\pi}{2}.$$

If the shell is completely transparent and surrounds the star like a narrow halo, the contour is

$$A\,(x) = \frac{1}{\pi\sqrt{1-x^2}}.$$

The same contour is obtained for a rotating ring without self-absorption. A completely transparent narrow ring would, of course, give a discontinuous contour with two sharp maxima at $x = \pm 1$ and with zero intensity for all other values of x. The observed contour alone does not permit us to distinguish between a ring and a spherical shell.

But, if we now consider that at phase 32.2 days the violet emission component is

[11] *Ap. J.*, Vol. 98, Pl. IV, 1944.

[12] Unsöld, *op. cit.*, p. 328.

completely eclipsed, while at phase 1.8 days the red component is almost completely eclipsed, it is clear that the diameter of the G3 star must be larger than the height of the stream above the A5 star. We shall see that the G3 star must be much larger than the A5 star. If the inclination is 81°, as results from Shapley's orbit, the unobscured portion of a spherical halo around the A star would result in a great strengthening of the emission between the maxima, at phase 0.9 day. I do not believe that such a strengthening is observed and I therefore incline toward the view that the stream is concentrated approximately toward the orbital plane.

If the photometric elements were known with sufficient accuracy, we could obtain the contours of a partly obscured spherical shell and of a flat ring by a graphical construction recently employed for a study of the rotational contours of absorption lines in U Cephei.[13] But the inclination and the value of k are not known accurately; and we must, therefore, content ourselves with the qualitative statement that the observations are more nearly in accord with the hypothesis of a stream in the orbital plane than with the hypothesis of a rotating spherical shell.

If this conclusion is correct, we infer that at phases 32.1 and 32.2 days the entire approaching cusp of the stream is eclipsed, while at phase 1.8 days only the major portion of the receding cusp of the stream is eclipsed. It is not entirely clear what this asymmetry means. Perhaps the distribution of the nebulous material around the A5 star is unsymmetrical in density or extent—the receding branch of the stream being larger or denser. But, if that were so, the roles of the two streams should be reversed at phases near 16 days. Yet, there is no evidence to show that at 16 days the violet emission components are stronger than the red. It is perhaps more reasonable to think of a small inclination of the stream to the orbital plane causing the G3 star to eclipse completely the approaching stream before mid-eclipse but only partially the receding stream after mid-eclipse.

It is noteworthy that the eclipse of the nebulous stream begins at phase 29.3 days and ends at phase 2.8 days. It lasts, therefore, only 5.8 days, or only 0.6 day longer than the photometric eclipse. In the case of SX Cas the eclipse of the nebulous streams lasted 5.7 days, while the photometric eclipse lasted 3.7 days. It is possible that, because of the large scatter in the photometric observations of RX Cas and the partial character of the eclipse, the duration of the photometric eclipse may be somewhat less than 5 days.

The total widths of the emission lines correspond to a velocity of ± 200 km/sec. Because of turbulence and instrumental broadening, the actual velocities of the two streams are probably of the order of ± 150 km/sec—exactly as in SX Cas.

The height of the stream above the photosphere of the A5 star must be somewhat less than the diameter of the G3 star, because the latter causes a total eclipse of the approaching stream at phases 32.1 and 32.2 days. Because of the uncertainty in the exact phase of mid-eclipse—0.75 day as observed, or 0.00 day as extrapolated from Blažko's formula—it is impossible to derive the height of the stream accurately. But it should be remarked that the spectrographic phases of maximum obscuration of each of the two streams—namely, 32.1 days and 1.8 days—are symmetrical with respect to phase 0.8 day, which is almost precisely the deepest point of my observed light-curve. Geometrical considerations demand that the photometric eclipse be less than 5.8 and more than 2.0 days. We shall probably not be far from the truth if we take the mean, namely, 3.9 days. This is probably still compatible with the light-curves of Wendell and of Martinoff. We do not yet know the ratio of the radii of the two stars. Shapley gave $k = 1$, but we shall see that probably $r_G = 3.9 r_A$. In that case we can derive the height of the stream, x, by assuming a central eclipse:

$$\frac{2r_G + 2r_A}{3.9} = \frac{x}{1.0},$$

whence

$$x = 2.5 r_A .$$

[13] *Ap. J.*, 99, 236, 1944.

The ratio of the radii can be obtained from the spectral types of the two stars and from the fact that at about λ 4000 the total luminosities of the two components are equal. Hence,

$$r_G^2 J_G = r_A^2 J_A .$$

Assuming for the temperatures of the two stars that

$$T_G = 5000^\circ \mathrm{K} ,$$

$$T_A = 8000^\circ \mathrm{K} ,$$

we find from Planck's law that at λ 4000

$$\frac{J_A}{J_B} = 15$$

and hence that

$$\frac{r_G}{r_A} = 3.9 .$$

Aside from the bright lines of *H*, the spectrum of RX Cas shows at maximum light a weak emission line between the absorption lines *Ca* I 4226 and *Fe* II 4233. During the eclipse this line is greatly enhanced; at phase 32.1 days it is visible as a very weak emission line, while at the same time there appears a somewhat stronger emission line on the red side of *Fe* II 4233. The normal emission is, therefore, caused mostly by Fe^+. Another remarkable emission feature occurs on both sides of the line *Mg* II 4481. This line changes little in intensity during the eclipse. It is quite clearly visible as a broad, diffuse double emission with weak central absorption. At phase 32.1 days this emission line is very little, if at all, enhanced. This may be partly due to the great strength of the G3 continuous spectrum at λ 4481, but I do not think that this explanation is sufficient. While *H* and *Fe* II change in a similar manner, *Mg* II remains almost unaffected. I have no explanation to offer for this strange behavior. Incidentally, the occurrence of *Mg* II in emission is in itself somewhat unusual.

During the principal eclipse, and especially at phases 32.1 and 32.2 days, several other emission lines are present. Among these, *Ca* II K is especially noteworthy. It is narrow and weak and all concentrated on the red side of the narrow absorption line. There is another weak line on the red side of what is apparently *Ni* II 4067. There are several other weak emission lines of *Fe* II, and possibly a few other lines. Among the *H* lines the emission intensities are not entirely uniform. The line *H* 9 3835 is especially weak, which is undoubtedly caused by absorption of *Mg* I 3838.

This phenomenon of absorption is one to which I have called attention on several occasions. It is, of course, well known among the late-type variables. But it also occurs in spectra of early type, such as in the case of the violet wing of double *Hγ* in SX Cas[14] or in the ultraviolet members of the Balmer series in VV Cephei.[15] The case of *H* 9 in RX Cas is especially instructive. The continuous spectrum in this region is so weak that there can be no question of a suppression of the bright line through the photographic superposition of an absorption line. The absorption must take place within the emitting stream of *H* atoms or above it. This conclusion has far-reaching consequences. Indeed, since we know that in RX Cas and SX Cas the emission of *H* is produced in a stream high above the normal reversing layer of the A star, we must conclude that some of the A-type absorption lines are produced at least as high. We had already reached the same conclusion for SX Cas from other considerations. But, if the absorption lines in these stars can be produced at such a high level, why is it not equally possible that many absorption lines of the late-type variables are produced in extended shells, and not within

[14] *Ibid.*, p. 101.

[15] *Ibid.*, p. 74.

the conventional limits of the reversing layers? This is important in view of the fact that some recent studies have placed the source of the emission lines in the spectrum of Mira Ceti below the reversing layer.[16] If we understand the reversing layer to designate that region of the star's atmosphere in which the continuous optical depth increases from 0.1 to 3.7 within a thickness of about 170,000 km,[17] then these studies would require a mechanism for the production of the bright lines which is altogether different from that which operates in the shells of Be and Ae stars. But, if the disturbing absorption lines are produced in a tenuous envelope whose optical depth for continuous radiation is relatively small, then there is no compelling reason why the emission lines of even a late-type variable may not be produced in an outer nebulosity where geometrical dilution operates and where conditions of equilibrium are not fully realized. There remains the troublesome question of the source of excitation of the *H* lines. But this is almost equally difficult for both theories.

We turn to the examination of the absorption-line spectrum. There are marked changes during the two eclipses: near phase 0 the G3 star predominates, while near phase 16 days the A5-features are strengthened. But there are other conspicuous changes which cannot be attributed to the eclipses. The most notable of these changes occurs at phases 7.8 and 8.8 days. The absorption line *Fe* II 4233 is exceedingly weak at these phases, while other absorption lines of *Fe* II and *Ti* II are also weakened to such an extent that the entire spectrum presents a very different aspect from that observed at other phases. This remarkable weakening of some of the A5 absorption features may affect *Ca* II K, but the evidence is not wholly convincing. This line is present at both phases, and it is weaker than at phases 13.8 and 2.8 days; but the change is less conspicuous than in the case of *Fe* II 4233. This weakening of the A5 absorption lines cannot be caused by the strengthening of the G3 spectrum at maximum of light, because there is no such weakening of the A5 lines at phase 24 days, where the total light is again at a maximum. However, we observe at phases 7.8 and 8.8 days another interesting phenomenon: the central absorption cores of $H\beta$ are missing, although they are conspicuous at all other phases. The central absorptions of $H\gamma$ and $H\delta$ are present, but they give one the impression of being covered by emission. At other phases these absorption lines stand out as real depressions in the underlying continuous spectrum. It is tempting to connect this phenomenon with the weakening of the other A5 absorption lines, despite the fact that the radial velocities from the *H* absorption cores do not agree with the velocities from the *Ca* II K line. We conclude that at one elongation the emission of the stream produces a contour without a deep central depression. There is no such effect at the other elongation.

A somewhat similar phenomenon was observed in SX Cas. But in that star the suppression of the central *H* absorptions occurred at both elongations, being more conspicuous at the one preceding principal light minimum. Perhaps the difference in the behavior of the stars may be attributed to the asymmetry of the bright lines in RX Cas during principal eclipse. In SX Cas the asymmetry was in the opposite sense, if it was at all present: the violet emission component after mid-eclipse reached a greater intensity than the red emission component before mid-eclipse.

The evidence is strongly in favor of the hypothesis that the A5 features are variable in character and intensity, being produced, at least in part, in a tenuous stream of gas and not in a normal stellar reversing layer. On the other hand, the G3 spectrum apparently does not change and presents no anomalies.

The spectrum of the G star exhibits a somewhat unusual appearance. The multiplet of *Fe* I ($a^3F_4 - z^5G_5^o$) is characterized by very strong lines of λ 4383 and λ 4415, while the intermediate line, λ 4404, is abnormally weak. In α Persei[18] the relative intensities of

[16] R. M. Scott, *Pub. A.A.S.*, **10**, 234, 1942.

[17] Unsöld, *op. cit.*, p. 146, Table 37.

[18] Dunham, *Contr. Princeton U. Obs.*, No. 9, 1929.

these lines are 9:9:9. In the sun they are 15:10:8. In RX Cas, I estimate the intensities in the ratio 10:3:7. It is possible that the suppression of λ 4404 is caused by the overlying emission of a line produced in the A-type stream; but, if so, it is difficult to identify this line. There are a number of strong lines of *Ti* II in the vicinity—for example, λ 4407.7—but no lines of *Ti* II have been definitely found to show emission lines, even at the time of eclipse. The absorption line *Fe* I 4383.55 in RX Cas may be blended with *Fe* II + *Mg* II 4384.41.

IV. THE VELOCITY CURVES

In a star whose spectrum is G3 and is, moreover, blended with a source of type A5, most of the absorption lines are seriously blended; and it is not always possible to be certain of the identifications. After a few preliminary measurements I chose the star lines listed in Table 2. The lines of *Ca* I, *Fe* I, V I, *Sr* II, and *Y* II belong to the G3 spectrum.

TABLE 2

STAR LINES MEASURED IN RX CASSIOPEIAE

	H	*Fe* I	*Ti* II	*Ca* I
Hδ	4101.74	3997.40	4012.37	4226.73
Hγ	4340.47	4005.25	4289.84	
		4045.82	4301.99	*Sr* II
	Fe II	4063.60	4307.90	4077.71
	4173.45	4071.75	4443.80	4215.52
	4178.87	4143.87		
	4233.16	4260.49	*Ca* II	*Mg* II
	4351.77	4325.77	3933.67	4481.23
		4383.55		
	V I	4404.75	*Y* II	
	4416.49		3982.58	
			4309.63	

The line of *Ca* II K belongs to the A5 spectrum. The line *Fe* II 4233 probably belongs mostly to the A5 spectrum, but the other *Fe* II lines are blended. The lines of *Ti* II are probably also blended, but I have attributed them to the G3 spectrum. The lines of *H* behave in a peculiar manner and are probably blends of lines of the A5 and G3 spectra. The results of the measurements are given in Table 3.

The velocity-curves are shown in Figures 2–7. The curves for the mean of *Fe* I, *Ca* I, *Ti* II, *V* II, and *V* I and for *Sr* II represent the motion of the G3 star. Principal light-minimum occurs while the G3 star is in front. There appears to be, however, an appreciable shift of spectrographic conjunction from principal mid-eclipse. The velocity-curve is symmetrical, and conjunction takes place at phase 30.3 = −2.0 days. The minimum observed by me was at phase +0.75 day, and this latter phase was also symmetrical with respect to the changes of the bright *H* lines. Although the scatter of the radial velocities is large, it is impossible to reconcile the velocity-curve with a time of conjunction at phase +0.75 day. It will be necessary, at some future occasion, to investigate whether the time of photometric minimum really represents the time of conjunction. The A5 star of the system is a very strange object, and the light-curve may contain features which are not caused by the simple process of geometrical eclipse.

Pending the explanation of this discrepancy, we shall assume that the velocity-curve of the G3 star represents its orbital motion. The elements of this orbit are

$P = 32.315$ days
$\gamma = -24$ km/sec
$K = 36$ km/sec
$e = 0.0$
$T =$ phase 30.3 days (passage through γ velocity)

$a \sin i = 1.6 \times 10^7$ km

$$\frac{m_2^3 \sin^3 i}{(m_1 + m_2)^2} = 0.16\odot$$

These elements are remarkably similar to those which would have resulted from the corrected velocity-curve of SX Cas.

The velocity-curve from the line of *Ca* II K (Fig. 3) is entirely different from that of the lines belonging to the G3 star. Although the scatter is large and cannot be reduced by

TABLE 3

RADIAL VELOCITIES OF RX CASSIOPEIAE

PLATE	DATE 1944	U.T.	PHASE	RADIAL VELOCITY					
				Mean *Fe* I, *Ca* I, *Ti* II, *V* I, *V* II	*Sr* II	*Ca* II K	*H*	*Fe* II 4233	*Mg* II
CQ 2754...	Jan. 20	1:43	26.09	−45.7	−77.9	.....	−33.0	−18.9	−38.9
2758...	20	7:02	26.31	−42.8	−24.0	.....	−24.7	+ 9.3	−14.2
2763...	21	6:33	27.29	−48.1	−45.7	+ 3.7	−39.6	− 5.2	−10.5
2767...	22	1:50	28.09	−19.6	−27.3	+59.3	−30.2	+ 5.5	+ 1.6
2775...	23	6:41	29.29	−33.1	−29.0	+41.0	−28.5	+ 9.4	+ 9.9
2777...	24	3:07	30.14	−28.8	− 4.9	.....	−17.2	+16.3	−39.8
2782...	25	2:08	31.11	− 6.6	+ 3.1	.....	−27.9	+ 5.6	+ 9.7
2784...	25	5:30	31.24	− 8.4	+ 8.0	+ 8.4	− 3.4	+ 4.8	−31.3
2789...	26	1:47	32.09	−19.0	−25.8	+ 3.0	−30.2	− 1.6	−40.0
2790...	26	3:53	32.18	−22.9	−17.0	+47.1	−11.8	−81.8	−11.3
2792...	27	4:55	0.90	− 4.2	−13.8	.....	+ 2.7	− 6.4	+13.1
2795...	28	1:51	1.78	−17.9	−13.8	−34.1	−17.5	+15.6	+17.1
2800...	29	1:56	2.78	− 3.2	−10.4	−23.6	−50.3	−20.7	+ 4.2
2808...	30	5:01	3.91	+ 4.0	−11.9	− 3.0	− 9.4	+15.1	+32.6
2813...	31	2:38	4.81	+11.5	− 1.0	−13.8	−15.8	+22.1	+44.6
2821...	Feb. 3	2:00	7.78	+10.4	+ 9.6	−30.9	−28.4	.....	−28.7
2827...	4	8:10	8.79	+ 5.4	−10.8	−33.6	−25.4	+18.0	+68.8
2835...	5	1:42	9.77	− 2.7	+58.6	.....	−18.5	.....	+11.9
2836...	9	2:09	13.79	−19.3	−14.5	−26.8	−17.3	−25.9	+ 2.6
2846...	10	2:03	14.78	−22.1	−26.1	−28.4	−11.7	−36.6	+11.2
2862...	11	3:55	15.86	−29.5	.....	.....	−13.9	.....	+ 7.1
2864...	12	2:17	16.80	−27.4	−25.8	−22.4	−21.9	−15.6	+11.0
2873...	13	3:34	17.85	−48.4	−34.3	−19.9	−33.4	−51.8	+18.9
2880...	14	2:44	18.81	−28.7	−27.2	− 0.4	−25.0	− 8.6	+18.9
2888...	15	2:09	19.79	−38.7	−51.1	+ 6.3	−27.2	.....	+22.8
2895...	16	2:08	20.79	−61.3	−54.5	.....	−39.1	+16.6	−18.2
2900...	17	2:40	21.81	−75.3	.....	.....	−10.5	.....	+18.5
2907...	18	2:07	22.79	−57.7	−57.5	+38.2	−26.2	+27.3	−26.1
2911...	19	2:33	23.81	−40.5	−46.4	+39.6	+ 1.3	+42.1	+22.6
2919...	20	3:20	24.84	−75.6	−92.7	+ 9.8	− 9.3	+ 7.7	−30.3
2970...	Mar. 4	2.52	5.50	− 3.6	−18.1	−34.8	−45.0	−33.8	+26.5
2978...	5	3:22	6.52	+ 6.6	−16.4	−19.5	−53.4	−62.8	−39.0
2991...	7	2:30	8.49	+22.0	−10.1	−25.5	−36.5	.....	+38.7
3002...	9	3:07	10.52	− 2.9	−15.0	−31.5	−38.4	.....	+14.7
3004...	10	4:08	11.56	−15.8	−34.6	−43.8	−52.0	−52.1	+14.6

repeated measurements of the same plates, three features stand out clearly: (*a*) the trend is opposite to that of the G3 star, so that we are concerned with a line belonging to the A5 star, (*b*) the γ-velocity is much greater than the value of −24 km/sec obtained for the G3 star, and (*c*) the curve is unsymmetrical, having a shallow and broad minimum and a somewhat peaked maximum. If the curve is interpreted in the usual way, we find the following elements:

P = 32.315 days e = 0.18
γ = − 3 km/sec ω = 37°
K = 34 km/sec T = phase 30.3 days (periastron passage)

These elements are not compatible with the ones deduced for the G3 star. They are, however, distinctly similar to the elements of the A6 star in the system of SX Cas. We must probably conclude that they are spurious and that the velocity-curve of the A5

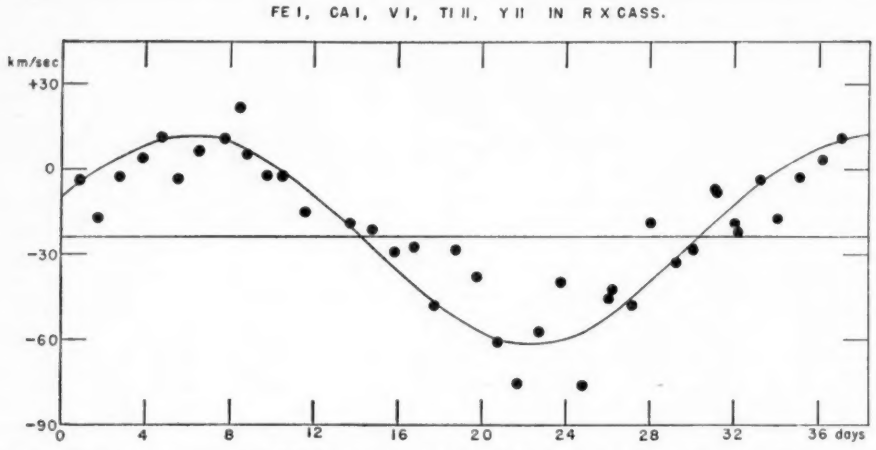

FIG. 2.—The velocity-curve of RX Cassiopeiae obtained from lines of *Fe* I, *Ca* I, *V* I, *Ti* II, and *Y* II. This curve represents the motion of the G-type component of the binary.

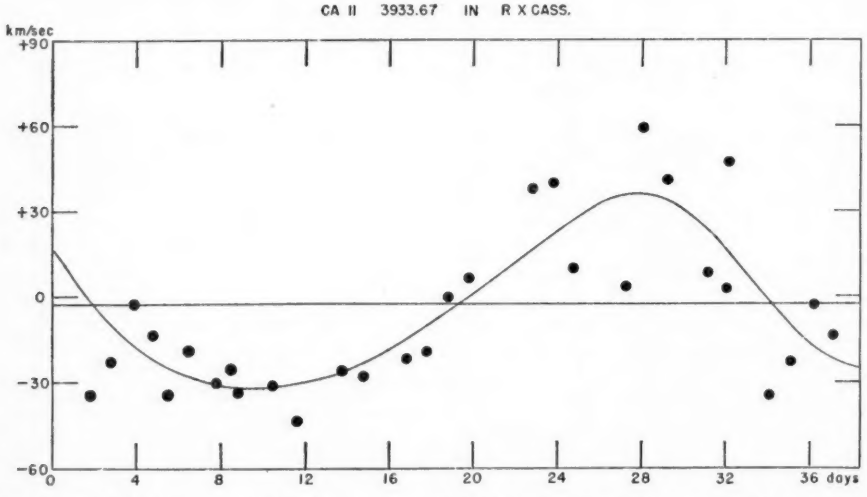

FIG. 3.—The velocity-curve of RX Cassiopeiae obtained from the line *Ca* II K, which belongs to the A-type component of the binary. Notice that the velocity of the system does not agree with that of the curve in Fig. 2. There is also a suggestion that the minimum is flatter than the maximum.

star in RX Cas is subject to distortions which are produced in the gaseous stream whose properties we discussed in the preceding section. It is unfortunate that the lack of precision of the measurements does not permit us to go further. I am unable to explain the large scatter of the measures near maximum radial velocity. The line is narrow and easy to measure, and duplicate measurements agree within a few kilometers. But there may exist accidental plate errors which prevent us from getting more consistent results for this single line.

A word of caution may be added at this point. The star is probably far enough away to show a weak interstellar *Ca* II K line, which would be blended with the much stronger line of the A5 star. From the B-type stars we know that the average velocity of the inter-

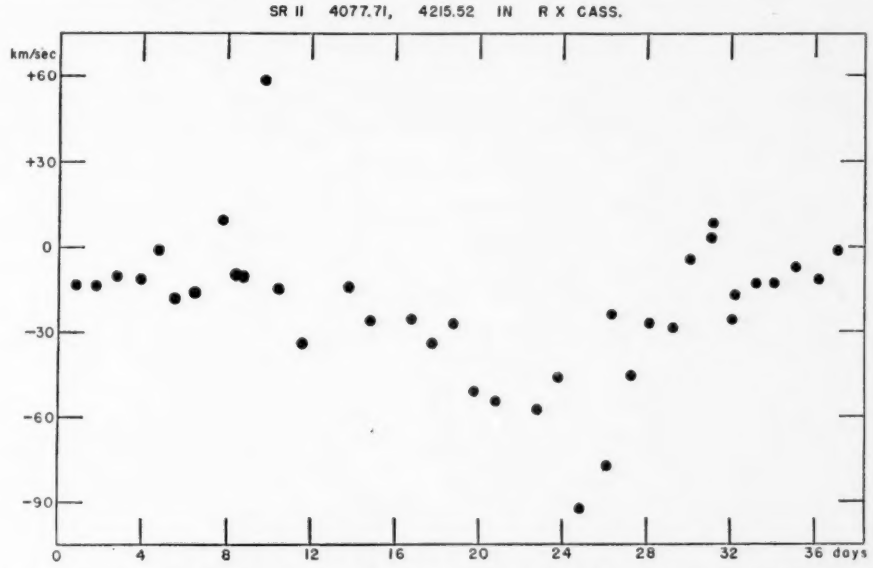

FIG. 4.—Radial velocities from two lines of *Sr* II. The trend of the curve agrees with that of Fig. 2, and the lines undoubtedly belong to the G-type component.

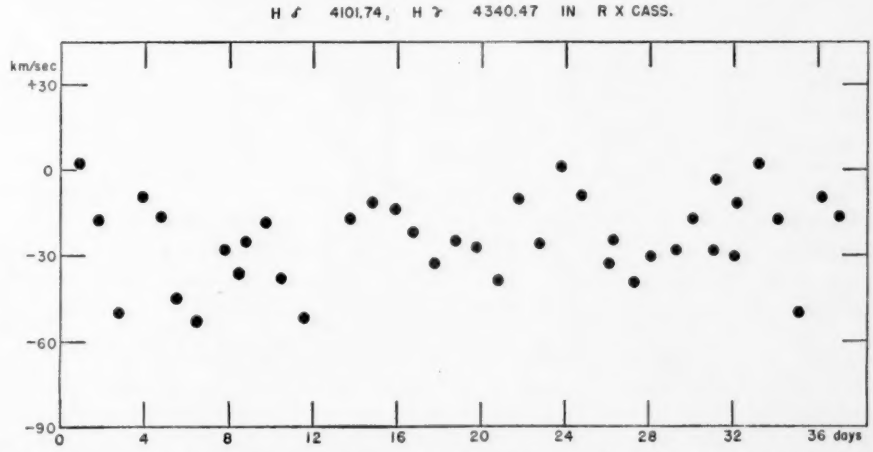

FIG. 5.—Radial velocities from two hydrogen lines in RX Cassiopeiae. There is no change within the errors of the measurements, but the mean is close to that of the velocity of the system as determined from the lines of the G-type star.

stellar lines in the vicinity of RX Cas (galactic longitude about 105°) is of the order of −15 km/sec. It is not very probable that this blending, if it has any effect at all, can account for the difference in γ between the G3 star and the A5 star. To accomplish this, the interstellar velocity would have to be positive.

The velocity-curve for the *H*-absorption cores shows no periodic variation, and the mean is about −20 km/sec. It is impossible to decide to what extent blending of the G3 and A5 spectra is important. But it is clear that the *H* velocities, in the mean, represent

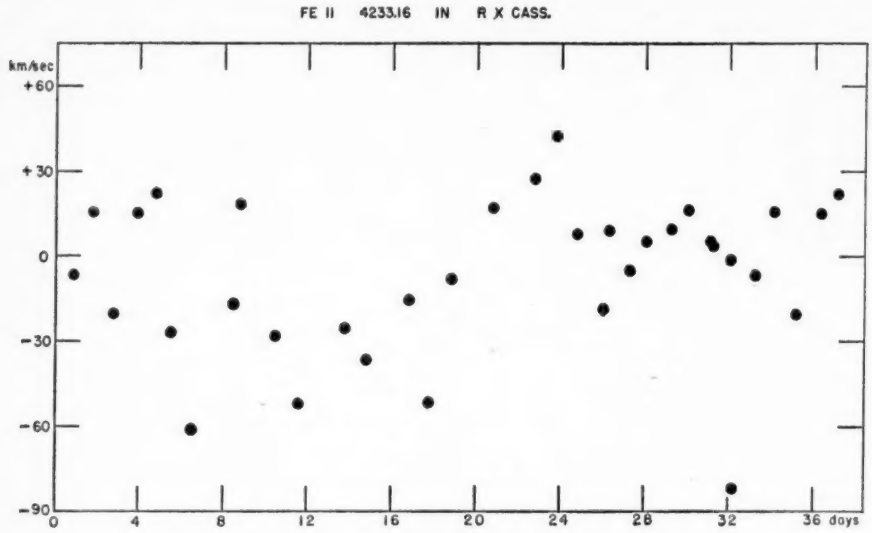

FIG. 6.—Radial velocities from a line of *Fe* II

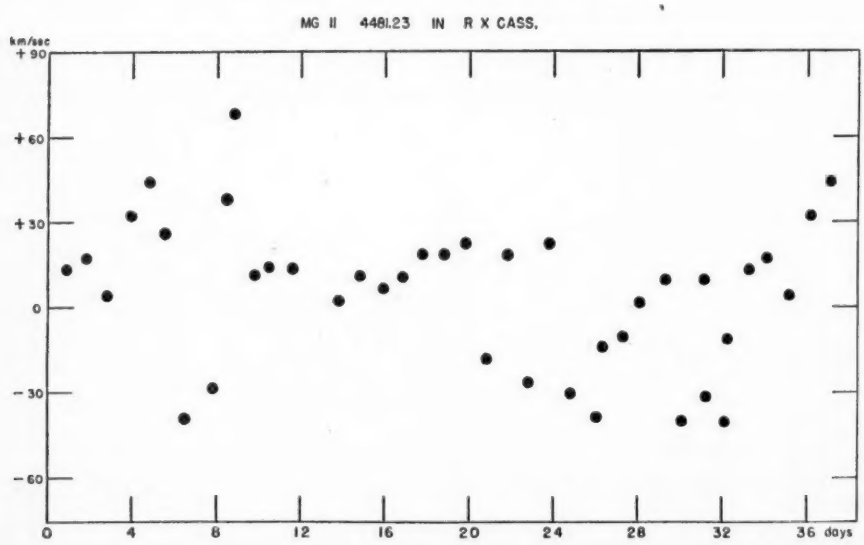

FIG. 7.—Radial velocities from a line of *Mg* II

the γ-velocity of the G3 star and, therefore, presumably the velocity of the system. The lines *Fe* II 4233 and *Mg* II 4481 give such a large scatter—perhaps because of blending —that no conclusion is possible. Both lines are concentrated near $V = 0$ km/sec, in the mean.

It is possible that the remarkable difference in γ which we have found for the two components of RX Cas was also present in the measures of SX Cas. It was found[19] that, during those phases of the principal eclipse of SX Cas where the G6 component should clearly predominate, the lines of *Ca* I and *Sr* II gave a decidedly greater negative velocity than had been expected. But this will have to be verified. If the difference in the two values of γ should be found to be an essential property of both systems, it may be argued that the velocity-curve for the G star represents the true velocity of the system. In that case the interpretation of the motions of the streams given for SX Cas will have to be somewhat modified. But the essential features will probably remain the same.

V. DISCUSSION

It has already been pointed out by Shapley that the photometric light-curve by Wendell leads to a set of elements which are rather poorly determined. The same is true of the light-curve by Martinoff. The difficulty rests partly in the fact that there is no phase

TABLE 4

SMOOTHED LIGHT-CURVE OF RX CASSIOPEIAE

Phase	$(1-l_1)$	$(1-l_2)$	Mean $1-l$	θ	$\cos^2\theta$	l^2
0	0.50	0.50	0.50	0°	1.00	0.25
1	.39	.45	.42	11	0.96	.34
2	.30	.32	.31	22	0.86	.48
3	.22	.23	.22	33	0.70	.61
4	.16	.16	.16	45	0.50	.71
5	.11	.10	.10	56	0.31	.81
6	.07	.05	.06	67	0.15	.88
7	.04	.02	.03	78	0.04	.94
8	.02	.01	.02	89	0.00	.96
9	.02	.03	.02	100	0.03	.96
10	.03	.07	.05	111	0.13	.90
11	.04	.13	.08	123	0.30	.85
12	.07	.20	.13	134	0.48	.76
13	.12	.25	.18	145	0.67	.67
14	.18	.28	.23	156	0.84	.59
15	.25	.29	.27	167	0.95	.53
16	0.28	0.28	0.28	178	1.00	0.52

of constant light at minimum and partly in the large amount of curvature exhibited by the light-curve between the minima. Light-curves of this character are very difficult to analyze, and the solution is often quite indeterminate. However, with the help of the spectrographic data there is some hope that the elements may be derived with a reasonable degree of precision.

The following discussion is based largely upon the light-curve by Martinoff. In this light-curve the secondary minimum occurs about 0.84 day later than phase $P/2 = 16.16$ days. Since Wendell's light-curve gave a small shift in the opposite direction and since the material is very uncertain, it is best to ignore any possible eccentricity (and rotation of the line of apsides) and to use a smoothed light-curve obtained by taking the mean intensities for phases $\pm p$. This has been done in Table 4.

In order to rectify the light-curve by the conventional methods,[20] we make use of the following expression for the light received by us at any time during the eclipse of the smaller star by the larger (principal eclipse):

$$l = l_1 + (1-a)\, l_2 = (1-\epsilon^2 \sin^2 i \cos^2\theta)^{1/2} \quad [L_1 + (1-a)\, L_2],$$

[19] *Ap. J.*, **99**, 99 and 100, 1944.

[20] H. N. Russell, *Ap. J.*, **36**, 64, 1912.

where ϵ is the eccentricity of the meridian section of each star, so that the semimajor axis of the spheroid is, in terms of the semiminor axis:

$$a_1 = \frac{b_1}{\sqrt{1-\epsilon^2}}.$$

Outside of the eclipse, $\alpha = 0$ and $L_1 + L_2 = 1$. Hence,

$$l^2 = 1 - \epsilon^2 \sin^2 i \cos^2 \theta .$$

In Figure 8 I have plotted l^2 against $\cos^2 \theta$, following Russell's procedure for the determination of $\epsilon \sin i$. The observations between $\theta = 0°$ and $\theta = 90°$ differ systematically from those obtained between $\theta = 90°$ and $\theta = 180°$. If we draw a straight line only through the points between $\theta = 0°$ and $\theta = 90°$, we obtain the beginning of the principal eclipse at $\cos^2 \theta = 0.82$ or $\theta = (360/P)\delta t = 24°$. Hence, $\delta t = 2.15$ days. This agrees satisfactorily with the spectroscopic determination $\delta t = 2.0$ days.

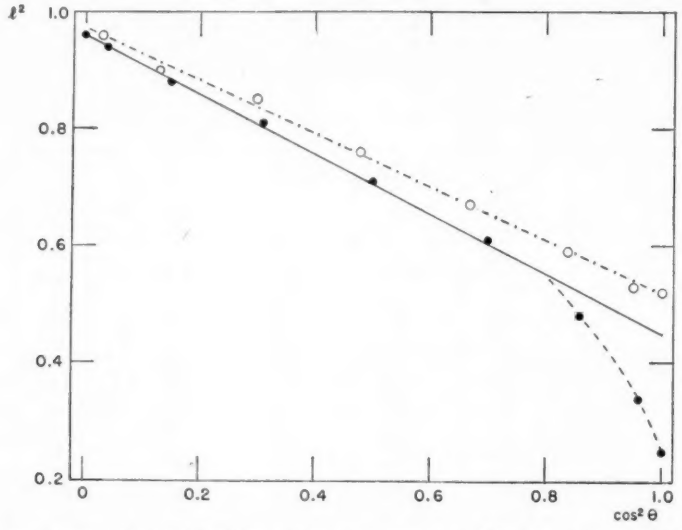

FIG. 8.—Determination of the ellipticity of the components. Solid circles, $\theta = 0°$ to $90°$; open circles, $\theta = 90°$ to $180°$.

However, unless we introduce the effect of reflection, we cannot reconcile the observations between $\theta = 90°$ and $\theta = 180°$ with this determination of the ellipticity effect. Because of the spectroscopic complications, it is undesirable to evaluate the reflection effect; and we shall content ourselves with the conclusion that a straight line satisfactorily fits all observations between $\theta = 90°$ and $\theta = 180°$. Hence, the secondary minimum is entirely accounted for by the ellipticity effect; any real secondary eclipse must be too small to be observable.

The ellipticity of the stars is found from the extrapolation of the straight line in Figure 8. At $\cos^2 \theta = 1$ we have

$$l_{\text{ell}}^2 = 0.45 = 1 - \epsilon^2 \sin^2 i .$$

Hence,

$$\epsilon \sin i = 0.74 ; \qquad \epsilon > 0.74 ; \qquad \frac{b}{a} < 0.67 .$$

This is an exceptionally small value of b/a. Gaposchkin[21] records that the smallest value known in 1938 was $b/a = 0.69$ for AG Virginis (undarkened solution).

[21] "Variable Stars," *Harvard Obs. Mono.*, No. 5, p. 60, Cambridge, 1938.

Since the conventional rectification of the light-curve has not given a measurable value for λ_2, the light at the middle of secondary eclipse, we must have recourse to the spectrographic observations. The spectral types of the two components are known; and the surface brightnesses resulting from them are, at λ 4000, in the ratio

$$\frac{J_A}{J_G} = 15 \quad (\text{at } \lambda 4000) .$$

With the same temperatures we find for the effective visual region of the spectrum, where the observations by Martinoff were made,

$$\frac{J_A}{J_G} = 7.3 \quad (\text{at } \lambda 5500) .$$

The light-curve gives directly for principal mid-eclipse $\Delta m_1 = 0.76$ mag., and for secondary mid-eclipse $\Delta m_2 = 0.38$ mag. If there were no ellipticity effect, we should have

$$\frac{1-\lambda_1}{1-\lambda_2} = \frac{J_A}{J_G} = \frac{0.50}{0.30} = 1.7 .$$

This is obviously not compatible with the spectrographic determination of J_A/J_G. In order to obtain such compatibility, we must attribute to the ellipticity effect

$$\Delta m_{ell} = 0.33 \text{ mag.} ,$$

leaving for the true eclipses

$$\Delta m_1 = 0.43 \text{ mag.} ,$$

$$\Delta m_2 = 0.05 \text{ mag.}$$

This gives

$$\frac{1-\lambda_1}{1-\lambda_2} = \frac{J_A}{J_G} = \frac{0.327}{0.045} = 7.3 .$$

The ellipticity found in this way must be less pronounced than the one found from the observations of the light-curve between $\theta = 0°$ and $\theta = 90°$ because of the systematic difference discussed previously in connection with Figure 8. We now have, in keeping with $\Delta m_{ell} = 0.33$ mag.:

$$l_{ell} = 0.74 ; \qquad l_{ell}^2 = 0.55 = 1 - \epsilon^2 \sin^2 i ,$$

$$\epsilon \sin i = 0.67 ; \qquad \epsilon > 0.67 ; \qquad \frac{b}{a} < 0.74 .$$

It is probable that the final value of the effective eccentricity is

$$\epsilon \sin i = 0.7 .$$

With the help of the spectroscopically determined values of $1 - \lambda_1$ and $1 - \lambda_2$ we may next determine the fraction α_0 of the area of the smaller star which is eclipsed when $\theta = 0°$:

$$\alpha_0 = 1 - \lambda_1 + \frac{1-\lambda_2}{k^2} .$$

We use

$$k = \frac{1}{3.9} = 0.257 .$$

The result is $a_0 = 1.007$, which is impossible because a_0 cannot exceed 1. We therefore assume that $a_0 = 1.00$ and that the eclipse is total. Since we do not observe a constant minimum of light and since the A5 spectrum never disappears, we must conclude that the eclipse is grazing; that is, that the beginning (and the end) of totality occurs at $\theta'' = 0$. It is possible that in deriving the value of k from the surface brightnesses of the two stars we exaggerated their difference in size. This determination rested upon the assumption that the temperatures of the two stars are known (from their spectral types) and that $L_A = L_G$ at λ 4000. It is improbable that this wave length can be in error by as much as $\pm$ 500 A. But making two extreme assumptions—λ = 3500 A and λ = 4500 A —and retaining the same temperatures as previously, we find:

	$\lambda = 3500$ A	$\lambda = 4000$ A	$\lambda = 4500$ A
J_A/J_G	21	15	11
k	0.22	0.26	0.30

The change in k is slight; but it is, nevertheless, sufficient to change a_0 from 1.00 to about 0.83, thereby making the eclipse a partial one. But it is useless to continue with these refinements. In the first place, we do not know with sufficient precision the values of $1 - \lambda_1$, and especially of $1 - \lambda_2$. In the second place, the temperatures of the stars are not known accurately. It may, for example, be possible that, since some of the absorption features of the A-type spectrum are attributed to a stream, the real type of the star involved in the stream may not be known. For the beginning of the partial phase of the eclipse we have

$$\theta' = 24^\circ .$$

We then make use of the equation for the distance between the centers of the apparent stellar disks:[22]

$$\delta^2 = \cos^2 i + \sin^2 i \sin^2 \theta .$$

Hence, for the beginning of the eclipse and for its middle we have two equations, from which we can eliminate i and a_1:

$$a_1^2 (1 - \epsilon^2 \sin^2 i \cos^2 \theta') (1 + k)^2 = \cos^2 i + \sin^2 i \sin^2 \theta' ,$$

$$a_1^2 (1 - \epsilon^2 \sin^2 i \cos^2 \theta'') (1 - k)^2 = \cos^2 i + \sin^2 i \sin^2 \theta'' .$$

Remembering that $\theta'' = 0$ and $\theta' = 24^\circ$, we find

$$\left.\begin{aligned} i &= 75^\circ , \\ a_1 &= 0.50 , \\ a_2 &= 0.13 , \\ L_1 &= 0.67 \\ L_2 &= 0.33 \end{aligned}\right\} \text{in visual light} .$$

I am indebted to Dr. Newton L. Pierce, of Princeton University, for a list of references to photometric observations of RX Cas; to Drs. Helen Steel, Carlos U. Cesco, and Jorge Sahade for a part of the spectrograms used in this paper; and to Miss J. Ringstad for help in the computations.

[22] Russell, *Ap. J.*, **35**, 321, 1912.

RECENT PROGRESS IN ASTROPHYSICS

RUSSIAN INVESTIGATIONS OF ECLIPSING VARIABLES

"ON THE SMALLER EFFECTS IN ECLIPSING VARIABLES" BY D. J. MARTINOFF[1]

Martinoff points out that in the decade preceding 1941 an intensive investigation of the fine effects of eclipsing variables has been carried on in the Soviet Union and elsewhere. In many cases, however, the available theoretical methods were not very satisfactory.

The major purpose of Martinoff's paper is to examine whether it is possible to determine the fine effects from the existing light-curves. By "fine effects" he understands especially the dissimilarity of the components and the orientation of their axes. In addition, he deals with the problem of the reflection effect and considers Krat's criticism of Russell's paper in 1939.

Martinoff computes light-curves for a hypothetical eclipsing system with given relative dimensions. He derives a set of well-known formulas, involving the eclipsed area (α), the ellipticity of the components (ϵ), their relative total brightness (L), the ratio of radii (k), and the elongation angle (θ). He also adds the reflection effect. After some discussion of the four well-known expressions for the reflection effect—those of Eddington (1926), Milne (1927), Pike (1931), and Krat (1934)—he expresses a preference for the formulas of Eddington and Milne as against those of Pike and Krat.

He then computes the light-curves for three models with similar components and compares the results with those that would be obtained with the assumption of dissimilar components. Computations were made for the case of uniform brightness; and the results are that the deviations for curves of similar and dissimilar components do not amount to more than 0^m02, and the differences between computed and adopted values are within the same limit. In other words, we are not able at present to deduce the dissimilarity of the components from moderately good light-curves. The computations were repeated for nonuniform brightnesses of the components and gave even less determinate results, as Martinoff had expected.

In discussing the reflection effects given by Eddington, Milne, Pike, and Krat he considers that Pike's formula, and its improvement by Krat, should not be adopted uncritically; the formulas of Eddington and Milne are preferable. After some criticism of Krat's method for rectifying the reflection effect he proposes the following rectification formula (a development of Russell's):

$$l_{\text{rect}} = \frac{l_{\text{obs}} + b\,(1+\cos\theta) + C\sin^2\theta}{a+b+c} \cdot \frac{1}{\left(1-2\left(\frac{c}{a}+C\right)\cos\theta\right)^{1/2}}.$$

Martinoff's general conclusion is that "there has been some haste in the methods and an absence of the right instinct toward the observational material; in consequence, the results obtained upon fine effects prior to 1941 should be considered doubtful, if not erroneous." In other words, more common sense should be used in the interpretation of eclipsing variables.

[1] *A.J. Soviet Union*, **19**, 63, 1942.

"THE REFLECTION EFFECT IN ECLIPSING VARIABLES" BY M. G. ODINZOV[1]

While Martinoff's paper deals with the question of how far the fine effects can be determined from the light-curve, Odinzov's paper is dedicated to the single problem of the reflection effect. He first points out that, although there is no unanimous agreement on the form of the reflection effect, it is possible to combine the results in a satisfactory solution. He does not pretend to solve the whole problem; he excludes the physical and treats chiefly the geometrical side of the effect. He discusses principally the problem of the forms of the components and touches upon some other related questions.

1. *Spherical stars.*—From the beginning to the end he uses, as his fundamental formula for the reflected radiation, that obtained by Milne in 1927. This law is a function of the relative brightness of the primary star and of the geometrical properties of the second (reflecting) component, which is small, relative to the distance between the centers. Odinzov derives some formulas, which were given also by other authors, notably by Krat. Before coming to his expression for the reflection effect, he mentions that the intensity of reflected radiation follows the law of darkening at the limb, a result first pointed out by Krat. Then Odinzov points out that the discrepancy between an exact expression for the reflected radiation and an approximate one given first by Eddington and again rederived by Krat and Odinzov is by no means great—a discrepancy amounting to not more than 1 per cent. Krat in 1934 thought that the discrepancy could amount to as much as 30 per cent.

Odinzov evaluates the *change* of reflected radiation (L_{r_2}) with phase (Φ) by a method similar to that of Milne, whose transformation of the variables he adopts:

$$\left.\begin{aligned} L_{r_2}(\Phi) &= \frac{L_1}{4\pi}\left[\, r_2^2 f_M(\Phi) + r_2^3\left(\frac{3}{2}\cos^2\frac{\Phi}{2} - 1\right)\cos^2\frac{\Phi}{2}\,\overline{M}(\Phi)\,\right] \\ &= \frac{L_1}{4\pi}\, r_2^2 f_M(\Phi) + r_2^3 f_0(\Phi) \ldots\ldots, \end{aligned}\right\} \tag{1}$$

where r_2 is the radius of the reflected component. For small phase angles equation (1) is practically identical with

$$L_{r_2}(\Phi) = \frac{L_1}{4\pi}\left(r_2^2 + \tfrac{3}{4} r_2^3\right) f_M(\Phi) \ldots\ldots \tag{2}$$

The distribution of the reflected radiation over the disk is treated graphically, the cases shown being those for $\Phi = 15°$, $30°$, and $45°$. The displacement (X) of the center of gravity of the reflected radiation (which is very important for spectroscopic binaries with close components) is given by the formula

$$X = -r_2\left[\sin\tfrac{1}{2}\Phi + (0.06 + 0.2\, r_2)\sin\Phi + 0.08\sin 2\Phi \ldots\ldots\right. \tag{3}$$

2. *Ellipsoidal stars.*—Odinzov starts from the rotation ellipsoids with an ellipticity, ϵ, with their major axes, a, in alignment. The analysis obviously becomes more complicated; but he overcomes the difficulties by applying simplifications similar to those used for treating spherical components, and finds

$$L_{r_2}(\Phi, \epsilon) = L_{r_2}(\Phi, 0) + \frac{L_1}{4\pi^2}\, a^2\epsilon^2\left[\int\frac{\partial}{\partial\epsilon^2}\left(\frac{\cos\alpha\cos\theta}{R^2}\right)\sqrt{(1-\epsilon^2)\,(1-\epsilon^2\nu^2)}\, d\omega \ldots\ldots\right. \tag{4}$$

[1] *A.J. Soviet Union*, **19**, 80, 1942.

After many lengthy but simple transformations, he obtains

$$L_{r_2}(\Phi, \epsilon)\frac{L_1}{4\pi}(a^2+\tfrac{3}{4}a^3-\tfrac{6}{5}\epsilon^2a^2)\,f_M(\Phi)+\frac{L_1}{4\pi}\times\epsilon^2a^2\frac{4\bar{M}(\Phi)}{15\pi}\sin^3\Phi\ldots., \quad (5)$$

where $f_M(\Phi)$ is Milne's function and $\bar{M}(\Phi)$ can be put equal to unity in most practical cases.

He derives the shift of the center of gravity in a manner similar to that employed for spherical stars and gives one example for $\Phi = 45°$.

3. *Stars with axes out of alignment.*—If the major axes are turned relative to the line of centers, making an angle II with it, he derives a more complicated formula for the reflected radiation, depending upon phase (Φ), ellipticity (ϵ), and the angle (II):

$$\left.\begin{aligned} &L_{r_2}(\Phi,\epsilon)\frac{L_1}{4\pi}\left[a^2+\tfrac{3}{4}a^3-\frac{\epsilon^2a^2}{2}(1+\tfrac{7}{5}\cos^2\Pi-\tfrac{1}{5}\sin^2\Pi\cos^2 i)\right]f_M(\Phi)\\ &+\frac{L_1}{4\pi^2}\epsilon^2a^2\bar{M}(\Phi)\left[(\tfrac{4}{15}\cos^2\Pi-\tfrac{1}{3}\sin^2\Pi\sin^2 i)\sin^3\Phi+\tfrac{4}{15}\sin^2\Pi\sin^2 i\sin^2\Phi\right]\\ &+\frac{L_1}{4\pi^2}\epsilon^2a^2\times\tfrac{1}{12}\sin 2\Pi\sin i\bar{M}(\Phi)\sin\Phi[5.142-\Phi+\tfrac{3}{2}\sin 2\Phi]\ldots., \end{aligned}\right\} \quad (6)$$

where i is the inclination of the orbit.

It is of interest, as he points out, to consider in passing that the co-called "periastron effect" (the difference in height of the maxima) cannot be explained by a lack of alignment of the ellipsoids. The amount of the asymmetry of the reflected radiation produced by this cause is computed, using equation (6) but putting $-\Pi$ instead of $+\Pi$. He applies his computed result to a visual light-curve given by Dugan for RV Ophiuchi and finds that his results are not in agreement with observation. He concludes that a lack of alignment cannot explain the periastron effect.

4. *Practical application.*—In the rectification of a light-curve for the reflection effect, he recommends the use of the formula given by Martinoff (see the foregoing review). A second approximation may also be made; and here he assumes that the whole discrepancy between theory and observation is caused by the secondary component and that therefore equation (5) can well be used. He then suggests the introduction of a certain "effective" radius for the star, depending on the phase, with total darkening at the limb and an intensity equal to the value of the reflection at a given phase. He has, therefore, to employ the function of limb darkening, for which he recommends the use of the tables of Zessewitsch. No actual example is given.

5. *Test of formulas.*—It is well known that the computed reflection in the majority of cases is larger than the observed one. The observed effect is in itself not large; it amounts in most cases to less than 0.05 of the total light of the system. From the twenty-three values published by the reviewer in 1932 the mean difference between the computed and observed reflection effect is +0.008. Krat found in 1934 a discrepancy of as much as 0.019 from eighteen eclipsing variables. The explanation given by Krat as early as 1934, in terms of the "effective frequency" of radiation for the different components, does not seem probable to Odinzov. An attempt by Kopal in 1939 to explain it by the introduction of the bolometric correction should also be considered unsuccessful, because Kopal's formula for computing the effect seems to be in error. Odinzov states that if the bolometric correction is correctly applied, the discrepancy becomes even greater.

Finally, Odinzov makes use of eighteen eclipsing variables for which Krat has applied his formulas in 1934. Odinzov does not give the details of his computations. He uses the computed ellipticities of the components, not the directly observed ones, in accordance with Walter's formulas. The latter are connected with the internal constitution of the stars.

Odinzov finds that the computed values of the reflected radiation are in the majority of cases smaller than the observed ones, a result that was anticipated by Eddington in 1926. The mean value of the difference for eighteen reflection effects as computed by Odinzov is −0.005, as may be seen from Table 1.

TABLE 1

COMPUTED AND OBSERVED REFLECTION EFFECTS

Star	L_1	a_1	a_2	Computed	Observed
RY Aqr	0.871	0.188	0.247	0.028	0.000
Y Cam	.974	.244	.238	.032	.041
R CMa	.941	.253	.244	.032	.015
RS CVn	.828	.128	.200	.023	.034
RZ Cas	.898	.259	.293	.031	.063
TV Cas	.884	.287	.314	.046	.074
TX Cas	.842	.567	.295	.011	.030
U Cep	.938	.200	.322	.038	.043
U CrB	.968	.196	.285	.042	.062
Z Dra	.869	.191	.222	.024	.032
TW Dra	.898	.211	.324	.032	.008
U Her	.658	.294	.359	.006	.036
RV Oph	.825	.129	.207	.023	.018
β Per	.939	.206	.243	.024	.045
RT Per	.859	.296	.264	.027	.022
X Tri	.875	.295	.336	.039	.018
W UMi	.917	.408	.324	.032	.038
Z Vul	0.867	0.323	0.300	0.038	0.030

S. GAPOSCHKIN

HARVARD COLLEGE OBSERVATORY
February, 1944

NOTES

NOTE ON THE SPECTRUM OF 12 COMAE BERENICES

Four plates of the spectroscopic binary 12 Comae Berenices were taken by O. Struve with the Cassegrain spectrograph of the 82-inch reflecting telescope at the McDonald Observatory, with a dispersion of 40 A/mm at λ 3933. The spectrum of this star is composite, being designated as gF4 + A by Trumpler.[1] An orbit from Lick Observatory spectrograms has recently been published by Julie M. Vinter Hansen.[2] Her measurements were made in the ordinary photographic region and refer to the F star. She states that "the spectral lines on her plates were rather weak due to the veiling of the spectrum of the primary by that of the secondary." At the suggestion of Dr. G. P. Kuiper, the four ultraviolet McDonald plates were measured in order to determine whether the spectrum of the A-type component is responsible for the absorption-line spectrum in the ultraviolet region. The measured values are shown in Table 1.

TABLE 1

Date	Plate	Measured Region	Number of Measured Lines	Radial Velocity (Km/Sec)	Mean Error
1943, July 7	CQ 2215	λλ 3610–3930	15	+19.5	±7.1
1943, July 7	CQ 2216	λλ 3490–4100	21	7.2	4.0
1943, July 7	CQ 2217	λλ 3430–3935	26	10.6	4.8
1943, July 7	CQ 2218	λλ 3550–4105	17	+ 7.8	±4.4

The radial velocity computed for July 7, 1943, with the elements given by Miss Vinter Hansen, is +13.5 km/sec, a value that agrees reasonably well with our measures. The expected velocity of the secondary for the same date should be about −15 km/sec. We conclude that there is no evidence of the spectrum of the secondary, except for the line *Ca* II K (λ 3933.68), which gives −21.7 km/sec as the average of the four plates. Presumably, continuous Balmer absorption on the violet side of λ 3647 and confluence of the wings of strong Balmer lines in the A star sufficiently weaken the continuous spectrum of this star, to leave the metallic absorption-line spectrum of the F star essentially undisturbed. Most of the lines measured by us were due to *Fe* I and other metals. The few hydrogen lines included in the measurements show no systematic departure from the other lines.

CARLOS U. CESCO
JORGE SAHADE

YERKES OBSERVATORY
November 24, 1943

[1] *Lick Obs. Bull.*, **18**, 186, 1938.

[2] *Lick Obs. Bull.*, **19**, 101, 1940.

COMPLEX LINES IN THE SPECTRUM OF θ AURIGAE*

About twelve years ago an announcement was made of the variability of certain lines, due principally to *Cr* II, in the spectrum of the second-magnitude A star θ Aurigae.[1] A number of plates of ordinary one-prism dispersion were taken during the two years following; these served only to confirm the variability found earlier, without permitting a period to be found. The changes observed may be summarized as follows: At times the lines of *Cr* II as a group seem to be unusually strong; this change probably does not take place rapidly, as series of plates taken on the same night appear to be similar. When the *Cr* II lines are faint the whole line spectrum seems to be affected by a general weakening, with the exception of certain lines of *Fe* II and *Si* II and *Mg* II 4481, which appear of approximately constant intensity.

In the autumn of 1943 several coudé spectrograms of the star were obtained with the 82-inch reflector of the McDonald Observatory; these spectrograms show that certain lines are complex in appearance, with a suggestion in some cases of duplicity. Plate XXI shows the region λλ 4545–4595, as enlarged from a coudé spectrogram taken on November 22, 1943, and illustrates the complex structure of the *Cr* II lines at λλ 4555, 4558, and 4590. It does not seem likely that the apparent duplicity of some of the lines can be explained on the assumption of a system of two stars, as the spectrum has not been observed with sharp, single lines; it is more probable that the structure is a phenomenon associated with the atmosphere of a single star. The star θ Aurigae belongs to the class of peculiar A stars in which the *Si* II lines are abnormally strong.

W. A. Hiltner
W. W. Morgan

Williams Bay, Wisconsin
February 1944

* *Contributions from the McDonald Observatory, University of Texas*, No. 90.

[1] *Ap. J.*, **75**, 423, 1932.

THE CONTINUOUS ABSORPTION COEFFICIENT OF THE NEGATIVE ION OF HYDROGEN: A CORRECTION

Dr. S. Chandrasekhar has kindly drawn my attention to the fact that there is an error in equation (35) in my paper in the January issue of the *Astrophysical Journal*.[1] The coefficients of $\mathfrak{Z}_6$, $\mathfrak{Z}_5$, $\mathfrak{Z}_4$, $\mathfrak{Z}_3$, and $\mathfrak{Z}_2$ in this equation should respectively be $3 \cdot 4!$, $-4 \cdot 5!$, $\frac{5}{3} \cdot 6!$, $\frac{2}{3} \cdot 7!$, and $-\frac{1}{3} \cdot 8!$, instead of $\frac{1}{3} \cdot 4!$, $-\frac{16}{3} \cdot 5!$, $3 \cdot 6!$, $-\frac{2}{3} \cdot 7!$, and $+\frac{1}{3} \cdot 8!$, as given. This error entails some further corrections. Thus, in equation (38) the coefficients of χ_{10} on the right-hand side of this equation should respectively be $+1$, $+6$, $+36$, $+240$, $+600$, -1680, and -6720, instead of $+1$, $+6$, $+44$, $+320$, $+1080$, $+1680$, and $+6720$, as given. Again, in equation (43) the numerical coefficients of $\mathfrak{L}_6$, $\mathfrak{L}_5$, $\mathfrak{L}_4$, $\mathfrak{L}_3$, and $\mathfrak{L}_2$ should respectively be 9.25451×10^{-2}, -1.03821×10^{-1}, 4.48888×10^{-1}, -2.15486×10^{-1}, and $+1.02609$, instead of 9.29071×10^{-2}, -1.04245×10^{-1}, 4.49261×10^{-1}, -2.15996×10^{-1}, and 1.02668, as given.

[1] **99**, 59, 1944.

PLATE XXI

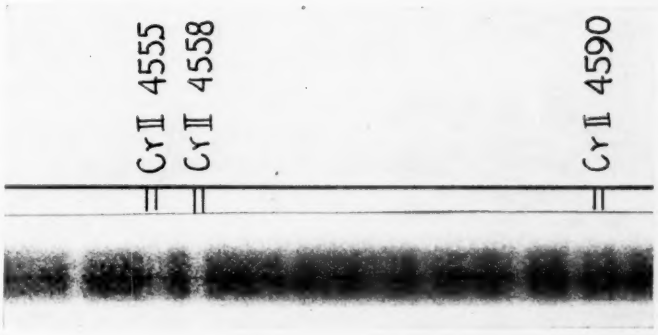

Coudé Spectrogram of a Short Region of θ Aurigae; Dispersion of Original Spectrogram: 3.3 A/mm

Fortunately, the foregoing errors do not introduce any substantial corrections to the table of absorption coefficients on page 68. The following table now replaces Table 8 of the paper.

THE CONTINUOUS ABSORPTION COEFFICIENT OF NEGATIVE HYDROGEN ION FOR DIFFERENT WAVE LENGTHS

λ (In Angstrom Units)	$\kappa_\lambda \cdot 10^{17}$ Cm^2	λ (In Angstrom Units)	$\kappa_\lambda \cdot 10^{17}$ Cm^2	λ (In Angstrom Units)	$\kappa_\lambda \cdot 10^{17}$ Cm^2	λ (In Angstrom Units)	$\kappa_\lambda \cdot 10^{17}$ Cm^2
1000.....	0.2783	4500.....	2.802	7000.....	3.934	10,000.....	3.172
2000.....	0.9611	5000.....	3.142	7500.....	3.955	12,000.....	1.993
2500.....	1.323	5500.....	3.438	8000.....	3.906	14,000.....	0.8484
3000.....	1.686	6000.....	3.674	8500.....	3.795	16,000.....	0.0803
3500.....	2.058	6500.....	3.840	9000.....	3.630	16,533.....	0.0000
40000.....	2.435			9500.....	3.419		

Finally, in equation (45) read 20.68 in place of 20.77.

LOUIS R. HENRICH

NEW YORK CITY
April 4, 1944

REVIEWS

Galaxies. By HARLOW SHAPLEY. ("Harvard Books on Astronomy.") Philadelphia: Blakiston Co., 1943. Pp. 229+126 figs. $2.50.

Only the day before this volume came to the reviewer's desk, a colleague returned several of the "Harvard Books on Astronomy" to the library, saying how interesting and well written they are. The present volume is no exception, and it serves the dual purpose of giving to the layman an attractive account of our present conception of the universe and to the astronomer the author's present views on the subject. As stated in the Preface, the work is based upon a series of lectures given nearly ten years ago, and naturally the author's views, like those of others, have been subject to constant expansion and revision in the interval.

To begin with, the title "Galaxies" has the approval of the reviewer. It has the advantage that we all know what the author is writing about, and a constant effort is not required to remind the public that there are two classes of nebulae. In general, the work is nontechnical; in fact, in scarcely any other field of astronomy are the latest results of research so easily adapted for exposition to the layman. Where the original methods of investigation are so simple there is little trouble in writing a nonmathematical book. As has been well said, for research of the solar system a seven-place logarithm table may be required, but in the metagalaxy one can get along very well with a ten-inch slide rule.

After an introductory chapter with some excellent instructions for the general reader, the author takes up the Magellanic Clouds as the nearest of the external systems and as sources of information and methods that can be applied farther out in space. One wonders how long it would have taken astronomers to evolve our present conception of the universe if the Harvard Observatory had not had a southern station and if Miss Leavitt had not found the period-luminosity relation for Cepheid variable stars. But, as Shapley points out, if instead of the amorphous Magellanic Clouds a regular spiral galaxy had been placed at the same distance, we now should be much further along in the study of outer systems. The Harvard observers have had something of a monopoly on the Magellanic Clouds, but their studies have been necessarily restricted to giant stars, since a dwarf star like the sun would have an apparent photographic magnitude 22.5 at the distance of one of the Clouds. Shapley tells a fascinating story of what studies of the Clouds have contributed to a knowledge of their structure, and one is rather staggered at the estimate of the possible number of dwarf stars they contain. If there are 200,000 stars brighter than absolute magnitude 0.0 in the Large Cloud, then on any reasonable basis the total number of stars in this Cloud is to be reckoned in millions. He does a real service in reminding us that the total luminosity of the Large Cloud is at least as great as that of the average galaxy. He also gives a list of ten contributions to the knowledge of stars and galaxies that have come from studies of the Clouds, or are on the way; but, as some of these items are of doubtful application to our Galaxy and other systems, he gives a word of caution under the heading of "Tools That Are Not Sharp Enough."

The chapter on the Milky Way as a galaxy is devoted almost wholly to the Harvard work on clusters and variable stars, a more general discussion of our own stellar system being left to another volume of the series, *The Milky Way* by Bok and Bok. It is interesting to note that the diameter of our Galaxy in its own plane is given as only about 100,000 light years, and it will be a good joke if Shapley has made the Galaxy too small. However, as he points out, the boundaries of all galaxies are so indefinite that any assigned dimension is without much significance unless the corresponding luminosity or star density is included.

The discussion of neighboring galaxies includes special reference to the new systems in Sculptor and Fornax discovered at Harvard. The reader is a little surprised to be introduced to the Andromeda nebula by the statement that Hubble's estimate of the distance may be wrong by more than 50,000 light years. A fairer statement would have been that Hubble began by getting a distance that was 500,000 light years nearer right than the estimates of many others. The importance of the Andromeda nebula, M33 in Triangulum, and the other galaxies of the local group, which give the best chance of being resolved into their stellar content, is well understood.

Hubble has said that there is plenty of material to occupy the full time of one observer on M31 alone. Shapley refers in several places to the spherical haze about our own and other galaxies, but it should be pointed out that this haze about the Andromeda nebula needs further confirmation. It was not found by Whitford in microphotometer tracings of Mount Wilson photographs, and there is no indication of a spherical form in the results of R. C. Williams on a Schmidt photograph from Mount Palomar.

When we get to the metagalaxy, we have a feeling that we are entering the author's own field; for, whether he invented the term or not, he at least has used it more than anyone else. Also we arrive at the familiar ground of attempting to show that Shapley's figures are too large. We soon come to the staggering distance of 1,600,000,000 light years, but we find that this is simply the hypothetical distance at which the Andromeda nebula would appear of magnitude 21.0, the assumed limit of the 100-inch reflector. Here the difficulty is that magnitude 21.0 smeared over the resulting area of 4″ in diameter would be quite out of reach of the 100-inch reflector. The central region alone, say 1″ across, would be about a magnitude fainter than the total, and the nebula would still be too faint to detect.

Again, in the last chapter, we read that the space density of galaxies appears to be uniform, on the average, within a sphere of perhaps half a billion light years in diameter. Taking the author's figures of magnitude 17.6 for the limit of the Harvard survey and absolute magnitude −15.2 for the average galaxy, the radius of the sphere comes out as 115,000,000 light years instead of 250,000,000. These slips are not errors in a technical discussion; they are simply overstatements in a popular book, but the name of the author carries such weight that the general reader is likely to accept a printed figure as an observed fact.

The last chapter, on the "Expanding Universe," includes much besides the expansion, and the author runs in a good deal of speculation, leaving the reader with a confused picture, but perhaps not more confused than the present state of our knowledge.

The typography and format of the book are pleasing. There are plenty of pictures, an average of more than one illustration or diagram to each double opening. Several of our old friends, both astronomers and galaxies, suffer from the rather harsh contrast of some of the reproductions.

Although the author makes an obvious effort to refer to the works of others in the same field—he even goes out of his way in places to give them due credit—the fact remains that history is not always best written by those who make it. The generally acknowledged sequence of the development and achievement of our present conception of galaxies is that, following the work of Miss Leavitt on Cepheid variables and of Bailey on clusters, it was, first, Shapley's work on the general system of globular clusters that enlarged the Galaxy to previously inconceivable dimensions and, second, Hubble's work on the Andromeda and other nebulae which placed them definitely as separate galaxies outside our own. Simple as these facts are, they do not stand out in the book; in fact, they are not there in recognizable form. Perhaps we should not expect the present author to emphasize them; but, as far as we can see, these two epoch-making events in the history of astronomy will stand out for all time.

We must end on a note of commendation. The little work is certainly delightful reading. One cannot help sharing the author's enthusiasm over his journeys in space, and we wish him many more of them, using his own quotation which has come from Stevenson to Jeans to Shapley: "To travel hopefully is a better thing than to arrive."

JOEL STEBBINS

Washburn Observatory
University of Wisconsin

ERRATUM

In the legend of Plate X, facing page 226, Volume **99**, the phase of the second spectrogram should be 2.318 days instead of 2.378 days.

INDEX TO VOLUME 99

INDEX TO SUBJECTS

PAGE

Z Andromedae, Spectroscopic Observations of AX Persei, RW Hydrae, CI Cygni, and. *Paul W. Merrill* 15

Astrophysical Research in France in 1940–1942. *P. Swings* 115

θ Aurigae, Complex Lines in the Spectrum of. *W. A. Hiltner and W. W. Morgan* . . . 318

Binary HD 214419, The Wolf-Rayet Spectroscopic. *W. A. Hiltner* 273

Binary Systems, On the Stability of. *S. Chandrasekhar* 54

α^2 Canum Venaticorum, Note on the Spectrum of. *W. A. Hiltner* 256

Cassiopeia, Analysis of the Milky Way in. *Robert H. Baker and Elaine Nantkes* . . . 125

RX Cassiopeiae, The Spectrum of. *O. Struve* 295

SX Cassiopeiae, The Spectrum of. *Otto Struve* 89

U Cephei, Note on the Problem of. *Zdeněk Kopal* 239

U Cephei, The Spectrographic Problem of. *Otto Struve* 222

VV Cephei, The Ultraviolet Spectrum of. *Otto Struve* 70

Color Indices of Proper-Motion Stars. *W. J. Luyten, P. D. Jose, and J. F. Foster* . . 244

Colors of Early-Type Stars in the Southern Milky Way. *Francis J. Heyden, S.J.* . . 8

12 Comae Berenices, Note on the Spectrum of. *Carlos U. Cesco and Jorge Sahade* . . . 317

Comet 1940c, On the Spectrum of. *N. T. Bobrovnikoff* 173

Comet Whipple-Fedtké-Tevzadze (1942g), The Spectrum of. *Andrew McKellar* . . . 162

Continuous Absorption Coefficient of the Negative Hydrogen Ion, The. *Louis R. Henrich* 59

Continuous Absorption Coefficient of the Negative Hydrogen Ion, The: A Correction. *Louis R. Henrich* 318

β Coronae Borealis, The System of. *F. J. Neubauer* 134

Curtis, Heber Doust, 1872–1942. *Robert R. McMath* 245

Curve of Growth, Line Intensities and the Solar. *K. O. Wright* 249

CI Cygni, and Z Andromedae, Spectroscopic Observations of AX Persei, RW Hydrae. *Paul W. Merrill* 15

Eclipsing Variables, Russian Investigations of: "On the Smaller Effects in Eclipsing Variables," by D. J. Martinoff, and "The Reflection Effect in Eclipsing Variables," by M. G. Odinzov. *S. Gaposchkin* 313

"Fraunhofer Lines along a Radius of the Solar Disk, The Variations in the Profiles of Strong," by J. Houtgast. *Lyman Spitzer, Jr.* 107

PAGE

Gravitational Field Arising from a Random Distribution of Stars, The Statistics of the. III. The Correlations in the Forces Acting at Two Points Separated by a Finite Distance. *S. Chandrasekhar* 25

Gravitational Field Arising from a Random Distribution of Stars, The Statistics of the. IV. The Stochastic Variation of the Force Acting on a Star. *S. Chandrasekhar* . . . 47

Helium in the Solar Atmosphere, Preliminary Note on the Behavior of. *Suzanne E. A. van Dijke* 121

RW Hydrae, CI Cygni, and Z Andromedae, Spectroscopic Observations of AX Persei. *Paul W. Merrill*. 15

48 Librae (HD 142983), A Note on the Shell Spectrum of. *W. A. Hiltner* 103

Line Intensities and the Solar Curve of Growth. *K. O. Wright* 249

Milky Way, Colors of Early-Type Stars in the Southern. *Francis J. Heyden, S.J.* . . . 8

Milky Way in Cassiopeia, Analysis of the. *Robert H. Baker and Elaine Nantkes* . . . 125

Negative Hydrogen Ion, The Continuous Absorption Coefficient of the. *Louis R. Henrich* 59

Negative Hydrogen Ion, The Continuous Absorption Coefficient of the: A Correction. *Louis R. Henrich* 318

Noncoherent Scattering, Notes on the Theory of. *Lyman Spitzer, Jr.* 1

Nova Puppis 1942, The Spectrum of. *Harold F. Weaver* 280

Orbits for the Spectroscopic Binaries HD 163181 and HD 78316 (76 κ Cancri), New. *Otto Struve* 210

Orion, Radial Velocities of the Four Stars of the Trapezium in. *Otto Struve and John Titus* 84

AX Persei, RW Hydrae, CI Cygni, and Z Andromedae, Spectroscopic Observations of. *Paul W. Merrill* 15

Proper-Motion Stars, Color Indices of. *W. J. Luyten, P. D. Jose, and J. F. Foster* . . 244

Proper-Motion Stars, Radial Velocities of. *Guido Münch* 271

Radial Velocities of the Four Stars of the Trapezium in Orion. *Otto Struve and John Titus* 84

Radial Velocities of Proper-Motion Stars. *Guido Münch* 271

Radial Velocities of 283 Stars of Spectral Classes R and N. *Roscoe F. Sanford* 145

Radiative Equilibrium of a Stellar Atmosphere, On the. *S. Chandrasekhar*. 180

Random Distribution of Stars, The Statistics of the Gravitational Field Arising from a. III. The Correlations in the Forces Acting at Two Points Separated by a Finite Distance. *S. Chandrasekhar* 25

Random Distribution of Stars, The Statistics of the Gravitational Field Arising from a. IV. The Stochastic Variation of the Force Acting on a Star. *S. Chandrasekhar* . . . 47

Reviews:

Banerji, A. C. *Recent Advances in Galactic Dynamics.* ("Lucknow University Studies," No. 15.) (S. Chandrasekhar) 124

Kingsland, J. C., and D. W. Seager. *Navigation.* (John Titus) 124

PAGE

Norton, Arthur P., and J. Gall Ingles. *Norton's Star Atlas and Telescopic Handbook.* (W. W. Morgan) 124

Shapley, Harlow. *Galaxies.* ("Harvard Books on Astronomy.") (Joel Stebbins) . . 320

Solar Atmosphere, Preliminary Note on the Behavior of Helium in the. *Suzanne E. A. van Dijke* 121

Solar Curve of Growth, Line Intensities and the. *K. O. Wright* 249

Solar Research in Belgium during 1942. *P. Swings* 118

Spectral Classes R and N, Radial Velocities of 283 Stars of. *Roscoe F. Sanford* . . . 145

Spectrographic Problem of U Cephei, The. *Otto Struve* 222

Spectroscopic Binaries HD 163181 and HD 78316 (76 κ Cancri), New Orbits for the. *Otto Struve* 210

Spectroscopic Observations of AX Persei, RW Hydrae, CI Cygni, and Z Andromedae. *Paul W. Merrill.* 15

Spectrum of θ Aurigae, Complex Lines in the. *W. A. Hiltner and W. W. Morgan* . . 318

Spectrum of α^2 Canum Venaticorum, Note on the. *W. A. Hiltner* 256

Spectrum of 12 Comae Berenices, Note on the. *Carlos U. Cesco and Jorge Sahade* . . 317

Spectrum of Comet Whipple-Fedtké-Tevzadze (1942g), The. *Andrew McKellar* . . . 162

Spectrum of Comet 1940c, On the. *N. T. Bobrovnikoff* 173

Spectrum of HD 218393, Rapid Changes in the. *Otto Struve* 75

Spectrum of 48 Librae (HD 142983), A Note on the Shell. *W. A. Hiltner* 103

Spectrum of Nova Puppis 1942, The. *Harold F. Weaver* 280

Spectrum of RX Cassiopeiae, The. *O. Struve* 295

Spectrum of SX Cassiopeiae, The. *Otto Struve* 89

Spectrum of VV Cephei, The Ultraviolet. *Otto Struve* 70

Spectrum Variable ϵ Ursae Majoris, The. *J. W. Swensson* 258

Stability of Binary Systems, On the. *S. Chandrasekhar* 54

Statistics of the Gravitational Field Arising from a Random Distribution of Stars, The. III. The Correlations in the Forces Acting at Two Points Separated by a Finite Distance. *S. Chandrasekhar* 25

Statistics of the Gravitational Field Arising from a Random Distribution of Stars, The. IV. The Stochastic Variation of the Force Acting on a Star. *S. Chandrasekhar* . . . 47

Stellar Atmosphere, On the Radiative Equilibrium of a. *S. Chandrasekhar* 180

Stellar Rotation and Large-Scale Currents. *Wasley Krogdahl* 191

Stellar Spectra, Notes on. *Otto Struve* 205

Ultraviolet Spectrum of VV Cephei, The. *Otto Struve* 70

ϵ Ursae Majoris, The Spectrum Variable. *J. W. Swensson* 258

Wolf-Rayet Spectroscopic Binary HD 214419, The. *W. A. Hiltner* 273

INDEX TO AUTHORS

PAGE

BAKER, ROBERT H., and ELAINE NANTKES. Analysis of the Milky Way in Cassiopeia . 125

BOBROVNIKOFF, N. T. On the Spectrum of Comet 1940c 173

CESCO, CARLOS U., and JORGE SAHADE. Note on the Spectrum of 12 Comae Berenices . 317

CHANDRASEKHAR, S. On the Radiative Equilibrium of a Stellar Atmosphere 180

CHANDRASEKHAR, S. On the Stability of Binary Systems 54

CHANDRASEKHAR, S. The Statistics of the Gravitational Field Arising from a Random Distribution of Stars. III. The Correlations in the Forces Acting at Two Points Separated by a Finite Distance 25

CHANDRASEKHAR, S. The Statistics of the Gravitational Field Arising from a Random Distribution of Stars. IV. The Stochastic Variation of the Force Acting on a Star . 47

FOSTER, J. F., W. J. LUYTEN, and P. D. JOSE. Color Indices of Proper-Motion Stars . . 244

GAPOSCHKIN, S. Russian Investigations of Eclipsing Variables: "On the Smaller Effects in Eclipsing Variables," by D. J. Martinoff, and "The Reflection Effect in Eclipsing Variables," by M. G. Odinzov 313

HENRICH, LOUIS R. The Continuous Absorption Coefficient of the Negative Hydrogen Ion 59

HENRICH, LOUIS R. The Continuous Coefficient of the Negative Ion of Hydrogen: A Correction 318

HEYDEN, FRANCIS J., S.J. Colors of Early-Type Stars in the Southern Milky Way . . 8

HILTNER, W. A. A Note on the Shell Spectrum of 48 Librae (HD 142983) 103

HILTNER, W. A. Note on the Spectrum of α^2 Canum Venaticorum 256

HILTNER, W. A. The Wolf-Rayet Spectroscopic Binary HD 214419 273

HILTNER, W. A., and W. W. MORGAN. Complex Lines in the Spectrum of θ Aurigae . 318

HOUTGAST, J. Recent Progress in Astrophysics 107

JOSE, P. D., J. F. FOSTER, and W. J. LUYTEN. Color Indices of Proper-Motion Stars . 244

KOPAL, ZDENĚK. Note on the Problem of U Cephei 239

KROGDAHL, WASLEY. Stellar Rotation and Large-Scale Currents 191

LUYTEN, W. J., P. D. JOSE, and J. F. FOSTER. Color Indices of Proper-Motion Stars . . 244

MCKELLAR, ANDREW. The Spectrum of Comet Whipple-Fedtké-Tevazdze (1942g) . . 162

MCMATH, ROBERT R. Heber Doust Curtis, 1872–1942 245

MARTINOFF, D. J. Recent Progress in Astrophysics 313

MERRILL, PAUL W. Spectroscopic Observations of AX Persei, RW Hydrae, CI Cygni, and Z Andromedae 15

MORGAN, W. W., and W. A. HILTNER. Complex Lines in the Spectrum of θ Aurigae . 318

PAGE

MÜNCH, GUIDO, Radial Velocities of Proper-Motion Stars. 271

NANTKES, ELAINE, and ROBERT H. BAKER. Analysis of the Mjlky Way in Cassiopeia . 125

NEUBAUER, F. J. The System of β Coronae Borealis 134

ODINZOV, M. G. Recent Progress in Astrophysics 314

SAHADE, JORGE, and CARLOS U. CESCO. Note on the Spectrum of 12 Comae Berenices . 317

SANFORD, ROSCOE F. Radial Velocities of 283 Stars of Spectral Classes R and N . . . 145

SPITZER, LYMAN, JR. Notes on the Theory of Noncoherent Scattering 1

SPITZER, LYMAN, JR. "The Variations in the Profiles of Strong Fraunhofer Lines along a Radius of the Solar Disk," by J. Houtgast. 107

STRUVE, OTTO. New Orbits for the Spectroscopic Binaries HD 163181 and HD 78316 (76 κ Cancri) 210

STRUVE, OTTO. Notes on Stellar Spectra 205

STRUVE, OTTO. Rapid Changes in the Spectrum of HD 218393 75

STRUVE, OTTO. The Spectrographic Problem of U Cephei 222

STRUVE, O. The Spectrum of RX Cassiopeiae 295

STRUVE, OTTO. The Spectrum of SX Cassiopeiae 89

STRUVE, OTTO. The Ultraviolet Spectrum of VV Cephei 70

STRUVE, OTTO, and JOHN TITUS. Radial Velocities of the Four Stars of the Trapezium in Orion 84

SWENSSON, J. W. The Spectrum Variable ϵ Ursae Majoris 258

SWINGS, P. Astrophysical Research in France in 1940–1942 115

SWINGS, P. Solar Research in Belgium during 1942. 118

TITUS, JOHN, and OTTO STRUVE. Radial Velocities of the Four Stars of the Trapezium in Orion 84

VAN DIJKE, SUZANNE E. A. Preliminary Note on the Behavior of Helium in the Solar Atmosphere 121

WEAVER, HAROLD F. The Spectrum of Nova Puppis 1942 280

WRIGHT, K. O. Line Intensities and the Solar Curve of Growth 249